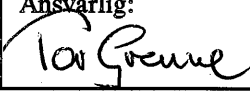


NGU Rapport 91.225

The Archaean-Proterozoic boundary beneath  
the Caledonides of northern Norway and  
Sweden:  
U-Pb, Rb-Sr, and  $\epsilon$ Nd Isotope data from  
the Rombak-Tysfjord area

Rapport nr. 91.225		ISSN 0800-3416	Gradering: Åpen
<b>Tittel:</b> The Archaean-Proterozoic boundary beneath the Caledonides of northern Norway and Sweden: U-Pb, Rb-Sr, and $\epsilon$ Nd isotope data from the Rombak-Tysfjord area.			
<b>Forfatter:</b> Romer, R.L., Kjøsnes, B., Korneliussen, A., Lindahl, I., Skyseth, T., Stendal, M. og Sundvoll, B.		<b>Oppdragsgiver:</b> NGU	
<b>Fylke:</b> Nordland og Troms		<b>Kommune:</b> Narvik, Tysfjord, m.fl.	
<b>Kartbladnavn (M=1:250.000)</b> Narvik Sulitjelma		<b>Kartbladnr. og -navn (M=1:50.000)</b> 1431.3 Skjomdalen 1431.4 Rombaken, m.fl.	
<b>Forekomstens navn og koordinater:</b> Diverse		<b>Sidetall:</b> 67	<b>Pris:</b> kr. 87,-
<b>Feltarbeid utført:</b>		<b>Rapportdato:</b> 28.4.92	<b>Prosjektnr.:</b> 67.2312.01
<b>Ansvarlig:</b> 			
<b>Sammendrag:</b> <p>The Baltic Shield includes an Archaean craton in northeastern Finland. Early Proterozoic accretions to this Archaean craton comprise of (1) the Svecofennian domain, which consists of island arc volcanic and sedimentary rocks that formed at 1.94 - 1.85 Ga and that between 1.83 and 1.78 Ga became intensely intruded by post-orogenic granites and (2) the Transscandinavian Granite Porphyry Belt (TGPB), which represents a 1.80 - 1.70 Ga magmatic arc at the western and southwestern margin of the Svecofennian domain. The TGPB granites extend across the boundary between the Archaean and Svecofennian crustal blocks. This boundary is in Finland a dextral strike-slip fault zone (Raahe-Ladoga zone) that to the west (Sweden and Norway) widens to a ca 250 km wide heterogeneous zone.</p> <p>TGPB granites occurring in the basement culminations of the 0.5 - 0.4 Ga Caledonian orogen of northern Scandinavia have a bimodal U-Pb zircon age distribution (<math>1791 \pm 10</math> Ma and <math>1711 \pm 26</math> Ma). The chemical composition of the older granites has magmatic arc affinity, while the one of the younger granites has within-plate affinity. Both granite generations have <math>\epsilon</math>Nd (T) values that suggest variable involvement of older crustal material in their formation. The older granites above the Archaean and Svecofennian domain have small to moderate involvement of Archaean material. The younger granites above the Archaean domain also have small to moderate Archaean crustal involvement, while the younger granites above the Svecofennian domain have moderate to dominant Archaean involvement. The strong Archaean involvement to the south of the Archaean craton is due to the melting of sedimentary rocks that originated from the Archaean craton.</p>			
<b>Emneord:</b>			
berggrunnsgeologi	prekambrisk	geokjemi	
granitt	geokronologi	isotopgeologi	

**The Archaean-Proterozoic boundary beneath the Caledonides of northern Norway and Sweden: U-Pb, Rb-Sr, and  $\epsilon_{Nd}$  isotope data from the Rombak-Tysfjord area**

Romer, R.L.<sup>1</sup>, Kjøsnes, B.<sup>2</sup>, Korneliussen, A.<sup>2</sup>, Lindahl, I.<sup>2</sup>, Skyseth, T.<sup>3</sup>, Stendal, H.<sup>4</sup>, and Sundvoll, B.<sup>5</sup>

<b>Contents</b>	<b>(page)</b>
1. Abstract	(4)
2. Introduction	(5)
3. Regional geology	(5)
4. Sample locations	(8)
5. Analytical methods and results	(13)
U-Pb results	(13)
Rb-Sr results	(20)
$\epsilon_{Sr}(T)$ results	(25)
$\epsilon_{Nd}(T)$ results	(26)
6. Geochemistry and petrology of the Early Proterozoic granitoids	(26)
Tonalites and trondhjemites	(31)
Older granites (ca 1.79 Ga)	(31)
Younger granites (ca 1.71 Ga)	(33)
Geochemical discrimination between younger and older granites	(36)
7. Constraints on the position of the Archaean-Proterozoic boundary beneath the Caledonides	(37)
8. The Transscandinavian Granite Porphyry Belt	(41)
9. Model	(42)
10. Summary	(50)
11. Acknowledgments	(50)
12. References	(51)

1 Department of Economic Geology, Luleå University, S-951 87 Luleå, Sweden

2 Norwegian Geological Survey, Box 3006, N-7002 Trondheim, Norway

3 Department of Geological Sciences, State University of New York at Buffalo, 4240 Ridge Road, Buffalo, NY 14226, U.S.A.

4 Geological Institute, University of Copenhagen, Øster Voldgade 10, DK-1350 Copenhagen K, Denmark

5 Mineralogisk-Geologisk Museum, Oslo University, Sars' Gate 1, N-0502 Oslo, Norway

## 1. Abstract

The Baltic Shield includes an Archaean craton in northeastern Finland. Early Proterozoic accretions to this Archaean craton comprise of (1) the Svecofennian domain, which consists of island arc volcanic and sedimentary rocks that formed at 1.94-1.85 Ga and that between 1.83 and 1.78 Ga became intensely intruded by post-orogenic granites and (2) the Transscandinavian Granite Porphyry Belt (TGPB), which represents a 1.80-1.70 Ga magmatic arc at the western and southwestern margin of the Svecofennian domain. The TGPB granites extend across the boundary between the Archaean and Svecofennian crustal blocks. This boundary is in Finland a dextral strike-slip fault zone (Raahe-Ladoga zone) that to the west (Sweden and Norway) widens to a ca 250 km wide heterogeneous zone.

TGPB granites occurring in the basement culminations of the 0.5-0.4 Ga Caledonian orogen of northern Scandinavia have a bimodal U-Pb zircon age distribution ( $1791 \pm 10$  Ma and  $1711 \pm 26$  Ma). The chemical composition of the older granites has magmatic arc affinity, while the one of the younger granites has within-plate affinity. Both granite generations have  $\epsilon_{\text{Nd}}(T)$  values that suggest variable involvement of older crustal material in their formation. The older granites above the Archaean and Svecofennian domain have small to moderate involvement of Archaean material. The younger granites above the Archaean domain also have small to moderate Archaean crustal involvement, while the younger granites above the Svecofennian domain have moderate to dominant Archaean involvement. The strong Archaean involvement to the south of the Archaean craton is due to the melting of sedimentary rocks that originated from the Archaean craton.

Proterozoic rocks exposed in the Caledonian basement culminations between Kvaløya and Sjøna formed close to the intersection of three plates: the Archaean plate in the north, the Svecofennian plate in the south and an unknown third plate to the west. Early Proterozoic crustal shortening across the area of the future Baltic Shield was initially accommodated within the Archaean craton to the northeast (granulite belts), but eventually became mainly concentrated at the border between the Svecofennian and Archaean plate and within the Svecofennian plate. The Svecofennian plate became destroyed, probably starting close to 1.94 Ga, when magmatic arc related tonalites intruded, and continuing until about 1.80 Ga, when the Svecofennian domain became consolidated. Buoyant fragments within the Svecofennian domain, that collided with the Archaean craton, were transported along major strike-slip shear zones to the northwest (e.g., Raahe-Ladoga zone), where they accumulated close to the intersection of the three plates. This accumulation to the northwest resulted in a westward widening heterogeneous zone of Archaean influence in the Svecofennian domain. After cessation of crustal destruction within the Svecofennian area, the third plate became destroyed at the western margin of the Baltic Shield, where it became subducted beneath these two plates and the TGPB rocks formed above the subduction zone.

## 2. Introduction

Reconstruction of the roughly northwest striking boundary between the Archaean and Svecofennian domain in northern Scandinavia (Fig. 1) involving  $\epsilon_{Nd}(T)$  data and U-Pb zircon geochronology suggests that this boundary continues beneath the Caledonian orogenic belt, passing through or between the basement culminations at Tysfjord, Rombak-Sjangeli, and Kvaløya (e.g., Öhlander et al., 1987). The reconstruction of this boundary bases on the assumption, that lithologic trends established to the east of the Caledonides continue undisturbed into the Caledonian orogenic belt. The basement culminations within the Caledonides were interpreted to be autochthonous parts of the Baltic Shield (Kulling, 1964; Gee and Zachrisson, 1979). This assumption is not strictly correct, as the basement culminations are intensely Caledonian imbricated antiformal stacks (Bax, 1989). For instance, at the eastern margin of the Rombak-Sjangeli window (Fig. 1) the Caledonian thrusting amounted to at least 50 km (Bax, 1989; Bax et al., 1991) and the amount of thrusting becomes increasingly larger to the west. However, the northwest to southeast directed Caledonian thrusting was roughly parallel to the strike of the Archaean-Proterozoic boundary, which therefore is not offset by the Caledonian crustal shortening.

Reconstruction of the Transscandinavian Granite Porphyry Belt (TGPB, Fig. 1), which consists of Early Proterozoic granitoids of probable island arc or magmatic arc affinity (Johansson, 1988; Zuber and Öhlander, 1990), suggests that this belt continues from southern Sweden to northern Norway beneath the Caledonides, where it is exposed in basement culminations (Eriksson and Henkel, 1983; Gaál and Gorbatshev, 1987). The boundary between the Archaean and Svecofennian domain should intersect with the TGPB in the area of the Tysfjord, Rombak-Sjangeli, and Kvaløya basement culminations (Fig. 1).

The scope of this paper is (1) to present geochemical data along with new isotope data and U-Pb zircon age determinations on granites from basement culminations in the Caledonian orogen along the EU 13 Geotranssect (Lofoten-Torneträsk-Kiruna-Malmberget Caledonide Deep Section), (2) to set constraints on the position and nature of the Archaean-Proterozoic boundary beneath the Caledonides, and (3) to investigate the relation between the granitoids in the basement windows and granitoids of the Svecofennian domain to the east of the Caledonides. We present a tectonic model to explain the age distribution and the geochemical characteristics of Early Proterozoic granitoids in the basement culminations of northern Scandinavian Caledonides.

## 3. Regional geology

The Baltic Shield displays a distinct age-zoned pattern with an Archaean core to the northeast and increasingly younger Proterozoic rocks to the southwest (Fig. 1). The craton grew by accretion of magmatic arcs during various orogenies. Each orogenic event reworked older crustal material along the margin of the craton and added mantle derived material to the crust (Gaál and Gorbatshev, 1987).

Archaean crust on the Baltic Shield (Fig. 1) has ages that cluster close to 2.7 Ga, when major crustal growth occurred and older parts of the craton became variably

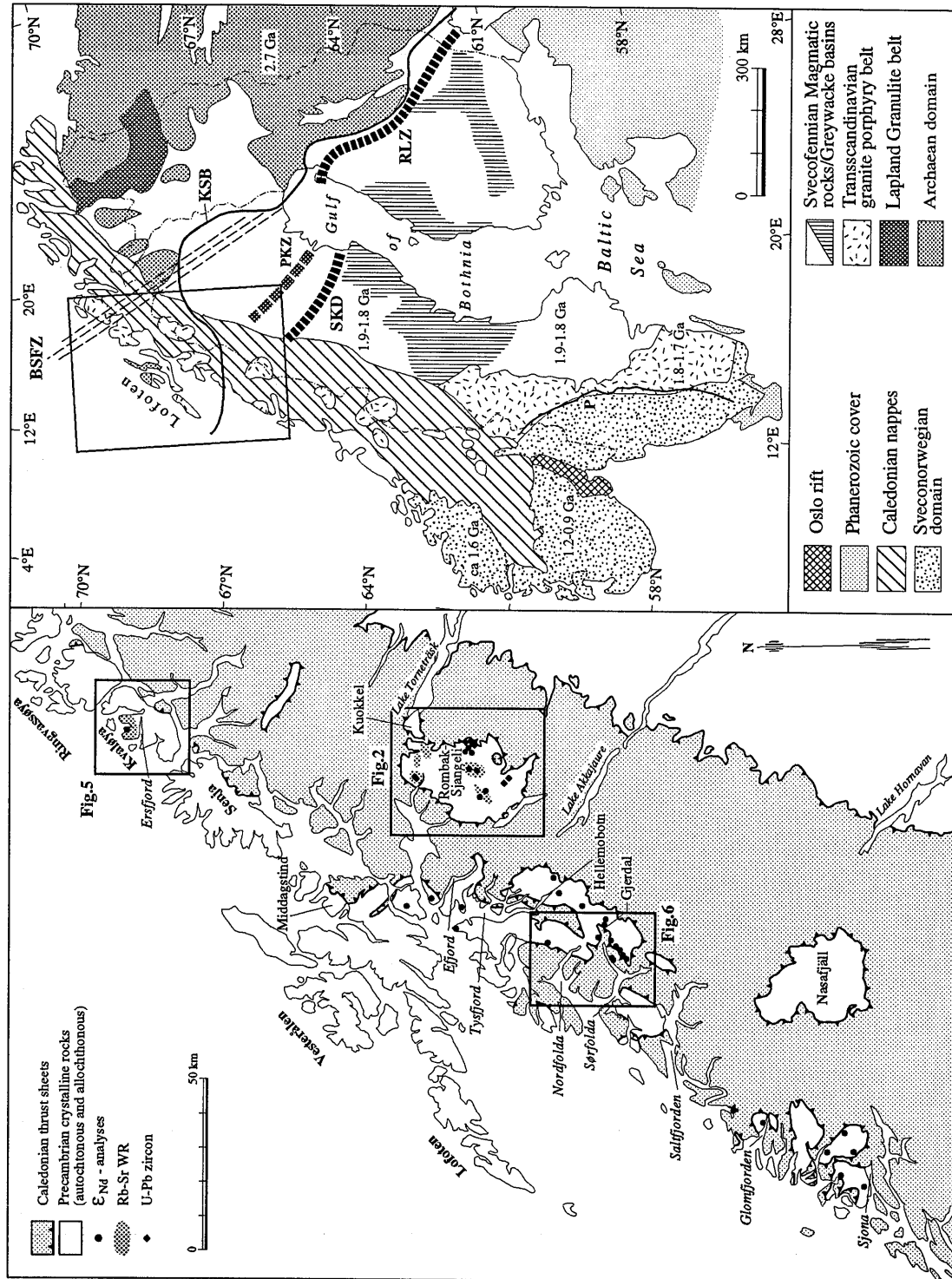


**Fig. 1:** Tectonic map of the Scandinavian Caledonides of northern Norway and Sweden (Nordkalott Project, 1988) and tectonic map of the Baltic Shield (simplified after Gaál and Gorbatshev, 1987). Suggested Archaean-Proterozoic palaeo-boundaries: Raahe-Ladoga Zone (RLZ) and Skellefte district (SKD; Lithology and sulfide deposits; Berthelsen, 1987), Piteå-Kåbdalis zone (PKZ; gravity and  $\epsilon_{Nd}$  (T) gradient; Öhlander et al., 1990), and Karelian-Svecofennian border (KSB; southern limit of geochronologically identified Archaean crust; Pharaoh and Pearce, 1984). Bothnian-Senja Fracture Zone (BSFZ) after Henkel (1991). P = Protogine zone.

metamorphosed (e.g., Jahn et al., 1984). Archaean crust occurs in eastern Finland and in the Lofoten and Vesterålen area (e.g., Griffin et al., 1978; Jacobsen and Wasserburg, 1978), northernmost Sweden (Öhlander et al., 1987), and eastern Finland (e.g., Huhma, 1986; Gaál and Gorbatshev, 1987). The Svecofennian (ca 1.8-1.9 Ga) accretion to the Archaean craton (Fig. 1) comprises mainly island and magmatic arc rocks. U-Pb zircon dating indicates two main periods of granitic magmatism. The older period at ca (1.94)-1.90-1.85 Ga (Skiöld, 1988) was probably mainly related to magmatism in volcanic arcs, while intrusions of the younger period (1.83-1.80 Ga; Skiöld, 1988) were due to the amalgamation of these arcs with the craton. Magmatism in Finland displays a similar dual age pattern, however, magmatic rocks corresponding to the Swedish granites appear to be older by 20 to 30 Ma (Vaasjoki and Sakko, 1988). Greywacke basins (e.g., Park, 1991) occur between the areas of Svecofennian magmatism and volcanism (e.g., northern Sweden, central Sweden, and southern Finland). These basins became extensively metamorphosed and migmatized during the late stages of the Svecofennian orogeny (ca 1.80-1.77 Ga).

Early Proterozoic rocks ranging in age from ca 1.8-2.0 Ga are subdivided into Svecofennian and Karelian units (see Gaál and Gorbatshev, 1987). Svecofennian refers to volcanic and sedimentary rocks that were deposited in an oceanic environment, while Karelian rocks mainly comprise of terrestrial sediments that were deposited on older continental crust (Gaál and Gorbatshev, 1987).

The Svecofennian area is to the south and west bordered by the Transscandinavian Granite Porphyry Belt (TGPB), which includes 1.79 - 1.70 Ga old granites and porphyries. The TGPB probably represents a magmatic arc related to an Early Proterozoic subduction zone (Johansson, 1988). The TGPB granitoids are geochemically not distinguishable from the Svecofennian rocks, yet they are, however, generally 50 to 100 Ma younger than the geochemically corresponding granites in the Svecofennian domain. Granitoids of the TGPB belong to a "paired" belt consisting of high-magnetic granitoids to the east and low-magnetic granitoids to the west. The belt is offset by a series of NW-SE striking fault zones (Eriksson and Henkel, 1983). TGPB rocks continue to the north beneath the Caledonides, where they are exposed in basement culminations such as Nasafjäll, Tysfjord, Rombak-Sjängeli, Senja and Kvaløya (cf. Eriksson and Henkel, 1983; Gaál and Gorbatshev, 1987). The original western limit of the Svecofennian rocks is not well known, as the Baltic Shield to the west of the Protogine zone (P in Fig. 1), an about 50-80 km wide zone of intense mylonitization, that truncates the TGPB to the west, was completely overprinted by the Sveconorwegian orogeny at ca 1.2-0.9 Ga.

The last major orogeny affecting the Baltic Shield was the Caledonian orogeny at ca 0.5-0.4 Ga that was related to the closure of the Iapetus ocean between the Baltic and Laurentian Shields. During this orogeny a pile of nappes was thrust in a piggy-back style from the northwest on the western margin of the Baltic Shield. The Early Proterozoic rocks in the basement windows (Fig. 1), which earlier were considered to represent autochthonous to para-autochthonous basement (Kulling, 1964; Gee and Zachrisson, 1979), were during the Caledonian orogeny intensely imbricated and thrust to form antiformal stacks in the basement culminations (Bax, 1989). The

basement culminations occur at locations where the margin of the continent Baltica was more intensely involved in the thrusting and shortening processes related to the Caledonian orogeny (Bax, 1989; Romer and Bax, 1990, 1992).

The different approaches to define the Archaean-Proterozoic boundary yield different results, because some methods measure the actual occurrence of Archaean rocks, while others only record the involvement of Archaean rocks in the protoliths of the younger rocks. The Archaean-Proterozoic boundaries defined by various methods coincide in Eastern Finland into a zone a few tens of kilometers wide (Vaasjoki and Sakko, 1988), while the variation of the boundary as estimated by the same methods spreads over more than 250 km in northwestern Sweden (Fig. 1). Projections of the Archaean-Proterozoic boundary across the Caledonides pass to the north, through, or to the south of the Rombak-Sjangeli basement culmination (e.g., Öhlander et al., 1987; Frietsch, 1988; Romer, 1991) depending on the used criteria to define the boundary. For instance, using published ages of intrusive rocks (e.g., Nordkalott Project, 1988), the border would pass far to the north of the Rombak-Sjangeli window, while the occurrence of quartzites that are correlated with Karelian continental sediments, aeromagnetic anomalies, and high  $\mu_1$  lead would position the boundary close to the northern margin of the Rombak-Sjangeli window (Romer, 1991).  $\epsilon_{Nd}(T)$  data and the volcanogenic exhalative sulfide ores, such as those from the Finnish sulfide ore belt and the Skellefte district, locate the boundary even far to the south (Fig. 1; e.g., Berthelsen and Marker, 1986).

#### 4. Sample locations

Sjangeli: The granitoid rocks in the Sjangeli area (Fig. 2) are dominated by the Early Proterozoic K-feldspar megacrystic granites, medium-grained equigranular granites, and minor lenses of gneiss. Regional Rb-Sr WR data (Gunner, 1981) yield an age of  $1780 \pm 85$  Ma ( $1\sigma$ ), which is close to the U-Pb zircon age of the older granites (Fig. 7i). However, the reported initial strontium isotopic composition ( $^{87}\text{Sr}/^{86}\text{Sr} = 0.700$ ) is anomalous low, suggesting that the regional approach involved originally heterogeneous, non-cogenetic material.

Tonalitic gneisses and two kinds of granite occur between the Sjangeli supracrustal belt and the eastern margin of the Rombak-Sjangeli basement culmination (Fig. 3). The gneisses border to the supracrustal belt and form a 300 to 500 m wide belt which to the east is intruded by weakly foliated coarse-grained granite. The original nature of the contact between the Sjangeli Supracrustal belt and the tonalite is not known, as the lowermost units of the Sjangeli supracrustal belt are intensely sheared, and the tonalite has a deformational fabric with the same orientation. The sheared contact became later faulted along NW-SE striking faults and NNE-SSW striking shear zones (see Fig. 3). The tonalite samples originate from three sites bordering the supracrustal belt. They were sampled 20 to 200 m beneath the Caledonian thrust plane.

The supracrustal belt and the tonalite became intruded by two generations of granite. The older granite is often weakly foliated, while the younger granite shows no internal fabric except for local flow-alignment of K-feldspar megacrysts. The



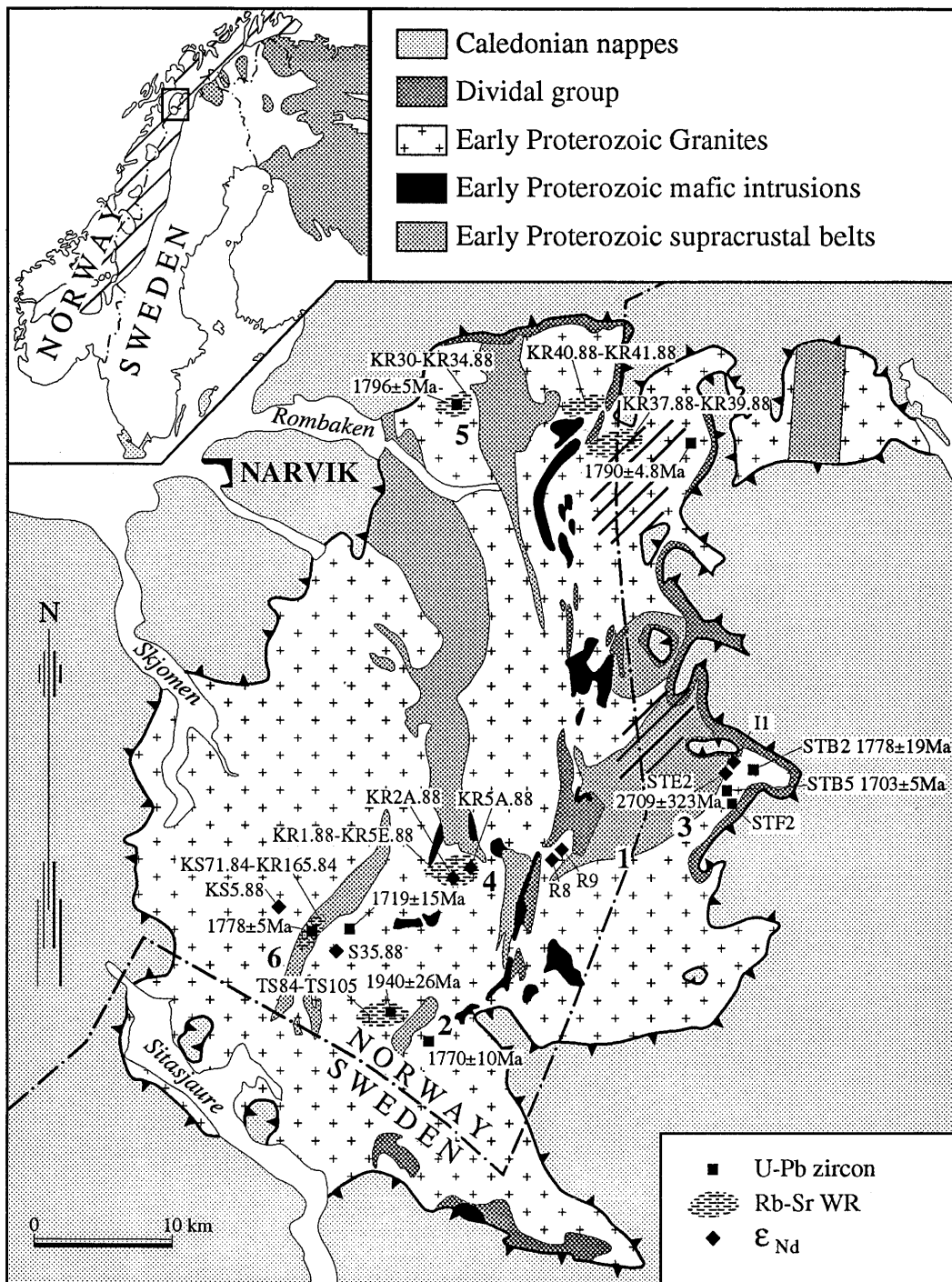


**Fig. 2:** Geological map of the Rombak-Sjängeli basement culmination (Romer, 1987 and unpubl. field data). Sample locations for chemical analyses,  $\epsilon_{Sr}(T)$ ,  $\epsilon_{Nd}(T)$ , and U-Pb dating are indicated. Geographic distribution of Caledonian-mobilized early Proterozoic lead (ruled) with high pre-1.8 Ga  $\mu$  and high post-1.8 Ga Th/U (data from Romer, 1989; Romer and Wright, subm.). U-Pb columbite age data is from Romer and Wright (1992). Locations: 1 = Cunojavre, 2 = Gautelis, 3 = Sjängeli, 4 = Stasjonsholmen, 5 = Svartdalen/Rombaksbotn, 6 = Sørdal.

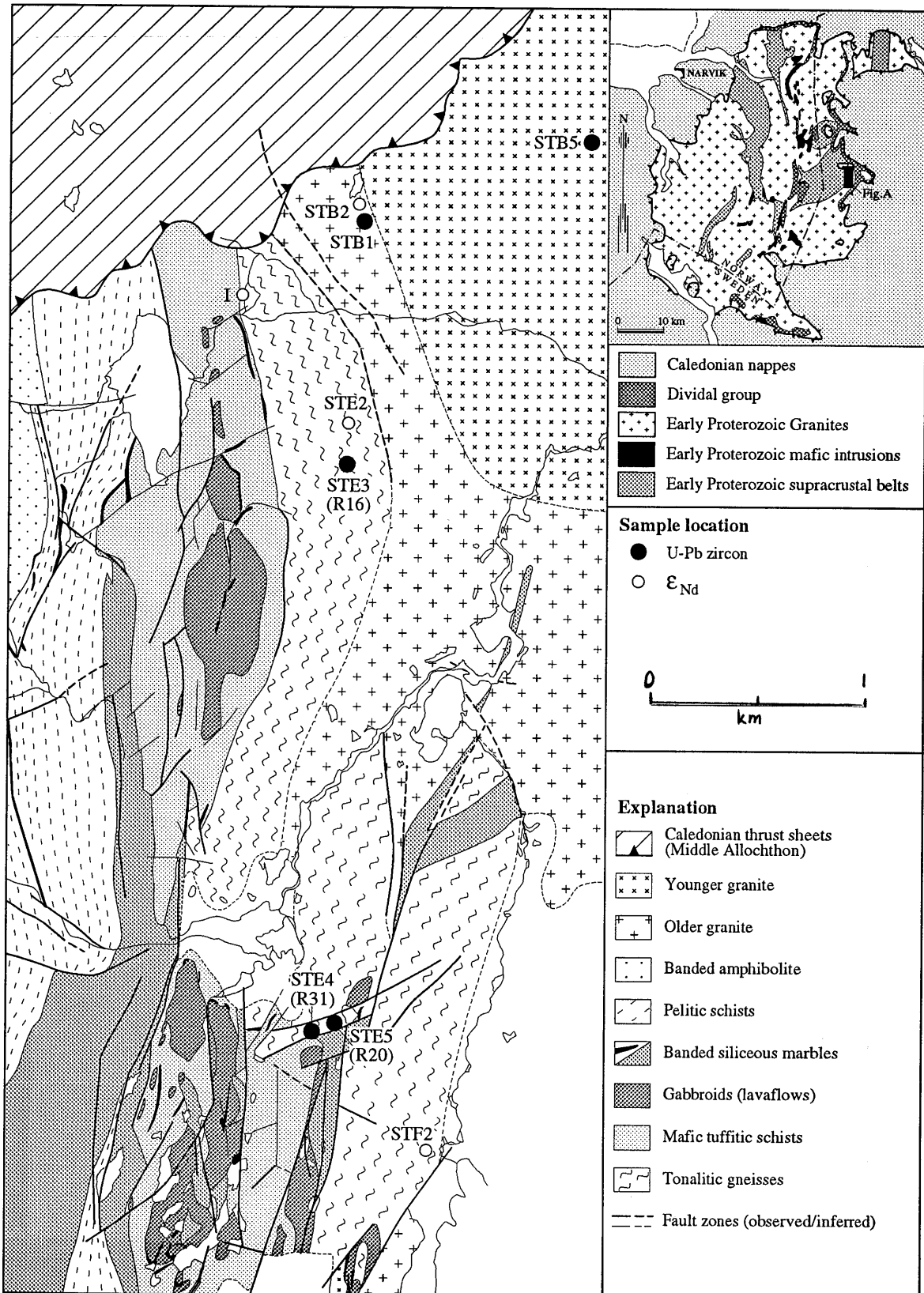


**Fig. 3:** Geological map of the Sjangeli area in the eastern part of the Rombak-Sjangeli basement culmination (Romer, 1987 and unpubl. field data). Sample locations for chemical analyses,  $\epsilon_{Sr}$  (T),  $\epsilon_{Nd}$  (T), and U-Pb dating are indicated.

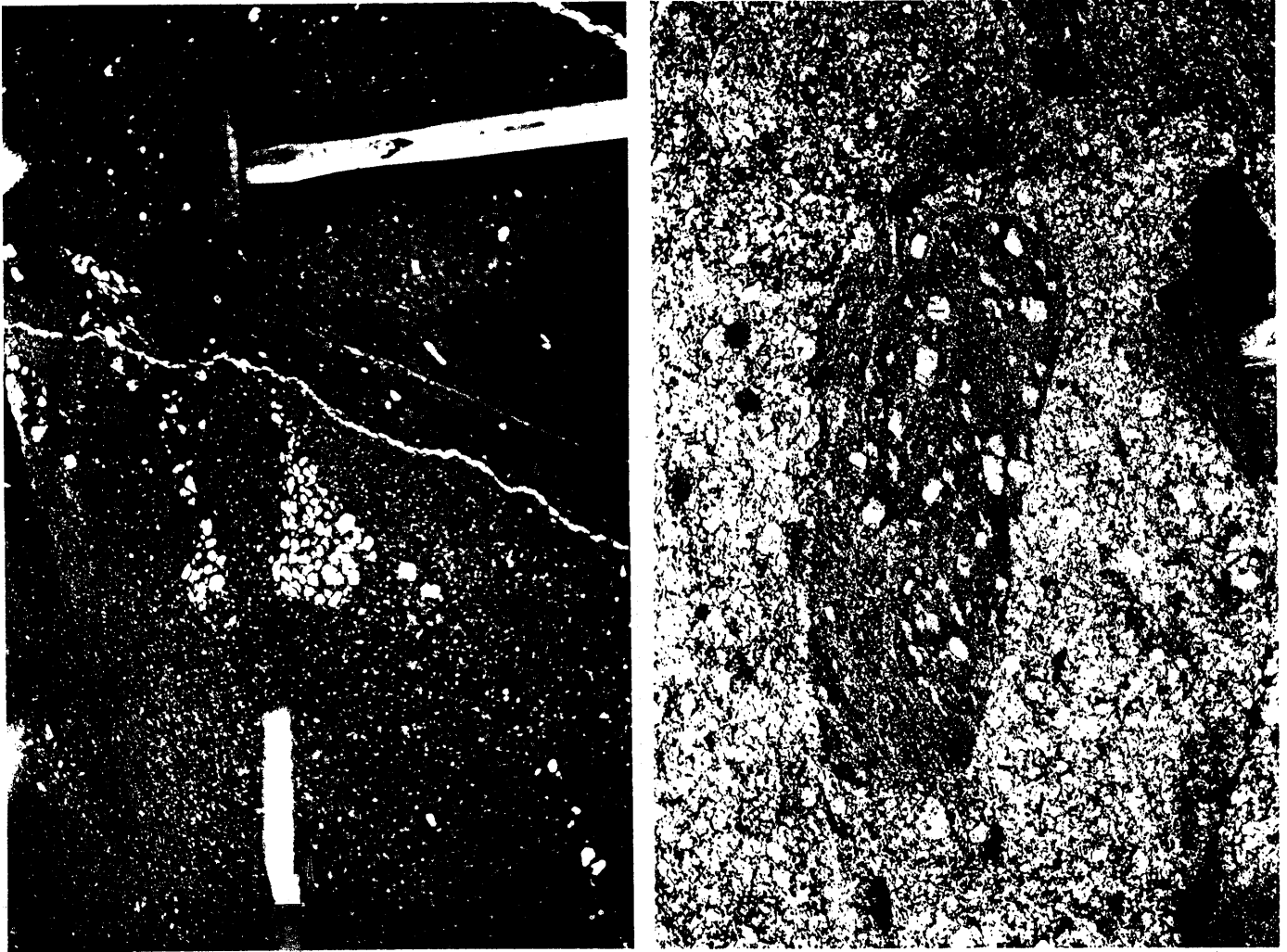


**Fig. 4:** Magma mixing and mingling structures at Stasjonsholmen (locality beneath bridge at the Stasjonsholmen Power Station). A: K-feldspar megacrysts in fine-grained mafic rock. B: K-feldspar megacrysts in the mafic enclave in the granite.

granites were sampled at two locations about 20-40 m beneath the Caledonian thrust plane (Fig. 3).

Gautelis: A gneissic tonalitic complex, that contains migmatitic mafic xenoliths and that is intruded by mafic dikes, is to the east overlain by a minor supracrustal belt. Both the supracrustal belt and the tonalite are intruded by granites (Fig. 2).

Sørdal, Stasjonsholmen, and Svartdal: At these three locations (Fig. 2), granites are either K-feldspar megacrystic or medium-grained equigranular. The granites of these three locations are very similar to the granites at Sjangeli, Kvaløya, and Tysfjord. Where contact relations can be observed, the equigranular granite is younger. Locally, granites contain enclaves, as for instance at Stasjonsholmen, where mafic enclaves in the K-feldspar megacrystic granites (Fig. 4) suggest magma mixing. At Sørdal, both granite generations intrude a minor mafic to intermediate volcanic belt (Fig. 2), which became metamorphosed to amphibolite facies.

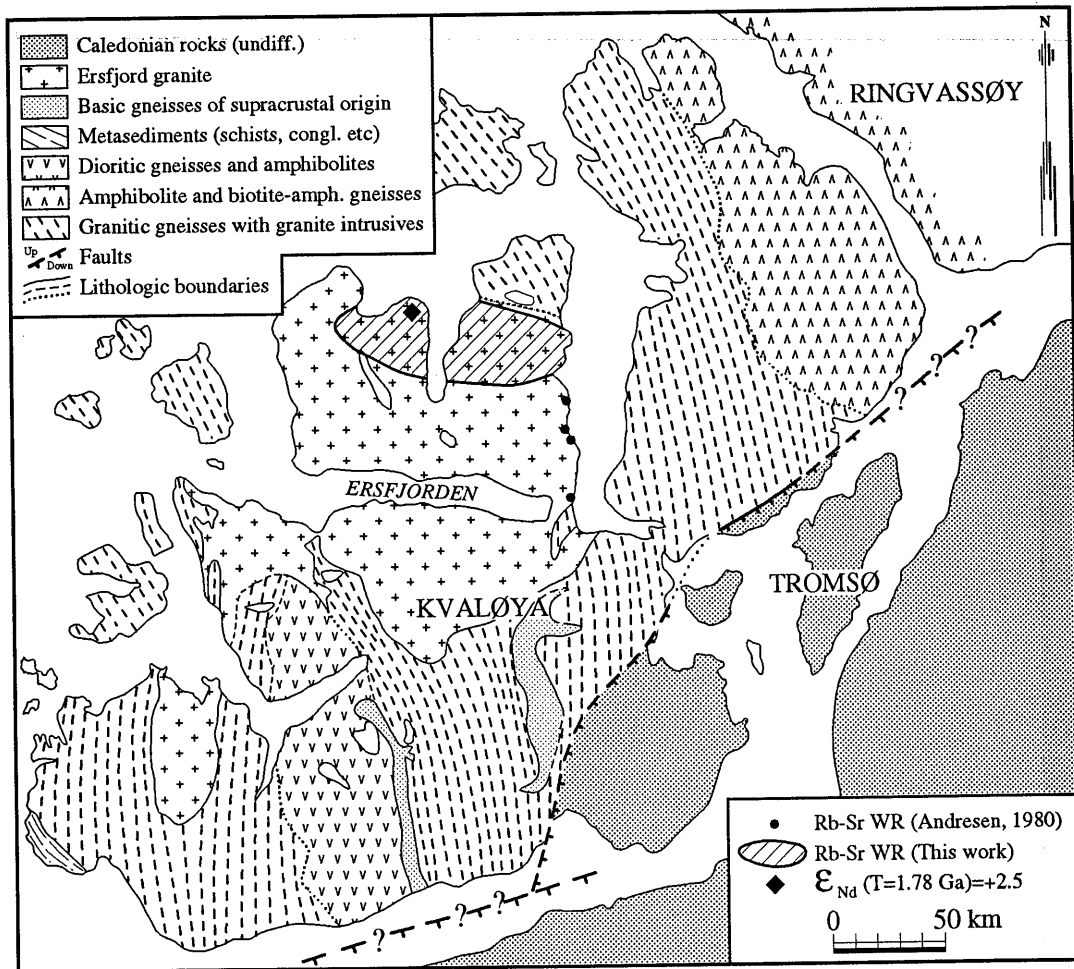


Fig. 5: Simplified geologic map of Kvaløya, northern Norway (Andresen, 1980)

**Kvaløya:** The Ersfjord granite covers about 80% of the northwestern part of Kvaløya (Fig. 5). The rock is a medium to coarse-grained reddish heterogeneous granodiorite that locally contains more fine-grained, weakly foliated aplitic sections. Pegmatitic veins occur at a few locations. The undeformed granite appears rather homogeneous, but often contains sections that are sheared, mylonitized and locally hydrothermal altered (Stendal and Petersen, 1989). The main part of the Ersfjord granite consists of a porphyric granodiorite in which 5-15 mm large elongated phenocrysts of alkali-feldspar occur in an equigranular more fine-grained groundmass of quartz and plagioclase with varying amounts of biotite, muscovite and zoisite. Epidote and allanite, chlorite, titanite, magnetite, apatite and zircon occur

accessoric. Andresen (1980) dated the Ersfjord granite from a sample suite from the eastern margin of the intrusion (see Fig. 5) and obtained a Rb-Sr age of  $1706 \pm 15$  Ma ( $1\sigma$ ). We sampled the same granite for Rb-Sr dating from the northern part of the intrusion. We obtained a Rb-Sr age of  $1779 \pm 19$  Ma ( $2\sigma$ ). The two age determinations differ beyond analytical uncertainties. The age difference suggests that the Kvaløya granite either consists of several differently aged intrusions or that at least one Rb-Sr age determination is erroneous.

**Southern Tysfjord:** Proterozoic rocks comprise in the southern Tysfjord area two tectonic windows in the Caledonides, the Tysfjord window and the Sommerseth window (Fig. 6). Heterogeneous, coarse-grained granites that usually are weakly foliated dominate in both windows. The deformational fabric is considered to be of Caledonian age (Andresen and Tull, 1986) as the fabric becomes more distinct as the contact to the covering sediments and the Caledonian nappes is approached (Stendal, 1981, 1990; Brattli and Prestvik, 1987). mm-sized magnetite disseminations are distinctive for the Sommerseth granite as well as for many granites belonging to the younger granite generation of the Transscandinavian Granite Porphyry Belt (TGPB).

## 5. Analytical methods and results

Zircon and titanite were separated by standard magnetic and heavy liquid procedures and purified by hand-picking. The analyzed fractions were acid washed with 6N HCl and 7N HNO<sub>3</sub> before dissolution. Some samples were spiked with a <sup>205</sup>Pb-<sup>235</sup>U tracer before dissolution, while the other samples were aliquoted after dissolution and spiked with a <sup>208</sup>Pb-<sup>235</sup>U tracer. Samples for U-Pb analysis weighted from 4 mg to less than 0.1 mg. Lead and uranium ion-exchange chemistry were carried out as described by Krogh (1973). The lead and uranium were measured on a Finnigan MAT262 multicollector mass spectrometer at Rice University, Houston TX.

Rb-Sr and Sm-Nd chemistry follow standard laboratory procedures (Mearns, 1986). The analyses were performed on a VG354 multicollector mass spectrometer at the Mineralogical-Geological Museum, Oslo University. <sup>86</sup>Sr/<sup>88</sup>Sr and <sup>146</sup>Nd/<sup>144</sup>Nd were normalized to 0.1194 and 0.72190, respectively. During the measurement period, NBS 987 yielded  $0.71023 \pm 2$  ( $2\sigma$ ) and the La Jolla Standard gave  $0.511850 \pm 8$  ( $2\sigma$ ).

**U-Pb results:** Zircons from all analyzed granites of the basement culminations have a simple crystal shape with tetragonal prisms (100) and tetragonal pyramids (101). Other crystal faces are extremely rare. The zircon morphology is typical for alkalic to subalkalic granites (e.g., Pupin, 1985). The zircons from the tonalitic gneiss at Sjangeli are distinctly brown colored and completely transparent. These zircons show prism faces after (100) and (110) and pyramidal faces after (201). The pyramid tops are slightly corroded. Their morphology is typical for plagiogranites and trondhjemitites (e.g., Pupin, 1985). Most of the zircons are translucent to opaque due to their high U-contents. They are either white, pink, or black. All of them are metamict, the black ones are in addition highly fractured. A minor fraction of zircons was perfectly transparent, varying in color from colorless to honey and brown. Only transparent inclusion-free zircons were analyzed, except for the Gautelis tonalite, for which no transparent zircons could be obtained.

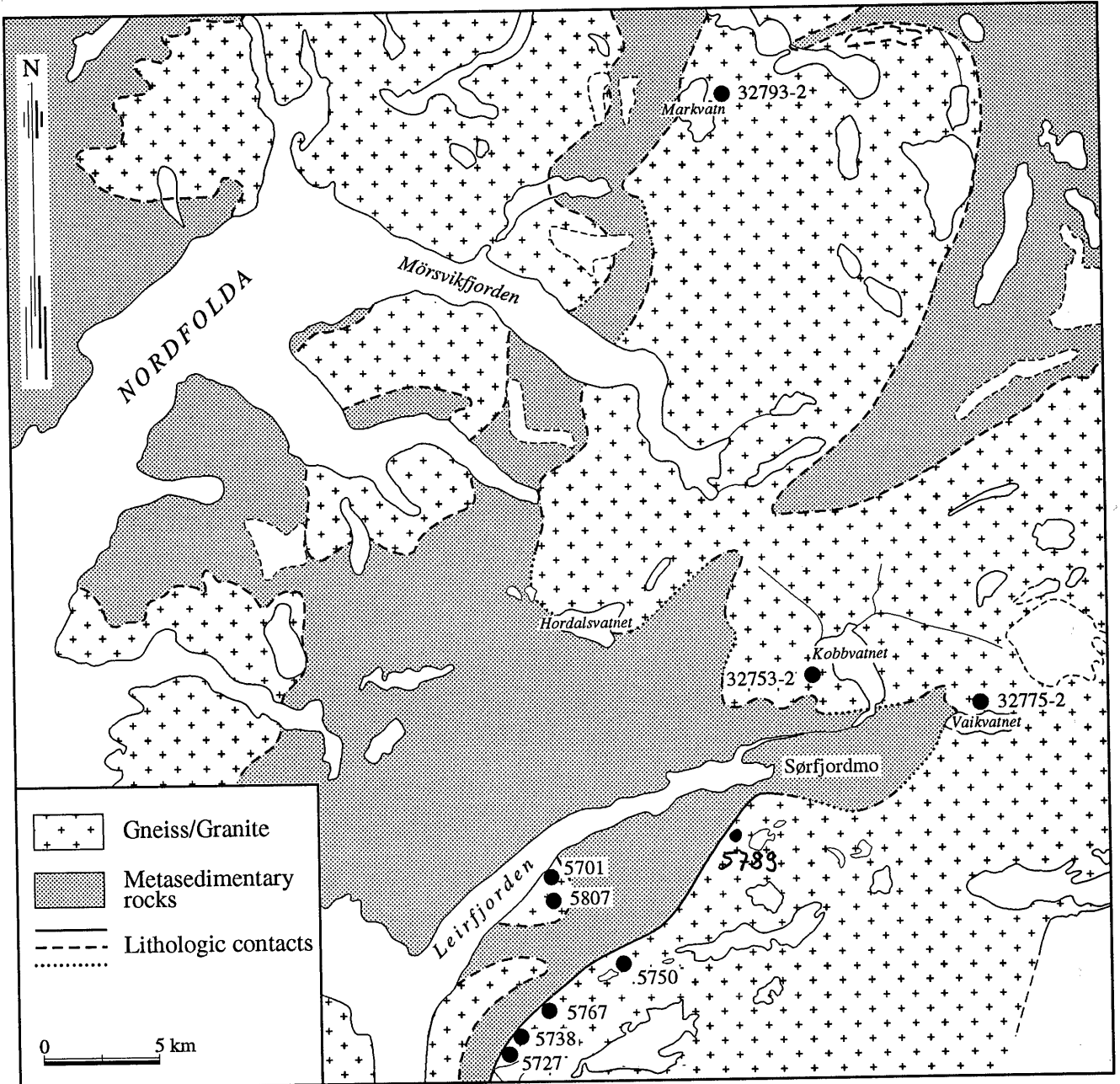


**Fig. 6:** Simplified tectonic map of the southern Tysfjord area, northern Norway (modified from Stendal, 1981).

**Sjangeli:** Zircons were separated from the two granites and the tonalitic gneiss east of Sjangeli. The transparent zircons of both the gneiss and the granites did not contain older cores. The discordia through the two points of the STB1 granite sample yields an upper intercept of  $1778 \pm 19$  Ma and a lower intercept of  $297 \pm 55$  Ma (Fig. 7c), while the two fractions from the STB5 granite sample have an upper intercept of  $1703.3 \pm 4.4$  Ma and a lower intercept of  $-3 \pm 40$  Ma (Fig. 7d). Zircons from the two granites do not fall on a common discordia.

The four analyzed fractions from the tonalitic gneiss fall to the right of the discordias for the Sjangeli granites, which indicates that the gneiss is older. Three of the four samples define a discordia with a rather large MSWD = 65. The intercepts of the discordia with the concordia curve are  $2709 \pm 323$  and  $530 \pm 627$  Ma (The  $2\sigma$  errors are multiplied by the square root of the MSWD). The zircon system of the tonalitic gneisses was affected during the Caledonian orogeny, but not during the Svecofennian magmatism and metamorphism. The fourth sample, deviating from the discordia through the zircons (Fig. 7b), is a titanite and falls between the discordias of the granites and the tonalite. The U-Pb system of the titanite probably was partially open during the Caledonian (ca 0.4 Ga) and the Svecofennian (ca 1.8 Ga) orogenies, and thus, the titanite composition falls in the concordia diagram in the triangular area defined by the 0.4, 1.8, and 2.7 Ga coordinates on the concordia curve (shaded in Fig. 7b).

**Gautelis:** The Gautelis tonalite is stratigraphically overlain by the Gautelis supracrustal belt (Skyseth and Reitan, 1990), which is a sequence of impure marbles and turbiditic psammitic to pelitic sedimentary rocks with intercalated mafic to acid volcanic rocks. The Gautelis supracrustal belt is intruded by the Gautelis granite. Zircons were separated from both the tonalite and the granite. The two analyzed inclusion-free transparent zircon fractions from the granite define a discordia of  $1769.6 \pm 9.2$  Ma.

Zircons from the Gautelis tonalite have numerous opaque inclusions. Aliquots from the two least magnetic fractions were analyzed after purification by separation by hand and a mild acid wash. They yielded highly discordant U-Pb ages (Table 1: Z-T-2 and Z-T-4). Splits of the least magnetic fractions were subjected to a strong acid leach in concentrated HF for 3 days on a hot plate. These samples were subsequently leached during 3 days with 6N HCl and twice during 3 days with 7N HNO<sub>3</sub>. Less than 1 mg remained from more than 15 mg starting material. The residual contained cores that previously were not visible in the translucent zircons. The cores have the same clear brown color and shape as the zircons from the Archaean tonalitic gneiss at Sjangeli. There is no sign of mechanical or magmatic corrosion on the cores. The cores from the two fractions were recombined to one sample, while the core free leached mantles were analyzed as two samples (Z-T-3/4L and Z-T-2L). The leaching process dissolved the metamict parts of the zircon and decreased the total contents of U and Pb (Table 1). Leaching increased the  $^{206}\text{Pb}/^{204}\text{Pb}$  ratios from 430 to 2000-6000 (Table 1). The intercept ages calculated from the four untreated zircon fractions of the Gautelis tonalite are  $1939 \pm 106$  Ma (MSWD = 68), while the addition of the three leached fractions to the data set yields  $1940 \pm 26$  Ma (MSWD = 46). The lower intercepts are  $403 \pm 54$  Ma (four samples) and  $404 \pm 18$  Ma (seven samples),

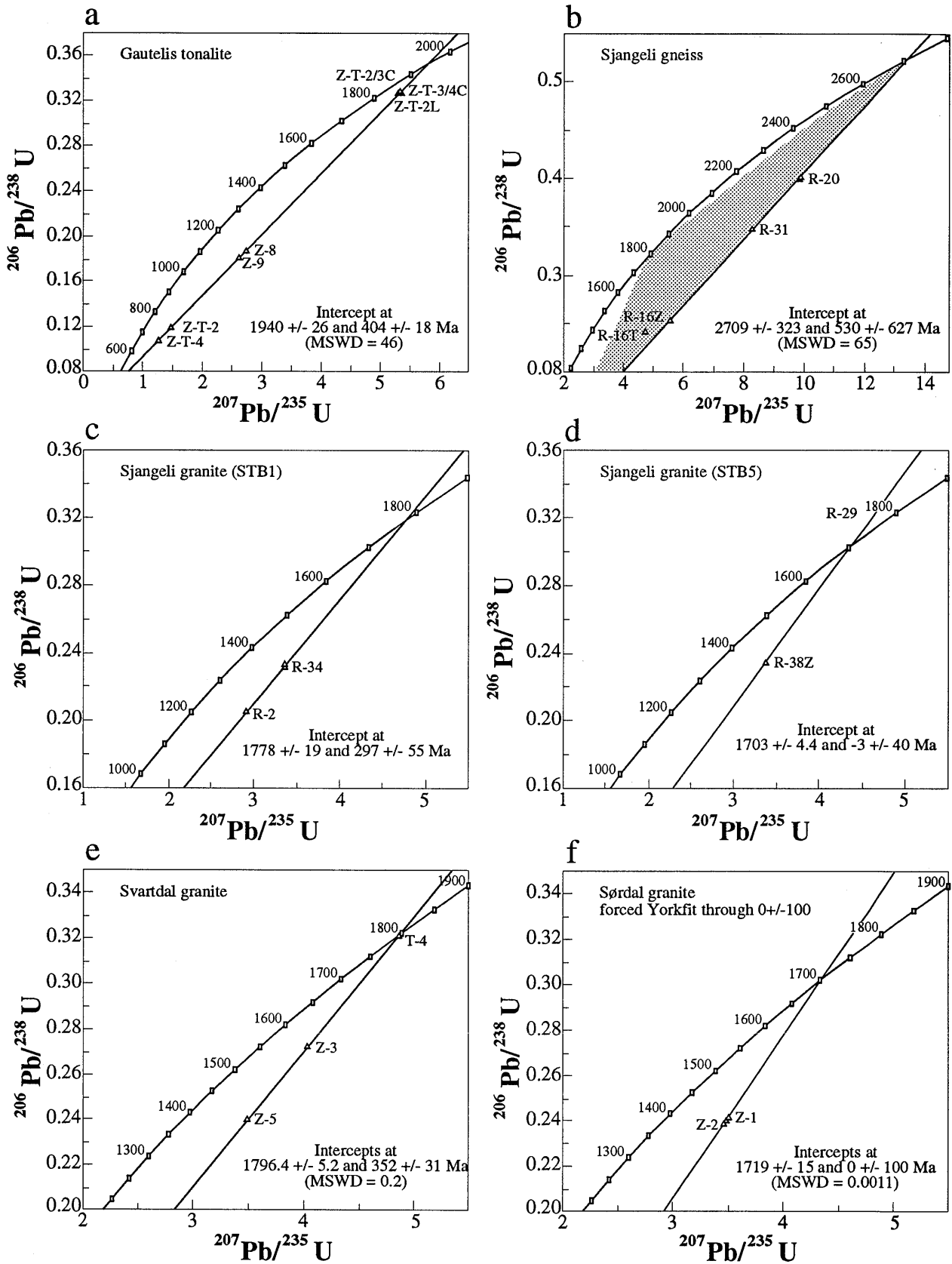


**Fig. 7:** Concordia diagram for zircons and titanites from the locations shown in Fig. 1. Intercepts and  $2\sigma$  errors were calculated with the program of Ludwig (1986). Granites fall into two age groups (pooled data in Figs. 7i and 7j).



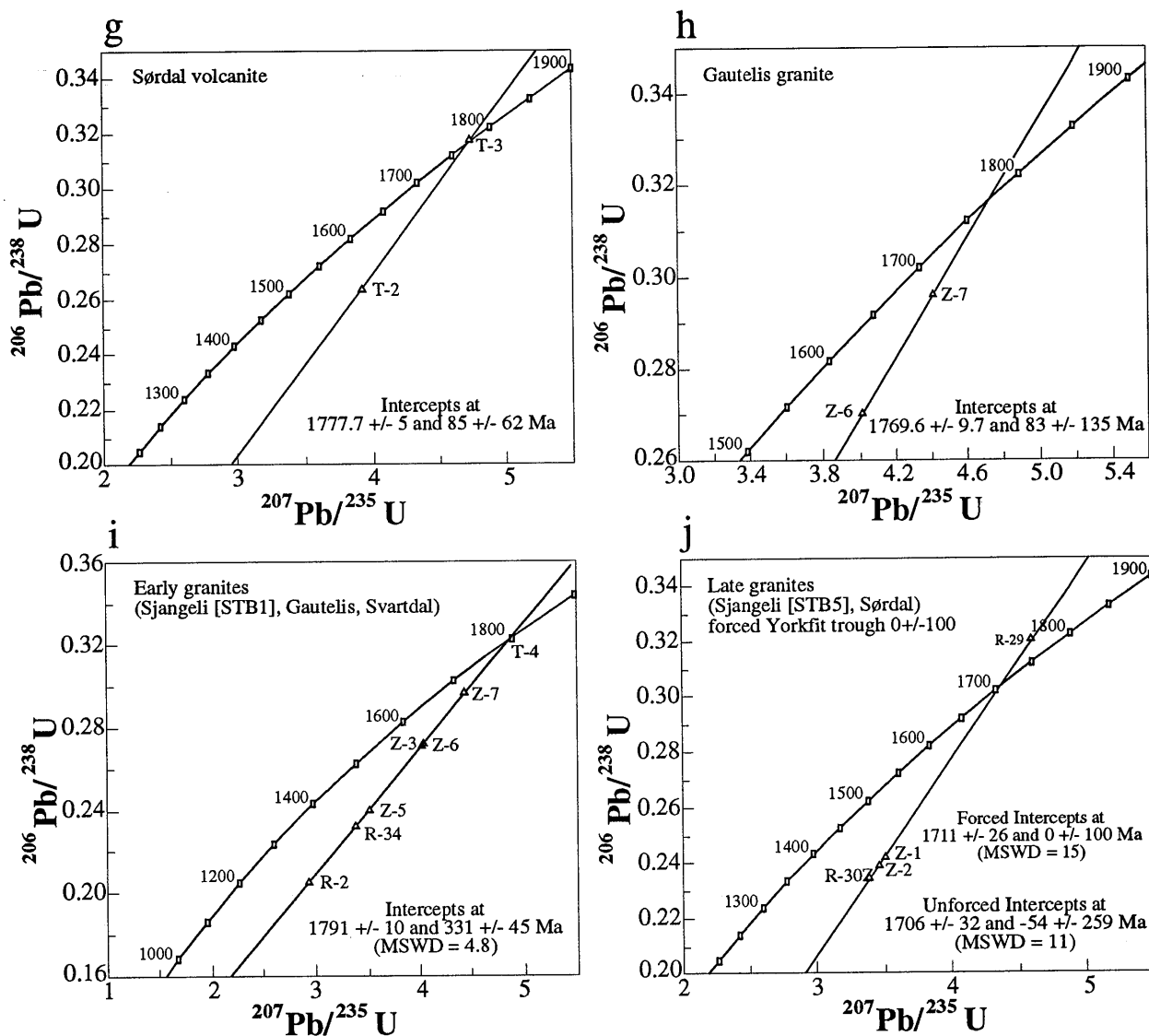


Fig. 7: Cont'd.

respectively (Fig. 7a). The coincidence of the intercepts suggests that the leaching procedure did not result in U-Pb fractionation of the undissolved material along a trajectory through the origin of the concordia diagram. The zircon mantles are related to a magmatic event or a pre-Svecofennian metamorphism at ca 1.94 Ga. Igneous rocks in the Svecofennian domain with ages close to 1.94 Ga are so far only known from the Norvijaure tonalite (Skiöld, pers. com., 1991:  $1926 \pm 13$  Ma) and from Finland (e.g., Kontinen, 1987). Tonalitic and granitoid intrusion of that age are related to volcanism and magmatism in volcanic belts and they probably represent exposed magma chambers related to the early stages of subduction related magmatism in these areas. In the Gautelis area, the tonalites are the oldest preserved rocks.

Sample	Wt. (mg)	U (ppm)	206Pb* (ppm)	measured ratios			atomic ratios			apparent ages (Ma)#		
				206Pb/204Pb	207Pb/206Pb	208Pb/206Pb	206Pb*/238U	207Pb*/235U	207Pb*/206Pb*	206*/238	207*/235	207*/206*
<b>Sørðal volcanite</b>												
T-2#	4.7	78.82	17.87	768.6	.12578	.48715	.26386	3.9349	.10816	1509.6	1620.9	1769±2 **
T-3	2.6	80.99	22.50	684.0	.12854	.46378	.32334	4.8481	.10875	1806.0	1793.3	1778±2
<b>Sørðal granite</b>												
Z-1#	1.5	325.4	67.40	658.3	.12589	.16504	.24111	3.4988	.10525	1392.5	1527.0	1719±2
Z-2#	1.0	171.6	35.16	187.4	.17776	.30684	.23850	3.4610	.10525	1378.9	1518.4	1719±2
<b>Gautelis Tonalite</b>												
Z-T-2#	1.8	847.1	85.68	444.4	.12229	.17652	.11772	1.4808	.09123	717.5	922.6	1451±2
Z-8#	<0.01	1564	250.4	222.3	.16725	.26532	.18635	2.7283	.10619	1101.5	1336.2	1735±2
Z-T-3/4L#	0.2	203.5	71.76	5380	.12163	.12893	.32673	5.3674	.11915	1822.5	1879.7	1943±2
Z-T-2/3C#	0.1	88.40	24.96	2060	.12355	.15421	.32871	5.3044	.11704	1832.1	1869.6	1911±2
Z-T-2L#	0.5	191.2	53.76	6540	.11976	.13970	.32726	5.3115	.11771	1825.1	1870.7	1921±2
Z-T-4	0.3	969.2	89.67	426.4	.11819	.16943	.10772	1.2717	.08562	659.5	833.1	1330±2
Z-9#	0.3	154.2	23.98	292.6	.15136	.21953	.18098	2.6174	.10489	1072.3	1305.5	1712±2
<b>Gautelis Granite</b>												
Z-7#	0.3	372.3	94.69	1389	.11780	.14374	.29601	4.4097	.10804	1671.5	1714.2	1767±2
Z-6	0.5	158.8	36.90	690.1	.12742	.16100	.27048	4.0197	.10779	1543.2	1638.2	1762±2
<b>Sjangeli Gneiss</b>												
R-20#	0.6	318.3	109.1	4610	.18225	.10779	.39899	9.8808	.17961	2164.3	2423.7	2649±2
R-16Z#	0.4	539.1	117.4	2960	.16397	.11937	.25347	5.5835	.15977	1456.3	1913.6	2453±2
R-31#	0.2	292.1	87.16	4020	.17519	.09817	.34740	8.2449	.17213	1922.2	2258.3	2578±2
R-16T#	0.4	155.2	32.70	1215	.15466	.17168	.24524	4.8771	.14424	1413.9	1798.3	2279±2
<b>Sjangeli Granite (STB1)</b>												
R-34#	0.4	281.6	56.20	1670	.11326	.11436	.23228	3.3661	.10510	1346.5	1496.5	1716±2
R-4T	0.1	26.15	4.359	214.4	.17008	.21368	.19400	2.8569	.10680	1143.0	1370.6	1746±2
R-2	1.3	29.76	5.236	197.9	.17213	.23903	.20478	2.9166	.10330	1200.9	1386.2	1684±2
<b>Sjangeli Granite (STB5)</b>												
R-29	0.3	222.2	61.94	796.2	.12145	.14970	.32448	4.6694	.10436	1811.7	1761.8	1703±2
R-30Z	0.4	305.3	61.55	418.6	.13690	.19627	.23467	3.3780	.10440	1358.9	1499.3	1704±2
<b>Svartdal Granite</b>												
Z-3	0.4	133.3	31.04	2793	.112411	.147180	.27112	4.0207	.107559	1546.5	1638.4	1758±2
Z-5	0.6	200.6	41.22	1930	.112792	.148226	.23918	3.4876	.105757	1382.4	1524.4	1728±2
T-4	0.6	135.2	37.22	714.8	.128721	.189953	.32041	4.8511	.109807	1791.7	1793.8	1796±2

Table 1: Uranium-lead isotopic data of zircons and titanites.

# # with 205Pb isotopic tracer

\* denotes radiogenic Pb, corrected for common Pb using the isotopic composition of 206Pb/204Pb = 15.3 and 207Pb/204Pb = 15.2 for Proterozoic zircons and titanites and 206Pb/204Pb = 13.5 and 207Pb/204Pb = 14.6 for Archaean ones. Total Pb processing blanks were less than 160 pg.

# ages calculated using the following constants: decay constant for 235U and 238U = 9.8485E-10 yr-1 and 1.55125E-10 yr-1, respectively; 238U/235U = 137.88.

\* \* The two-sigma uncertainties in the 207Pb\*/206Pb\* ages were calculated from the combined uncertainties in mass spectrometry (principally the uncertainty in the 206Pb/204Pb measured ratios) and an assumed uncertainty of ± 0.1 in the 207Pb/204Pb ratio used for the common lead correction.

**Sørdal:** The two analyzed samples from the Sørdal area include zircons from a granite and of titanites from intermediate volcanic rocks that were intruded by various granites. The zircons frequently had minor inclusions of ilmenite or hematite. The two analyzed transparent, inclusion-free zircon fractions have similar  $^{206}\text{Pb}^*/^{238}\text{U}$  and  $^{207}\text{Pb}^*/^{235}\text{U}$  ratios. The calculated age has, therefore, large uncertainties ( $1718 \pm 225$  Ma). As this age is identical with the apparent  $^{207}\text{Pb}^*/^{206}\text{Pb}^*$  age ( $1718 \pm 3$  Ma, Table 1) of both zircon fractions, the regression line through these samples was forced through the origin of the concordia diagram, which yielded a more constrained upper intercept of  $1719 \pm 15$  Ma (Fig. 7f). The very low MSWD value (MSWD = 0.0011) indicates that the forced fit, which assumes that the discordancy in the U-Pb system is solely due to recent lead loss, is a good approximation to the real conditions. An alternative fit through  $400 \pm 100$  Ma yields a poorer fit of the regression line (MSWD = 1.03) and an upper intercept ( $1798 \pm 28$  Ma). Although both upper intercept ages fall in the range obtained from other granites in the Rombak-Sjangeli window, we prefer the younger upper intercept age ( $1719 \pm 15$  Ma), as the dated Sørdal granite has the same trace element signature as other younger generation granites from the Rombak-Sjangeli basement culmination.

Titanites formed during the amphibolite facies metamorphism of intermediate volcanic rocks of the Sørdal area. Two transparent inclusion-free titanite fractions, one of which is slightly inverse discordant define an upper intercept age of  $1777.7 \pm 5$  Ma (Fig. 7g). This age probably represents the age of the amphibolite facies metamorphism of this supracrustal belt as it falls in the age range of the volumetrically dominant older granites (ca 1770 - 1790 Ma, see Fig. 7). Furthermore, the Sørdal supracrustal belt was probably in time and genetically related to the nearby Gautelis supracrustal belt, which is intruded and metamorphosed by ca 1.77 Ga old granites.

**Svardal:** Most zircons from the Svardal granite are honey colored, translucent tetragonal prismatic, crystals. Only few zircons were perfectly transparent. The two analyzed zircon fractions and the titanite fraction were perfectly transparent and core-free. The titanite is almost concordant, while the zircon fractions are variably discordant. The three samples fall on the same discordia (MSWD = 0.2) which intersects the discordia at  $1796.4 \pm 5.2$  Ma and  $352 \pm 31$  Ma (Fig. 7e).

**Pooled discordia lines:** The zircon and titanite data from the various granites strongly suggest that there occur two generations of granitoids in the Rombak-Sjangeli area. Pooling the zircon data from the older granites, that comprise the Svardal, Gautelis, and older Sjangeli granite (Fig. 7i), yield intercepts at  $1791 \pm 10$  Ma and  $331 \pm 45$  Ma (MSWD = 4.8). The younger granites include the Sørdal and the younger Sjangeli granite (Fig. 7j). Their pooled zircon data yield intercepts at  $1706 \pm 32$  Ma and  $-54 \pm 259$  Ma (MSWD = 11). Apart from the slight difference of the upper intercepts, the two discordia lines differ in their lower intercept. The older granites were affected by lead loss during the Caledonian orogeny at 400 Ma, while the younger granites were not affected by this event. The sampling sites for both groups of granites were similarly close to the Caledonian thrust plane and both groups of granites were locally affected by brittle to ductile deformation during the Caledonian orogeny. The contrasting response of zircons to the Caledonian orogeny probably reflects different U

contents of the analyzed zircons from the two kinds of granites. The analyzed zircons of the older granite generation have U contents around 300 ppm, while zircons of the younger granite generation have U contents from 30 to 200 ppm (Table 1). Due to their higher U contents, the zircons of the older granite generation had acquired considerable more lattice damage by 400 Ma and probably lost radiogenic lead more readily than the low-U zircons from the younger granites.

**Rb-Sr results:** Earlier Rb-Sr dating of granites from the Rombak-Sjangeli area (Heier and Compston, 1969) and Gunner (1981) comprised samples from the northern and the whole Rombak-Sjangeli window, respectively. The reported ages were  $1691 \pm 85$  Ma and  $1780 \pm 85$  Ma (both at  $1\sigma$  level). The strong scatter of the data and the anomalous low  $^{87}\text{Sr}/^{86}\text{Sr}$  initial ratio (0.700) suggest that the systems were either disturbed, for instance during the Caledonian orogeny, or that the sample set included non-cogenetic granitic intrusions of different age or different  $^{87}\text{Sr}/^{86}\text{Sr}$  initial composition. U-Pb zircon data indicate the presence of two generations of granite, as well as an older tonalite, and an Archaean gneiss. We sampled several granites for Rb-Sr whole-rock dating to investigate, whether the whole-rock systems became disturbed during the Caledonian orogeny and if the initial Sr-isotopic compositions were homogeneous. The Rb-Sr whole-rock data, with exception of the Kvaløya data, yield ages that are too young in comparison to the U-Pb zircon ages. The data further scatters widely suggesting that the isotopic systems were disturbed. As the recalculation of the strontium isotopic composition to the U-Pb zircon age in part yields impossible values, there must have been a post-crystallization change of the Rb/Sr ratio of some of these samples. A gain of rubidium and/or loss of radiogenic strontium can explain most of the disturbance of the data (impossible initial strontium compositions, too low ages, scatter of the data about the regression line in the isochron diagram). However, some of the non-ideality of the systems might also be due to a heterogeneous strontium isotopic composition at the time the granites formed. Inclined trends in the  $^{87}\text{Sr}/^{86}\text{Sr}$  (T) -  $1/\text{Sr}$  mixing diagram (T = time, at which the system was established) suggest such a heterogeneity (Faure, 1986). The sample suites that yield inclined mixing lines originate from the Svartdal and the Stasjonsholmen granites. Field evidence from the Stasjonsholmen granite also suggests such a magma mixing origin of these rocks (Fig. 4).

**Gautelis:** Eleven samples from the Gautelis tonalite have a very limited variation of the  $^{87}\text{Rb}/^{86}\text{Sr}$  ratio (0.135 to 0.705, Table 2) and they scatter widely (Figs. 8a and 8b) about a regression line (all points, equally weighted) that yields a reference date of 1510 Ma. This date is lower than the U-Pb zircon age, indicating that the Rb-Sr system either was open during the Caledonian orogeny or was heterogeneous when established. The slightly gneissic nature and the presence of secondary epidote in several samples indicate a later disturbance of the Rb-Sr system. A recalculation of the strontium isotopic composition to the U-Pb zircon age yields  $^{87}\text{Sr}/^{86}\text{Sr}$  ratios in the range 0.7026 to 0.7080 (Fig. 8d). None of the calculated initial isotopic compositions falls below the BABI strontium composition (Papanastassiou and Wasserburg, 1969), which suggests, that this later disturbance did not significantly change the Rb/Sr ratio in the samples. For instance, a Caledonian Rb gain would result in extremely low apparent  $^{87}\text{Sr}/^{86}\text{Sr}$  initial ratios and a Caledonian Rb loss would

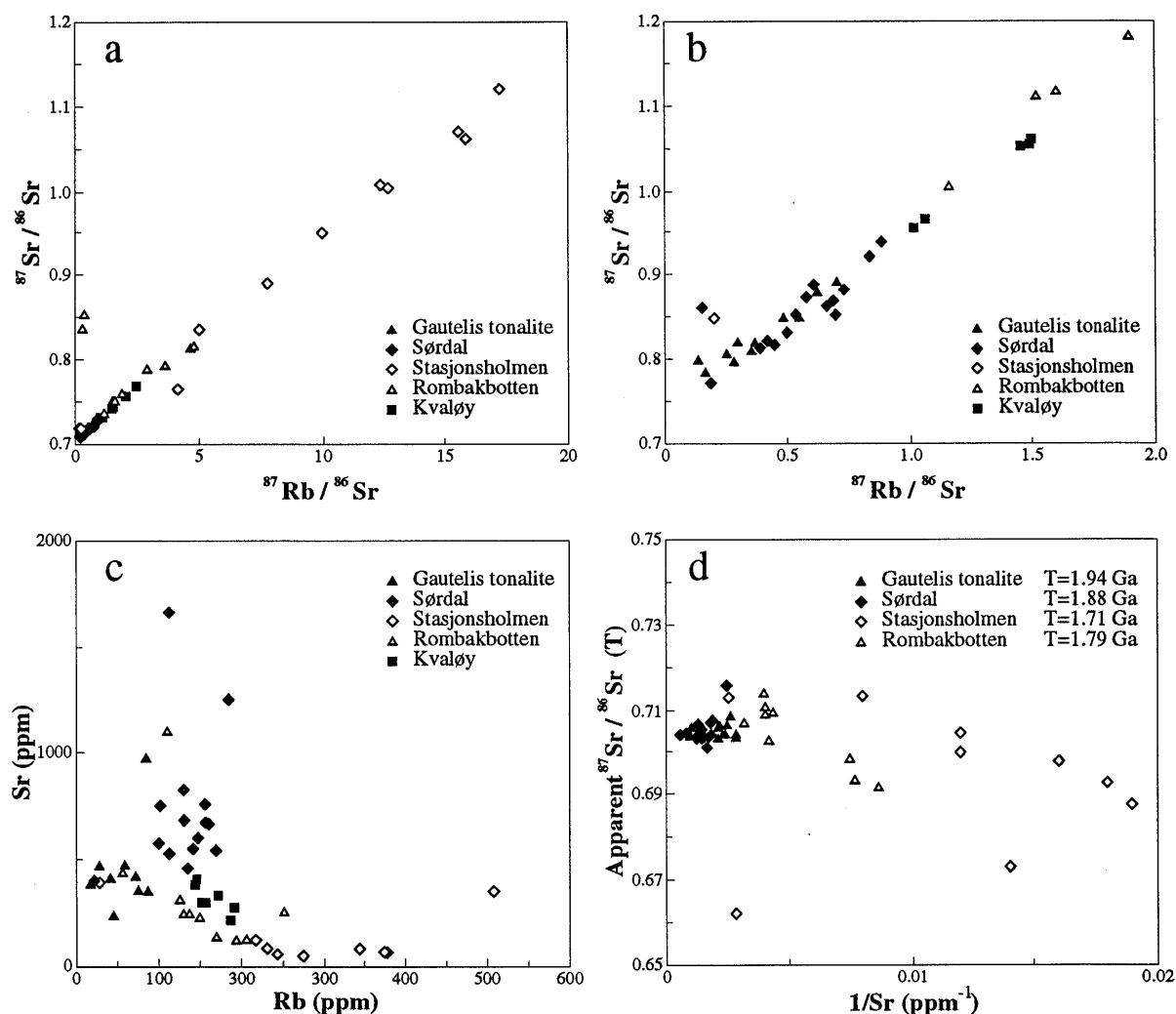


**Fig. 8:**  $^{87}\text{Sr}/^{86}\text{Sr}$  -  $^{87}\text{Rb}/^{86}\text{Sr}$  correlation diagram for Early Proterozoic plutonic rocks from the Rombak-Sjangeli and Kvaløya windows within the northern Scandinavian Caledonides. For sample locations see Figs. 1, 2, and 5.

yield very radiogenic apparent  $^{87}\text{Sr}/^{86}\text{Sr}$  initial ratios. The too low Rb-Sr age could be due either to partial homogenization of the  $^{87}\text{Sr}/^{86}\text{Sr}$  of the samples at Caledonian time or to a heterogeneous initial strontium isotopic composition. If a partial homogenization of the strontium isotopic composition did not change the Rb/Sr ratio of the various samples, this process will lead to decreased ages and excessive scatter (Roddick and Compston, 1977).

**Sørdal:** Similarly to the Gautelis Rb-Sr whole-rock system, the whole-rock Rb-Sr whole-rock system from the intermediate volcanic rocks at Sørdal does not define an isochron (Figs. 8a and 8b). Regression through all samples yields a reference line corresponding to a date of 1345 Ma, while the omission of two samples yields a reference line corresponding to a date of 1878 Ma. This second date is higher than the age of the granite that intrudes the Sørdal supracrustal belt and it is lower than the age of the Gautelis tonalite that is underlying the Gautelis supracrustal belt,

**Gautelis (Tonalite)**

sample	$^{87}\text{Sr}/^{86}\text{Sr}$	$^{87}\text{Rb}/^{86}\text{Sr}$	Rb (ppm)	Sr (ppm)	$^{87}\text{Sr}/^{86}\text{Sr}$ (T=1.94 Ga)
TS84/43	0.714230	0.2945	42.52	409.82	.7060
TS85/44	0.717850	0.5467	45.51	236.38	.7026
TS86A/45	0.713040	0.3578	59.17	469.41	.7030
TS86B/46	0.710120	0.1664	27.35	466.38	.7055
TS87/47	0.717780	0.4876	71.48	416.24	.7042
TS69/50	0.721620	0.6251	76.78	348.90	.7042
TS90/51	0.711760	0.1352	18.28	383.77	.7080
TS91/52	0.722740	0.7048	86.97	350.56	.7031
TS93/54	0.714420	0.3718	56.75	433.26	.7040
TS95/55	0.711600	0.2855	110.5	1098.0	.7036
TS105/64	0.712570	0.2525	86.06	967.22	.7055

**Sørdal (intermediate volcanic rock)**

sample	$^{87}\text{Sr}/^{86}\text{Sr}$	$^{87}\text{Rb}/^{86}\text{Sr}$	Rb (ppm)	Sr (ppm)	$^{87}\text{Sr}/^{86}\text{Sr}$ (T=1.88 Ga)
K71.84	0.708560	0.1917	112.61	1666.7	.7033
K74.84	0.720720	0.5818	156.72	765.09	.7050
K77.84	0.728630	0.8813	169.29	546.02	.7048
K79.84	0.722530	0.6054	113.21	531.24	.7062
K81.84	0.714630	0.4170	184.55	1256.3	.7033
K134.84	0.713640	0.3909	103.24	749.68	.7031
K135.84	0.720410	0.6893	161.92	667.16	.7018
K142.84	0.714090	0.4504	130.86	824.75	.7019
K143.84	0.718440	0.6978	148.61	604.78	.6996
K144.84	0.718360	0.5385	130.37	687.45	.7038
K145.84	0.715780	0.5008	101.14	573.28	.7022
K149.84	0.719620	0.6593	158.03	680.72	.7018
K155.84	0.726540	0.8347	135.63	461.77	.7040
K164.84	0.719270	0.1545	22.04	405.10	.7151
K165.84	0.721880	0.7307	142.3	553.16	.7021

**Table 2:** Whole rock Rb-Sr isotopic data from granites and tonalites of the Rombak-Sjangelj and Kvaløya basement culminations. The initial strontium isotopic composition is calculated for the U-Pb zircon age of the plutonic rocks assuming an undisturbed system. Values less than BABI (0.69898; Papanastassiou and Wasserburg, 1969) indicate a disturbed system and require later Rb-gain or radiogenic Sr-loss.

# initial strontium isotopic composition calculated for 0.4 Ga.

**Svardal (Rombakfjord; granite)**

sample	$^{87}\text{Sr}/^{86}\text{Sr}$	$^{87}\text{Rb}/^{86}\text{Sr}$	Rb (ppm)	Sr (ppm)	$^{87}\text{Sr}/^{86}\text{Sr}$ (T=1.79 Ga)
KR30.88	0.852460	0.3769	56.75	433.26	.8428#
KR31.88	0.835130	0.2890	110.47	1098.0	.8277#
KR32.88	0.815050	4.777	193.26	115.98	.6921
KR33.88	0.812320	4.616	208.05	129.17	.6935
KR34.88	0.792390	3.639	169.64	133.33	.6987
KR37.88	0.788150	2.885	253.18	250.88	.7139
KR38.88	0.757830	1.886	151.13	228.42	.7093
KR39.88	0.736490	1.155	127.37	313.63	.7067
KR40.88	0.749950	1.595	136.46	243.65	.7089
KR41.88	0.749300	1.510	130.29	245.69	.7104

**Stasjonsholmen (Granite)**

sample	$^{87}\text{Sr}/^{86}\text{Sr}$	$^{87}\text{Rb}/^{86}\text{Sr}$	Rb (ppm)	Sr (ppm)	$^{87}\text{Sr}/^{86}\text{Sr}$ (T=1.71 Ga)
KR1.88	1.003280	12.58	244.33	56.70	.6941
KR2A.88	1.120720	17.13	373.05	64.31	.6998
KR2B.88	1.008070	12.30	343.04	81.46	.7058
KR2C.88	1.062470	15.77	378.27	70.44	.6750
KR3.88	0.836810	5.009	217.55	124.76	.7137
KR4.88	0.891270	7.745	231.37	86.28	.7009
KR5B.88	1.070670	15.51	274.60	52.03	.6895
KR5C.88	0.717840	.2051	28.48	394.28	.7128
KR5D.88	0.764290	4.136	508.54	350.70	.6626

**Kvaløya (Granite)**

sample	$^{87}\text{Sr}/^{86}\text{Sr}$	$^{87}\text{Rb}/^{86}\text{Sr}$	Rb (ppm)	Sr (ppm)	$^{87}\text{Sr}/^{86}\text{Sr}$ (T=1.78 Ga)
KR9.88	0.730700	1.010	146.67	412.89	.7048
KR10A.88	0.743300	1.488	173.44	331.88	.7052
KR11.88	0.742520	1.481	156.13	300.13	.7046
KR12.88	0.731910	1.060	143.03	383.83	.7048
KR14.88	0.768790	2.493	187.65	214.77	.7050
KR15.88	0.755880	1.998	192.07	273.98	.7047
KR16.88	0.742220	1.445	153.69	302.72	.7052

Table 2: Cont'd.

which probably is coeval with the Sørdal volcanic belt. The obtained date of 1878 Ma could therefore be close to the correct age of the volcanic belt. The two omitted samples have higher Sr contents than the other Sørdal samples (Fig. 8c). The recalculated strontium isotopic compositions for 1.88 Ga (0.7018 to 0.7062, Fig. 8d) fall close to the range of the Gautelis tonalite. In contrast, the two samples omitted from the reference line give apparent initial  $^{87}\text{Sr}/^{86}\text{Sr}$  of 0.6996 and 0.7151, respectively, which suggests that these two samples probably suffered from later changes of their Rb/Sr ratio.

**Stasjonsholmen:** The Stasjonsholmen granite samples define a reference line corresponding to a date of 1659 Ma, which is lower than the estimated age of ca 1.71 Ga (in analogy to the Sørdal and Sjangeli samples). Two of the samples, that originate from Caledonian deformed parts of the granite, were omitted from the reference line, as their strongly radiogenic strontium isotopic composition at low  $^{87}\text{Rb}/^{86}\text{Sr}$  strongly suggests a later disturbance (Fig. 8a). These two excluded samples have lost Rb or received highly radiogenic strontium. Their distinctly higher Sr contents indicate the addition of radiogenic Sr (Fig. 8a). Highly radiogenic Sr compositions were also observed in other Caledonian deformed Early Proterozoic rocks. For instance, variably Caledonian sheared marbles from the Sjangeli greenstone belt (Fig. 2) have  $^{87}\text{Sr}/^{86}\text{Sr}$  varying from 0.7061 to 0.7649 (Romer, unpubl. data) and two Caledonian pseudotachylytes yield initial  $^{87}\text{Sr}/^{86}\text{Sr}$  of 0.830 and 0.805, respectively (Bax, unpubl. data). These data indicate, that highly radiogenic strontium was mobilized during the Caledonian orogeny and transported and precipitated along permeable deformation zones.

The recalculation of the strontium isotopic composition of the samples to 1.71 Ga yields impossible values suggesting that these rocks were no closed systems with respect to Rb and Sr, but instead experienced marked losses of radiogenic Sr or gains of Rb at some later time, such as the Caledonian orogeny. The selective loss of radiogenic Sr from minerals such as biotite could provide the radiogenic strontium observed in the marbles at Sjangeli, the pseudotachylytes, and the two excessively radiogenic Stasjonsholmen samples.

**Svartdal:** The Svartdal Rb-Sr whole-rock data define a reference line yielding a date of 1454 Ma, which compares unfavorably with the  $1796.4 \pm 5.2$  Ma U-Pb zircon age. Recalculation of the Rb-Sr data to 1.79 Ga yields for most samples impossible initial strontium isotopic compositions, which indicates that these samples have lost radiogenic strontium or increased their Rb/Sr ratio.

**Kvaløya:** The Rb-Sr whole-rock sample suite from Kvaløya is the only sample set presented here that defines a statistically valid isochron. The age of  $1779 \pm 17$  Ma ( $2\sigma$ ; MSWD = 0.456) falls within the range of TGPB granites (e.g., Jarl and Johansson, 1988), and the obtained initial of 0.7048 suggests a short crustal residence time of the protoliths before the granite formation. Earlier Rb-Sr whole-rock dating of the Ersfjord granite on Kvaløya yielded  $1706 \pm 15$  Ma ( $1\sigma$ , Andresen, 1980). The  $1706 \pm 15$  Ma and  $1779 \pm 17$  Ma Rb-Sr whole-rock ages differ beyond analytical uncertainties. The contrasting ages suggest that the Ersfjord granite could consist of two differently aged intrusions, similarly to the Sjangeli granite. Similar Rb-Sr whole-rock ages were obtained from other TGPB granites (Fig. 1): Granitic



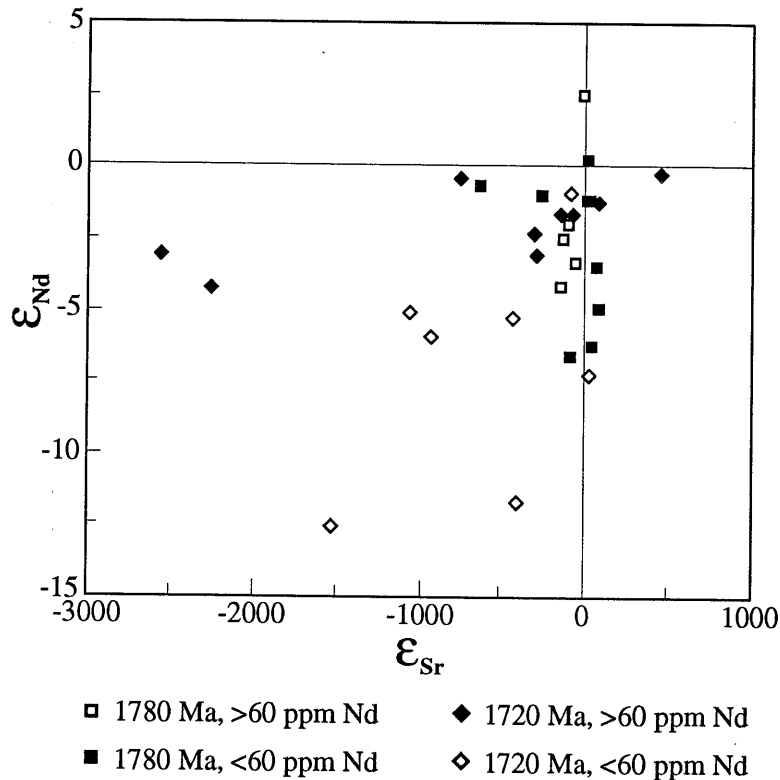


**Fig. 9:**  $\epsilon_{\text{Sr}}(T)$  vs.  $\epsilon_{\text{Nd}}(T)$  diagram for granites from Kvaløya to Sjona. Unaltered rocks should fall on a trend with a negative slope in the quadrant at the lower right side. Note the anomalously negative values for  $\epsilon_{\text{Sr}}(T)$ .

rocks from the Senja Island gave  $1746 \pm 93$  Ma and  $1768 \pm 49$  Ma, respectively (Krill and Fareth, 1984). The Tysfjord granite was dated at  $1742 \pm 46$  Ma (Andresen and Tull, 1986; Rb-Sr WR,  $2\sigma$ ) and the Middagstind quartz syenite was dated at  $1726 \pm 97$  Ma (Bartley, 1981; Rb-Sr WR,  $2\sigma$ ).

**$\epsilon_{\text{Sr}}(T)$  results:**  $\epsilon_{\text{Sr}}(T)$  are calculated from the isotopic composition of Sr, the  $^{87}\text{Rb}/^{86}\text{Sr}$  ratio, and the known age of the rock, if the system was not disturbed at a later time.  $\epsilon(T)$  values measure the deviation of a reservoir from a reference reservoir, which in the case of  $\epsilon_{\text{Sr}}$  and  $\epsilon_{\text{Nd}}$  is the Earth's chondritic mantle. As Rb is more enriched than Sr during crust generating processes, crustal rocks will with time develop positive  $\epsilon_{\text{Sr}}$  values. In contrast, rocks evolving in a reservoir, that is strongly depleted in Rb, will develop negative  $\epsilon_{\text{Sr}}$  values with time.

A rock suite consisting of mantle rocks that has experienced variable amounts of crustal contamination will fall in the  $\epsilon_{\text{Nd}} - \epsilon_{\text{Sr}}$  diagram on a hyperbolic trend from positive  $\epsilon_{\text{Nd}}$  at weakly negative  $\epsilon_{\text{Sr}}$  to distinctly negative  $\epsilon_{\text{Nd}}$  at highly positive  $\epsilon_{\text{Sr}}$ . The samples from the basement culminations of the Caledonides fall dominantly in the field of negative  $\epsilon_{\text{Sr}}$  values at negative  $\epsilon_{\text{Nd}}$  values (Fig. 9). Since Sm and Nd are rather immobile during metamorphic processes and do not fractionate much, the negative  $\epsilon_{\text{Nd}}$  values indicate the presence of an older crustal component at 1.8 Ga. In contrast, Sr

and Rb can strongly fractionate during metamorphic and magmatic processes. The negative  $\epsilon_{Sr}(T)$  demonstrates that the system became disturbed at some later time, e.g., during the Caledonian orogeny.

High-grade metamorphism would result in the depletion of Rb relative to Sr, and thus Rb-depleted rocks will develop negative  $\epsilon_{Sr}$  with time. The obtained  $\epsilon_{Sr}$  values (Table 3) are, however, too negative to be explained by the involvement of an older high-grade metamorphosed crust in the source of the ca 1.7-1.8 Ga granites. The alternative explanation is that the Rb/Sr ratio of rocks was altered later or that these rocks lost radiogenic strontium. Increased Rb/Sr or  $^{87}Sr$  loss would result in very negative  $\epsilon_{Sr}$  values. These two possibilities also could account for the too low apparent ages of the Rb-Sr isochrons (see above) and the too low  $^{87}Sr/^{86}Sr$  initial composition.

**$\epsilon_{Nd}(T)$  results:**  $\epsilon_{Nd}(T)$  of granites from Kvaløya in the north to Sjøna in the south vary from +2.5 to -12.6 (Table 3).  $T$  ranges from 1.71 to 1.78 Ga. The Early Proterozoic mantle had  $\epsilon_{Nd}(T=1.8 \text{ Ga})$  values close to +4 (Huhma, 1986), while Archaean crustal rocks had  $\epsilon_{Nd}(T=1.8 \text{ Ga})$  close to -12 (Skiöld et al., 1988). Positive  $\epsilon_{Nd}(T)$  values suggest that the protolith of the granites did not include large quantities of Archaean felsic crust and that the Sm/Nd ratio of the protolith did not change from the Sm/Nd ratio of the mantle a long time before the formation of the granites. In contrast, strongly negative  $\epsilon_{Nd}(T)$  values indicate the involvement of older (Archaean) felsic crust in the source of the granite. The contribution of older felsic crust is increasingly higher with more negative  $\epsilon_{Nd}(T)$  values. At  $\epsilon_{Nd}(T) \approx -12$ , the granite consists predominantly of reworked felsic Archaean crust. The  $\epsilon_{Nd}(T)$  values of both the older and the younger granites vary over a wide range, suggesting that both groups of granites involved variable amounts of old crustal rocks. The  $\epsilon_{Nd}(T)$  of the ca 1.78 Ga granites ranges from +2.5 at Kvaløya to -6.6 at Glomfjord (Fig. 10). The  $\epsilon_{Nd}(T)$  of the ca 1.72 Ga granites varies from 0.0 to -12.6 (Table 3). The younger granites involved in average larger amounts of older crustal material in their source than the older granites. However, there is a very wide range of overlap in  $\epsilon_{Nd}(T)$  values (Fig. 10).

## 6. Geochemistry and petrology of the Early Proterozoic granitoids

Geochemically, the granitoids fall into two main groups. One group comprises the 2.7 Ga and 1.94 Ga old tonalites and trondhjemites at Sjangeli and at Gautelis, respectively, while the other group comprises 1.71 Ga and 1.79 Ga old granites. The variation of  $SiO_2$  spans similar ranges in both rock suites: 60 to 77 wgt% for the tonalites and trondhjemites and 61 to 79 wgt% for the granites (Fig. 11). The trondhjemites and tonalites have lower  $K_2O$  and Rb contents and higher contents of  $Na_2O$ , CaO and MgO than the granites (Fig. 11). Because of the contrasting alkali and earth-alkali element contents, the trondhjemites and tonalites have higher  $CaO/(Na_2O+K_2O)$  ratios than the granites (Fig. 11h). The tonalites and trondhjemites are most clearly separated from the granites in diagrams involving trace and alkali

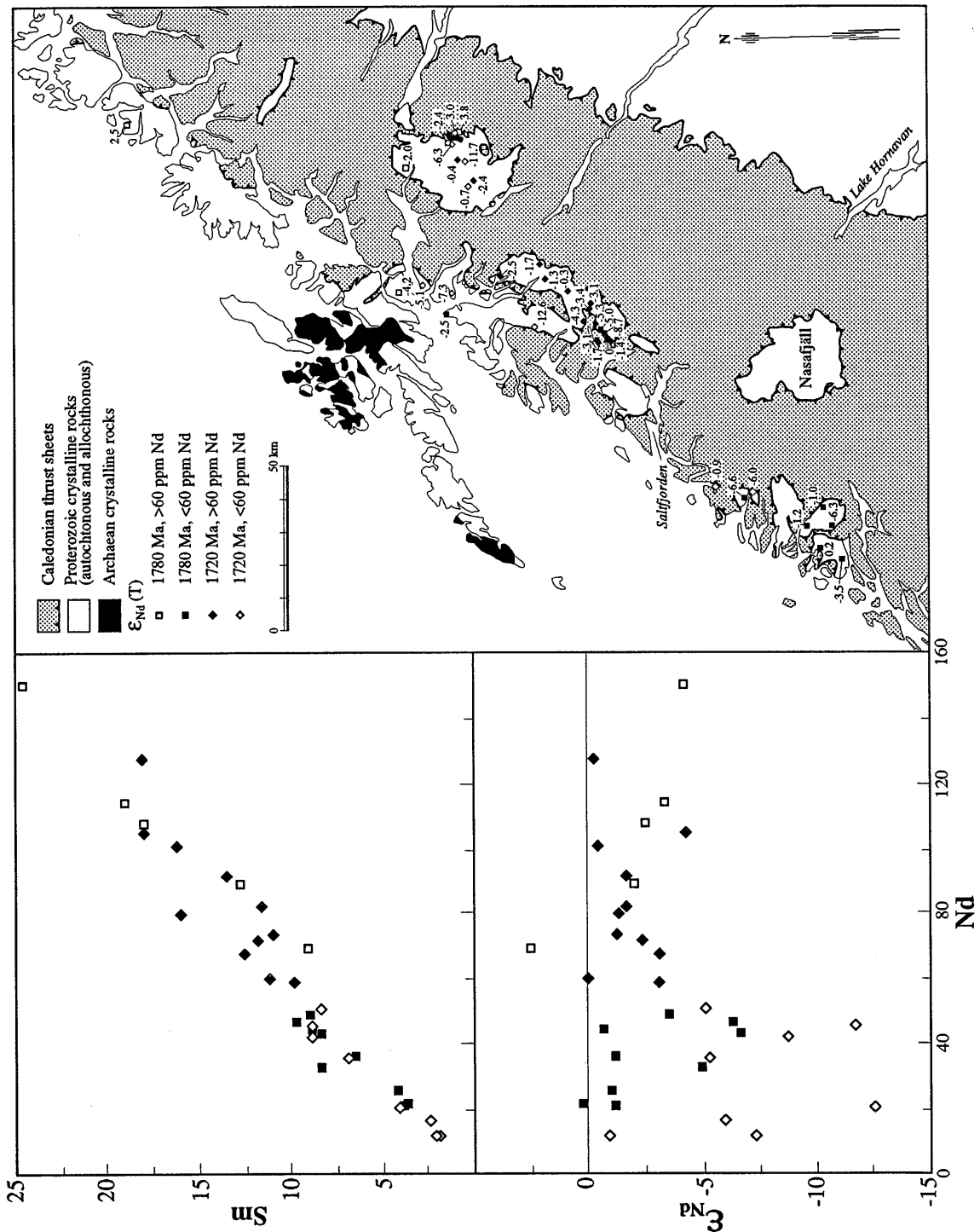


**Fig. 10:** Sm-Nd and  $\epsilon_{Nd}(T)$ -Nd diagram for granites from Kvaløya to Sjøna. Note the contrasting behavior of  $\epsilon_{Nd}(T)$  for the two granite generations at Nd contents above and below 60 ppm. Above 60 ppm Nd, the  $\epsilon_{Nd}(T)$  variation coincides, while at Nd contents less than 60 ppm, the  $\epsilon_{Nd}(T)$  for the younger generation of granites is markedly more negative. Geographic distribution of  $\epsilon_{Nd}(T)$  does not show systematic variations.

Sample	Sr	Rb	$^{87}\text{Sr}/^{86}\text{Sr}$	$^{87}\text{Rb}/^{86}\text{Sr}$	Nd	Sm	$^{143}\text{Nd}/^{144}\text{Nd}$	$^{147}\text{Sm}/^{144}\text{Nd}$	T	$\epsilon_{\text{Sr}}$	$\epsilon_{\text{Nd}}$
Archaean gneisses at Sjangeli											
STE2	329.3	75.0	0.73712	0.677	18.79	3.737	0.510856	0.1215	1780	247	-17.7
STF2	137.3	32.7	0.73343	0.707	82.16	11.71	0.510699	0.0870	1780	184	-12.8
I1	147.5	63.7	0.73764	1.28	26.96	3.627	0.510607	0.0822	1780	35.1	-13.5
Older granites from the Kvaløya, Rombak-Sjangeli, and Tysfjord basement culminations											
HS-5750	177.9	193.7	0.78812	3.113	32.63	8.363	0.511462	0.1179	1780	942.5#	-5.0
HS-32775-2	704.1	353.4	0.73432	1.427	113.8	19.02	0.511345	0.1011	1780	-65.8	-3.4
KR13.88	433.2	168.7	0.72965	1.107	69.08	9.142	0.511400	0.0800	1780	-15.6	2.5
KG3.88	157.6	188.2	0.78322	3.412	43.31	8.364	0.511362	0.1167	1780	-93.0	-6.6
KR33.88	130.2	207.8	0.81255	4.572	88.75	12.79	0.511251	0.0871	1780	-98.2	-2.0
IL88007	98.16	275.2	0.89979	8.103	150.4	24.57	0.511276	0.0987	1780	-143	-4.2
IL890142	158.7	115.7	0.75788	2.078	21.04	3.915	0.511715	0.1125	1780	32.4	1.2
IL890195	119.8	269.4	0.85887	6.471	107.5	18.00	0.511394	0.1013	1780	-131	-2.5
IL870320	220.6	222.1	0.77836	2.875	46.83	9.694	0.511478	0.1251	1780	34.5	-6.3
IL870390	99.13	227.7	0.85336	6.610	25.44	4.197	0.511451	0.0997	1780	-260	-1.0
IL870468	951.1	117.6	0.71215	.3510	36.29	6.441	0.511531	0.1073	1780	10.7	-1.2
IL870525	727.5	78.09	0.71078	.3046	21.8	3.610	0.511514	0.0998	1780	8.1	0.2
IL870577	178.9	219.8	0.79682	3.515	48.85	9.011	0.511460	0.1115	1780	63.1	-3.5
STB2	168.6	250.0	0.79075	4.43	61.65	9.979	0.511297	0.0988	1780	-358	-3.8
R8	158.5	91.7	0.75524	1.72	64.33	10.20	0.511345	0.0968	1780	125	-2.4
Younger granites from the Kvaløya, Rombak-Sjangeli, and Tysfjord basement culminations											
HS-5701	47.34	239.4	1.04810	14.83	58.88	9.871	0.511400	0.1013	1720	3690#	-3.1
HS-5727	-	-	-	-	79.83	16.03	0.511715	0.1214	1720	-	-1.4
HS-5738	9.763	360.9	3.55968	134.4	59.90	11.23	0.511695	0.1134	1720	29600#	0.0
HS-5767	25.83	245.9	1.16907	28.23	41.78	8.914	0.511429	0.1290	1720	4320#	-8.7
HS-5789	50.93	263.2	1.04633	15.15	35.60	6.881	0.511465	0.1168	1720	3640#	-5.3
HS-5807	55.22	247.0	1.02076	13.08	81.90	11.63	0.511297	0.0858	1720	-73	-1.7
HS-32753-2	39.36	360.2	1.21793	27.27	104.5	17.99	0.511368	0.1040	1720	-2260	-4.3
HS-32793-2	48.74	288.6	1.02301	17.32	20.49	4.100	0.511139	0.1209	1720	-1530	-12.6
KR2A.88	64.11	393.0	1.12104	18.10	45.39	8.871	0.511153	0.1181	1720	-412	-11.7
KR5A.88	52.00	299.9	1.06829	16.95	100.8	16.19	0.511492	0.0971	1720	-760	-0.4
KG1.88	27.24	229.3	1.25954	25.18	16.28	2.389	0.511110	0.0887	1720	-933	-6.0
KH51.88	67.30	241.5	0.94971	10.42	91.16	13.51	0.511338	0.0896	1720	-150	-1.7
KH60.88	45.90	287.3	1.16773	18.56	73.23	11.00	0.511374	0.0908	1720	90.5	-1.3
KG69.88	88.87	173.4	0.87306	5.627	127.5	18.09	0.511366	0.0858	1720	448	-0.3
KV73.88	27.49	448.3	1.78709	51.18	67.50	12.53	0.511526	0.1122	1720	-2570	-3.1
KS5.83	32.10	374.4	1.54271	35.81	44.41	8.874	0.511743	0.1208	1780	-643	-0.7
KS35.83	152.1	372.8	0.85536	7.052	71.61	11.79	0.511419	0.0996	1720	-306	-2.4
IL890007	22690	211.3	1.32003	28.01	50.53	8.389	0.511289	0.1004	1720	-1070	-5.1
IL890016	97.86	148.8	0.81169	4.359	11.66	1.833	0.511116	0.0950	1720	20.4	-7.3
U-268	50.76	231.5	1.02589	13.35	11.69	2.115	0.511604	0.1094	1720	-95	-0.9
STB5	49.16	320.0	1.1510	20.1	49.04	9.920	0.511657	0.1235	1720	-690	-3.0
R9	51.65	101.0	0.84632	5.85	31.54	5.307	0.511252	0.1027	1720	-11.4	-6.3

**Table 3: Whole-rock Rb-Sr and Sm-Nd isotopic data from granites and tonalites of the Kvaløya, Rombak-Sjangeli, and Tysfjord basement culminations.  $\epsilon_{\text{Sr}}$  (T) and  $\epsilon_{\text{Nd}}$  (T) calculated for the U-Pb zircon ages using the following constants:  $\lambda^{87}\text{Rb} = 1.42\text{E-}11 \text{ y}^{-1}$ ,  $(^{87}\text{Rb}/^{86}\text{Sr})_{0\text{UR}} = 0.0816$ ,  $(^{87}\text{Sr}/^{86}\text{Sr})_{0\text{UR}} = 0.7045$ ,  $\lambda^{147}\text{Sm} = 6.54\text{E-}12 \text{ y}^{-1}$ ,  $(^{147}\text{Sm}/^{144}\text{Nd})_{0\text{CHUR}} = 0.1966$ ,  $(^{143}\text{Nd}/^{144}\text{Nd})_{0\text{CHUR}} = 0.512638$ . #  $\epsilon_{\text{Sr}}$  (T) Calculated for 400 Ma.**

elements, such as Rb, Y+Nb, and K<sub>2</sub>O, as they have distinctly lower Rb and K<sub>2</sub>O contents than the granites (Fig. 12). Geochemically, the tonalites define a much more coherent group than the granites. Each granitic intrusion has its own field in the Harker and Peacock diagrams (Fig. 11) and has a peraluminous calc-alkaline to alkaline character (Fig. 11h). The individual granite intrusions differ in Al<sub>2</sub>O<sub>3</sub>, CaO, Na<sub>2</sub>O, and K<sub>2</sub>O contents at comparable SiO<sub>2</sub> contents (Fig. 11). Furthermore they have very contrasting trace element contents, such as Ba, Rb, and Zr (see Fig. 12).

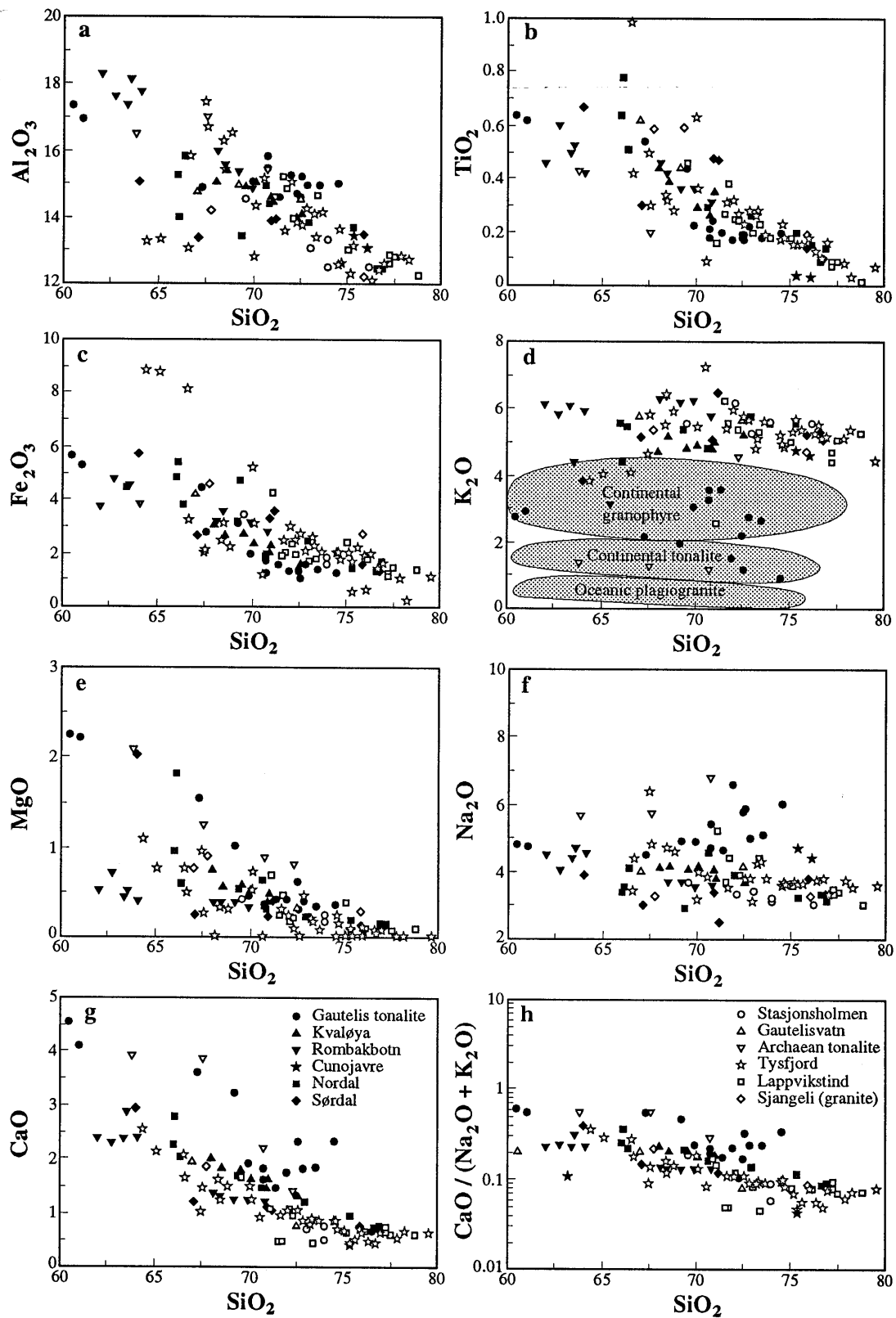


**Fig. 11:** Main element analyses of tonalites and granites from the Kvaløya, Rombak-Sjangeli, and Tysfjord basement culminations. Granite types are separated after geographic areas. Data from Table 4 (at the end of this report).

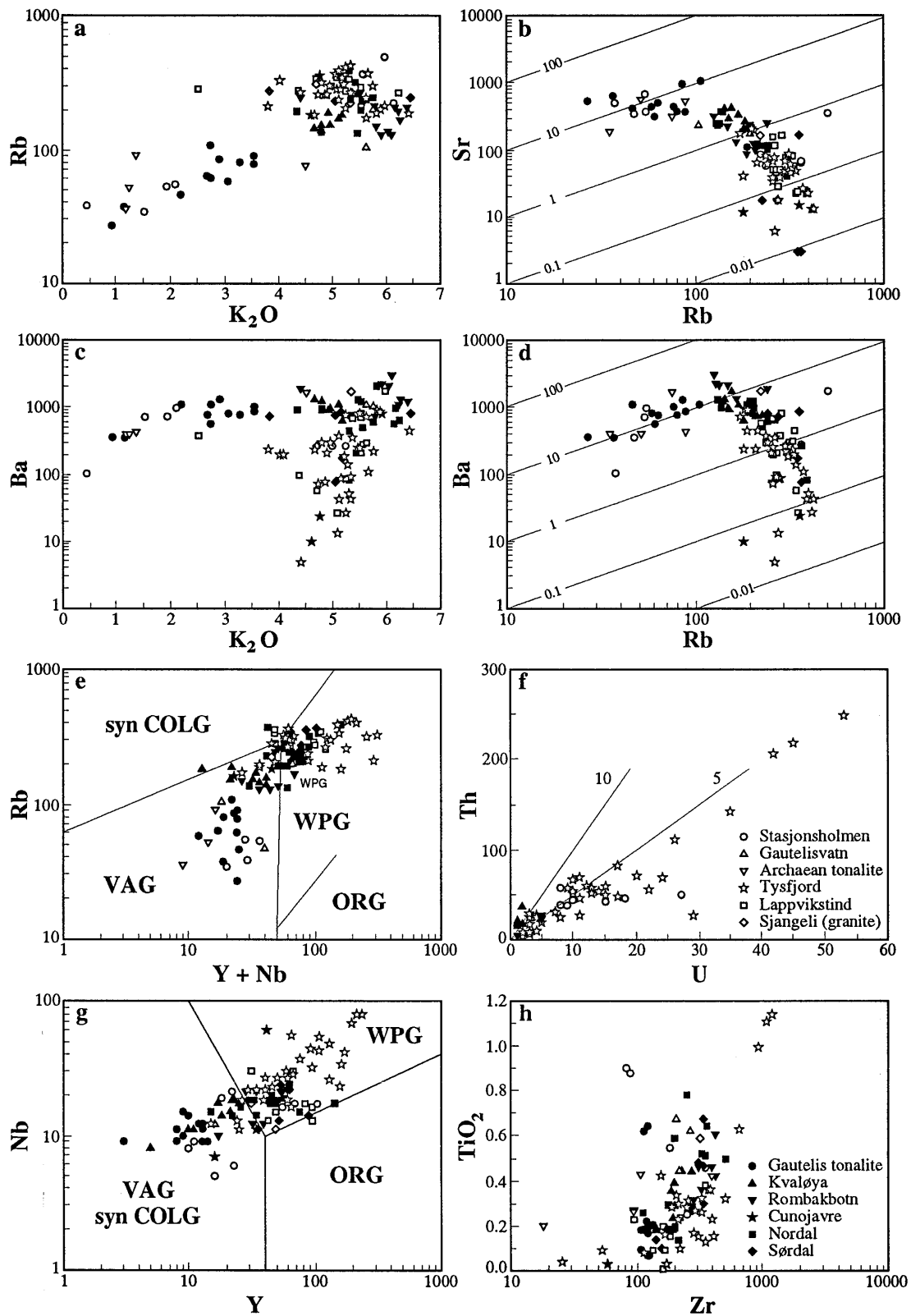


**Fig. 12:** Trace element analyses and discrimination diagrams for tonalites and granites from the Kvaløya, Rombak-Sjangeli, and Tysfjord basement culminations. Same symbols as for Fig. 11; granites are separated after geographic areas.

**Tonalites and trondhjemites:** The trondhjemite-tonalite rocks from the Sjangeli and Gautelis areas have high  $\text{Al}_2\text{O}_3$  contents (more than 15 wgt% at 70 wgt%  $\text{SiO}_2$ ) and classify as high- $\text{Al}_2\text{O}_3$  trondhjemites and tonalites (Barker, 1979). They have low  $\text{K}_2\text{O}$  and Rb contents. In the  $\text{SiO}_2$  -  $\text{K}_2\text{O}$  and Rb - Sr diagrams (Figs. 11d and 12b) they fall in the field for continental tonalites (Coleman and Donato, 1979). They are distinctly different from oceanic plagiogranites that have lower Rb, Sr, and  $\text{K}_2\text{O}$  contents and they differ from continental granophyres that have higher K and Rb contents (e.g., Arth, 1979; Coleman and Donato, 1979). The main and trace element chemistry of the tonalites from Gautelis and Sjangeli is identical with the one of continental trondhjemites, which suggests that their formation is not related with any oceanic crust forming processes. The main elements of the tonalites fall in the R1-R2 diagram (Fig. 13) in the field for pre- to post-collision related magmatism (Batchelor and Bowden, 1985) and trace element discrimination diagrams (Figs. 12e and 12g) suggest a volcanic arc setting (Pearce et al., 1984). Discrimination diagrams, where rock chemistry is linked to tectonic setting, suggest that the tonalites formed close to a destructive plate margin.

The Archaean tonalitic gneisses at Sjangeli and the Early Proterozoic tonalites and trondhjemites at Gautelis can not be distinguished geochemically. Main elements (Fig. 11) and trace elements (Fig. 12) have the same range of contents. The chemical identity suggests that both kinds of rocks were formed by similar processes in a comparable tectonic environment. However, they differ in U-Pb zircon age. The tonalites and trondhjemites at Sjangeli are ca 2.7 Ga old, while the ones at Gautelis are ca 1.94 Ga old (Figs. 7a and 7b).

Melting experiments of hydrated basaltic crust (Rapp et al., 1991) yield the same compositional variations as the trondhjemites and tonalites at Gautelis and Sjangeli. Melting of a mafic protolith at high pressures (>30 kbar) would generate high- $\text{TiO}_2$  melts (Rapp et al., 1991), while the tonalite and trondhjemites at Gautelis and Sjangeli have low  $\text{TiO}_2$  contents. Therefore, melting of a mafic precursor at high pressure is not likely. In contrast, melting at medium to elevated pressures (16-22 kbar) yields low to intermediate  $\text{TiO}_2$  contents in the melt and results in a distinct HREE depletion due to residual garnet in the source (Rapp et al., 1991). Such a HREE depletion is indicated by the normalized La/Yb of the tonalites at Gautelis (Skyseth unpubl. data).

**Older granites (ca 1.79 Ga):** The 1.79 Ga granites occur at Kvaløya, Sjangeli, Nordal, Gautelisvatn, Svartdal (Rombakbotn), Tysfjord (Hellembotn, Sørfolda), Efjord, Hogtuva, and Glomfjord (see Figs. 2, 5 and 6). They have  $\text{SiO}_2$  contents from 61 to 75 wgt%. The main elements define rather regular trends in the Harker diagrams (Figs. 11 and 14) with steadily decreasing oxide contents of  $\text{Al}_2\text{O}_3$ ,  $\text{Fe}_2\text{O}_3$ , and  $\text{TiO}_2$  as  $\text{SiO}_2$  contents increase. Usually the trends are scattered at the low silica end and become narrower defined as  $\text{SiO}_2$  increases. CaO and MgO deviate from simple trends in the Harker diagram. CaO increases from 2.0 to 3.5 wgt% as  $\text{SiO}_2$  increases from 61 to 65 wgt% and steadily decreases for  $\text{SiO}_2$  contents higher than 65 wgt%.  $\text{K}_2\text{O}$  and  $\text{Na}_2\text{O}$  show little changes with increasing  $\text{SiO}_2$  contents. They fall in the range of 4.5 to 6.3 wgt% and 3.0 to 4.7 wgt%, respectively. The older granites have

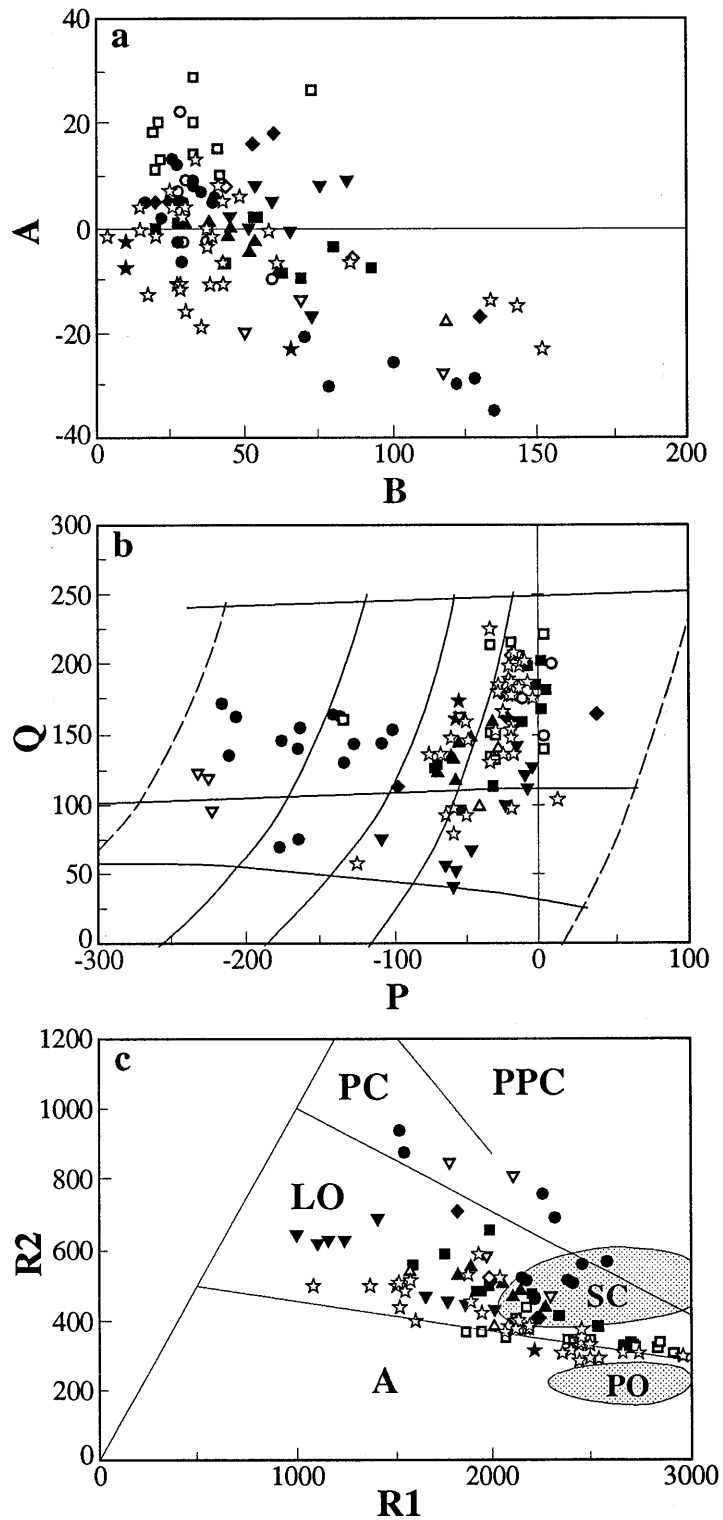


**Fig. 13:** Multi-element discrimination diagrams for tonalites and granites from the Kvaløya, Rombak-Sjangel, and Tysfjord basement culminations (after Debon and LeFort, 1983; Batchelor and Bowden, 1985). Granite types are separated after geographic areas. PC = post-collision uplift granites, PPC = destructive plate margin magmatism (pre-plate collision magmatism), LO = late-orogenic magmatism, A = anorogenic alkaline suite, SC = syn-collision granites (crustal melts), PO = post-orogenic granites (crustal melts).



TiO<sub>2</sub> contents less than 0.8 wgt%. Most of these granites have high Ba contents (1000 - 2500 ppm), intermediate Sr contents (100-400 ppm), and low Rb contents (100-300 ppm). They have low U (<10 ppm) and low Th (<30 ppm) contents. The Th/U ratios vary from 2 to 10 (Figs. 12f and 15f). They fall, however, often close to the higher end of that range.

In trace element discrimination diagrams, the older granites fall in the range of magmatic arc and volcanic arc granites (Figs. 12e, 12g, 15e and 15g; Pearce et al., 1984). In the R1-R2 multi-element classification diagram (Fig. 13), they fall in the field of late orogenic granites (see Batchelor and Bowden, 1985). In several of the trace element diagrams, the older granites fall on the continuation of the trondhjemite and tonalite trend. For instance in the Ba-Rb, Ba-K<sub>2</sub>O, and Rb-Sr diagrams (Figs. 12b, 12c, 12d and 16), the older granites fall in a rather narrowly defined cluster at high-Ba and high-Sr. In trace element discrimination diagrams (Figs. 12e and 12g), the older granites fall on a trend from the center of the volcanic arc granite field towards the field for within-plate granites. Trace element contents of the older granites fall, however, dominantly into the volcanic arc field.

The 1.79 Ga granites have low contents of U, Th, La and Rb (Table 4) which suggests that they are mainly derived from a source that was depleted in these elements. Potential source rocks could be lower crust or hydrated mafic rocks. Involvement of mafic crust is also suggested by slightly elevated MgO and CaO contents in granites with low SiO<sub>2</sub> contents. Most granites also have elevated Sr and Ba contents (Table 4).

**Younger granites (ca 1.71 Ga):** The 1.71 Ga granites occur at Sjangeli, Cunojavre, Nordal, Sjørdal, Stasjonsholmen, Lappvikstind, Tysfjord (Sjøfolda, Hellembotn, Gjerdal, Veikvatn), Efyord, and Glomfjord (Figs. 3 and 6). They have SiO<sub>2</sub> contents that vary from 64 to 79 wgt%. The main element oxides vary widely in the Harker diagrams (see Figs. 11 and 14). Al<sub>2</sub>O<sub>3</sub>, Fe<sub>2</sub>O<sub>3</sub>, TiO<sub>2</sub>, CaO, and MgO have a very wide range at low SiO<sub>2</sub> contents (below 72 wgt%) and the trends are irregular. At SiO<sub>2</sub> contents above 72 wgt%, the trends become closely defined and the oxide contents decrease in a regular manner as SiO<sub>2</sub> increases. TiO<sub>2</sub> is generally less than 0.4 wgt%. At low SiO<sub>2</sub> contents, however, TiO<sub>2</sub> contents can reach 1.2 wgt%. High TiO<sub>2</sub> contents closely correlate with high Fe<sub>2</sub>O<sub>3</sub> contents. K<sub>2</sub>O at SiO<sub>2</sub> contents higher than 72 wgt% falls in the range of 4.7 to 5.6 wgt%. At lower SiO<sub>2</sub> contents, the K<sub>2</sub>O contents increase with increasing SiO<sub>2</sub> contents from 3.5 wgt% to 7 wgt%, reaching a maximum at ca 71 wgt% SiO<sub>2</sub>.

The ca 1.71 Ga old granites of the TGPB have low to intermediate Ba contents (10-1000 ppm), low to intermediate Sr contents (3-200 ppm), and intermediate to high Rb contents (200-450 ppm). Zr contents vary from 100 to 1500 ppm. The contents of Y and Nb are enhanced in comparison with the ones of the older granites (Figs. 12 and 15). The younger granites have a wide range of La contents (20 to 800 ppm). Furthermore, the younger granites contain locally very high contents of U and Th (Figs. 12f and 15f).

The younger granites have very heterogeneous main and trace element compositions and trends in Harker diagrams scatter widely, especially at low SiO<sub>2</sub> contents (Fig. 11). This suggests, that the protoliths of these granites probably were

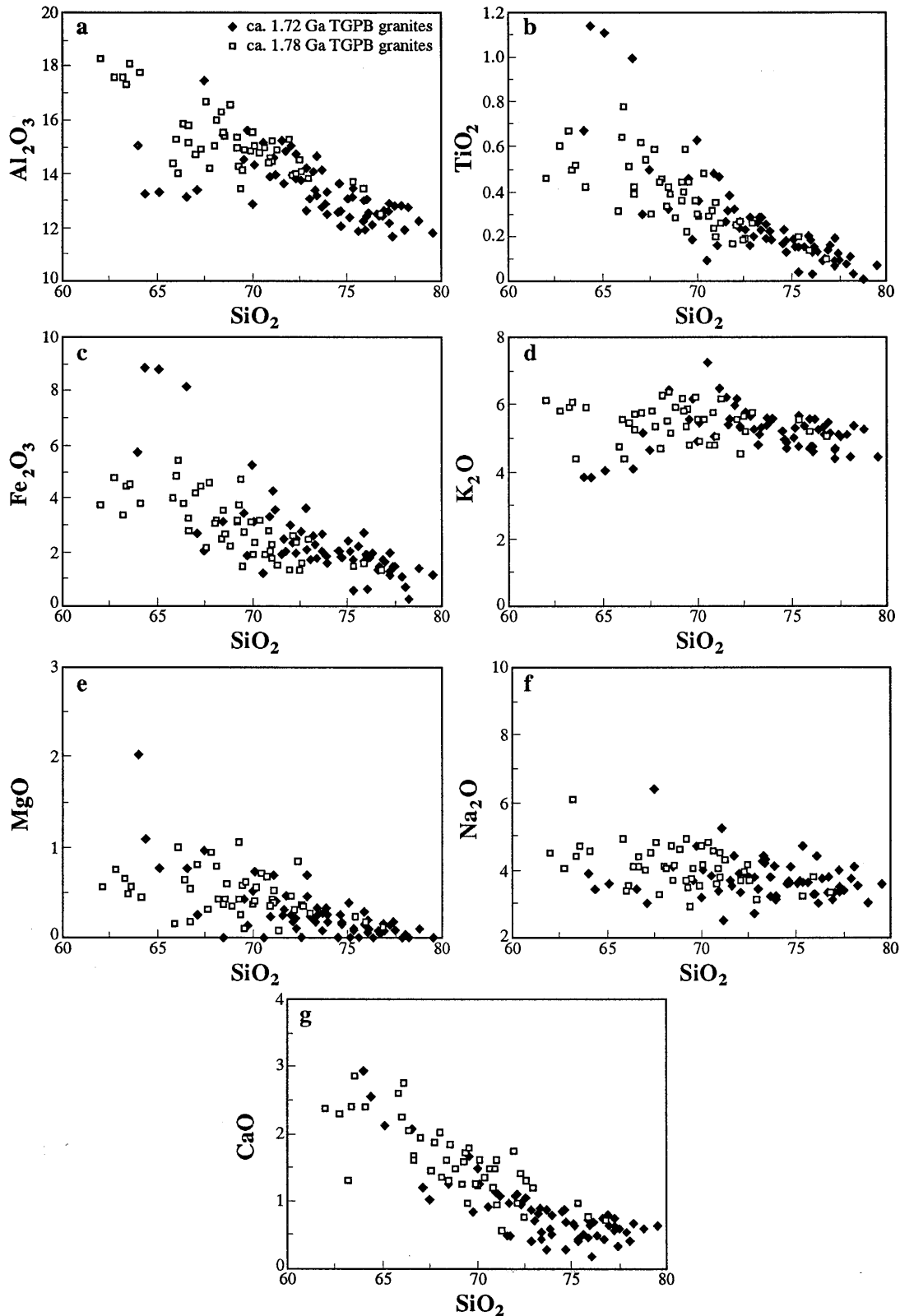


**Fig. 14:** Main element analyses of tonalites and granites from the Kvaløya, Rombak-Sjängeli, and Tysfjord basement culminations. Granites are separated into older (ca 1.78 Ga) and younger (ca 1.72 Ga) granites. Separation based on U-Pb ages. For granites with no geochronological data available, separation was made on basis of field occurrence and on trace element character (Rb, Ba, Sr), see text.

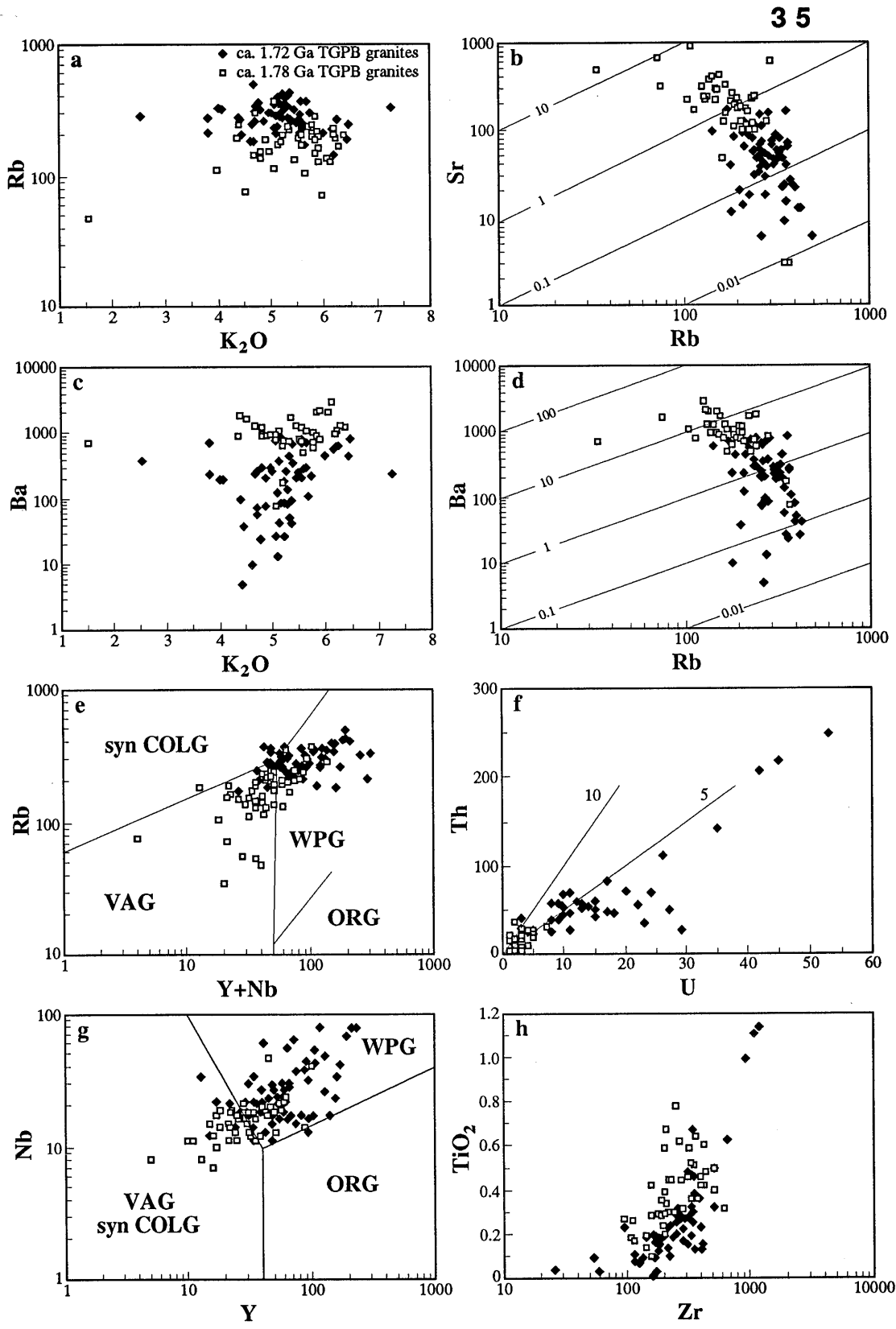


**Fig. 15:** Trace element analyses and discrimination diagrams for tonalites and granites from the Kvaløya, Rombak-Sjangel, and Tysfjord basement culminations. Granites are separated into older (ca 1.78 Ga) and younger (ca 1.72 Ga) granites. Separation based on U-Pb ages. For granites with no geochronological data available, separation was made on basis of field occurrence and on trace element character (Rb, Ba, Sr), see text.

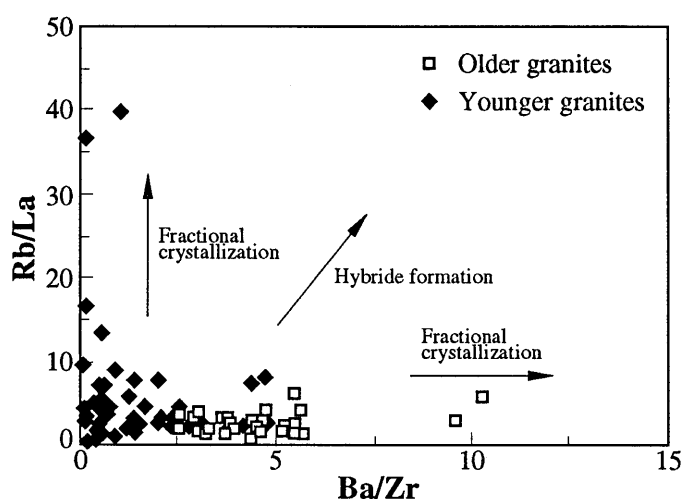


Fig. 16: Rb/La - Ba/Zr diagram for TGPB granitoids from the Kvaløya, Rombak-Sjangeli, and Tysfjord basement culminations.

very heterogeneous, and several geochemically and mineralogically different kinds of protoliths were involved in the formation of these granites.

***Geochemical discrimination between younger and older granites:***

The older and younger granites are distinguished rather clearly by means of trace element diagrams. In the Ba-Rb, Ba-K<sub>2</sub>O, Rb-K<sub>2</sub>O, and to a lesser extent the Rb-Sr and Ba-Sr diagrams, the two suites are clearly separated, as the Ba contents of the older granites are distinctly higher and their Rb contents are clearly lower than the ones of the younger granites. The older granites have Rb/La ratios less than 5 and Ba/Zr ratios larger than 2.5, while the younger granites have highly variable Rb/La ratios and Ba/Zr ratios less than 2.5 (Fig. 16). The two groups differ also in the Rb-(Y+Nb) and Nb-Y diagrams (Figs. 15e and 15g), where the older granites fall mainly in the field of volcanic arc granites while the younger granites predominantly fall in the field of within-plate granites. The data of the two granite generations overlap and form a continuous trend from little evolved volcanic arc rocks to very evolved within-plate granites. The geochemical evolution trend indicated by the trace elements corroborates with the one of the main elements (Fig. 13c). The older granites fall in the R1-R2 diagram in the field of late orogenic granites while the younger granites fall in and close to the fields of syn-collision and post-orogenic granites (Fig. 13c, Batchelor and Bowden, 1985). The trace elements, thus, not only differ the two generations of granites, they also suggest that these granites formed in different tectonic environments.

Differences between older and younger granites are not equally distinct in the main element compositions (Fig. 14). The younger granites have generally higher SiO<sub>2</sub> contents that vary from 65 wgt% to 79 wgt%, while the older granites have SiO<sub>2</sub> contents varying from 61 wgt% to 75 wgt%. At low SiO<sub>2</sub> contents, the younger granites have a considerably higher variability of other main element contents (e.g.,

Al<sub>2</sub>O<sub>3</sub>, Fe<sub>2</sub>O<sub>3</sub>, TiO<sub>2</sub>, MgO, CaO) than the older granites. In contrast, at high SiO<sub>2</sub> contents, the younger granites have a comparatively lower variability than the older ones.

In terms of source regions, the higher heterogeneity of the younger granites at low SiO<sub>2</sub> suggests that these granites have a higher variability of chemical and mineralogical composition in their source region. The  $\epsilon_{Nd}(T)$  values of the two granite generations also reflected a wider variation for the younger suite. Although there is considerable overlap of the data, the older granites have generally higher  $\epsilon_{Nd}(T)$  ranging from +2.5 to -6.6 than the younger granites whose  $\epsilon_{Nd}(T)$  span a wider range and vary from 0 to -12.6. The  $\epsilon_{Nd}(T)$  values suggest that both granite generations comprise variable amounts of reworked Archaean crustal material. Yet, the contribution of the Archaean crustal component varies from insignificant to moderate in the older generation granites, and from moderate to dominant in the younger granites.

## **7. Constraints on the position of the Archaean-Proterozoic boundary beneath the Caledonides**

**U-Pb data:** The oldest rocks are the Archaean gneisses at Sjangeli (2709 ± 323 Ma). The zircons are not detrital, thus revealing previously not recognized Archaean crust. The gneisses became deformed before the intrusion of the Early Proterozoic granites, as the granites are undeformed over large parts. Small xenoliths of gneiss occur in the granites in the northeastern part of the Rombak-Sjangeli window, the Kuokkel window and in Early Proterozoic granitoids exposed at the eastern erosional front of the Caledonides along Lake Torneträsk. These gneissic xenoliths are probably also of Archaean age. The presence of Archaean crustal remnants in the northern Rombak-Sjangeli window demonstrates that the Archaean-Proterozoic boundary goes through or to the south of this window.

Tonalites from the Gautelis area yield a U-Pb zircon age of 1940 ± 26 Ma (Fig. 7a). The tonalites probably formed in an island arc environment or continent marginal subduction related setting. They constrain the position of the Archaean-Proterozoic boundary *senso stricto* (i.e., the presence of non-detrital Archaean rocks) to the north of the Gautelis area (Fig. 2).

**Lithology:** Sediments deposited on and along the margin of the Archaean craton of Eastern Finland are often siliciclastic. The presence of Early Proterozoic siliciclastic sediments farther to the south, therefore, probably indicates the proximity of an older cratonic source. Such a source would be of Archaean age, as cratonic rocks of other ages are not known from northernmost Sweden. Most of the Early Proterozoic supracrustal rocks in the Rombak-Sjangeli area are intermediate to mafic rocks of volcanic arc affinity and are unlikely sources for voluminous siliciclastic sediments. Fluvial quartzites occur in the Kuokkel (Kopparåsen) greenstone belt (Fig. 2; Adamek, 1975). However no quartzites occur in supracrustal belts farther to the south. Clastic sediments in the Gautelis and Rombakbotn supracrustal belts (Fig. 2) have geochemical signatures of rocks from active continental margins that had passed through a weathering cycle (Sawyer and Korneliussen, 1989). Clastic sedimentary

rocks in the Early Proterozoic supracrustal belts of the Rombak-Sjangeli basement culmination, thus. suggest that the Archaean craton should be very close to the Kuokkal area and becoming increasingly more remote to the south and west.

$\epsilon_{Nd}(T)$  data: The  $\epsilon_{Nd}(T)$  values of granites in the basement culminations between Tysfjord and Kvaløya vary from samples with little or virtually no involvement of Archaean crust ( $\epsilon_{Nd}(T=1.78 \text{ Ga}) \approx +2.5$ ) to samples with very negative  $\epsilon_{Nd}(T=1.72 \approx -12.6)$ . Archaean crust would have  $\epsilon_{Nd}(T=1.8 \text{ Ga})$  of ca -12 (e.g., the gneissic tonalites at Sjangeli). From the zonation pattern of  $\epsilon_{Nd}(T \approx 1.8 \text{ Ga})$  from Sweden and Finland (Romer, 1991: compilation of data from, e.g., Huhma, 1986, Öhlander et al., 1987; Skiöld et al., 1988) the most negative  $\epsilon_{Nd}(T \approx 1.78 \text{ Ga})$  would be expected at Kvaløya to the north, while positive values would be expected in the Tysfjord and Sjona areas to the south. However, such a zonation is not observed (Fig. 10). The  $\epsilon_{Nd}(T)$  pattern of the granites of the basement culminations is highly irregular. The most positive  $\epsilon_{Nd}(T)$  value is observed at Kvaløya, i.e., closest to the Archaean craton. The  $\epsilon_{Nd}(T)$  values vary considerably even over very small distances (e.g., Stasjonsholmen, Rombak-Sjangeli window, Fig. 10), suggesting heterogeneous source regions and variable involvement of older crustal rocks in each granite. The very negative values from the Rombak-Sjangeli, Tysfjord, and Glomfjord basement culminations suggest that at least some granites incorporated significant amounts of material derived from the Archaean craton. The  $\epsilon_{Nd}(T)$  values do not define a clear-cut Archaean-Proterozoic boundary, at which no Archaean crustal component is present. The southernmost estimate of the Archaean-Proterozoic boundary to the east of the Caledonides is the Skellefte district with its massive sulfide deposits and mafic volcanic rocks (Berthelsen, 1987). The westward continuation of this boundary follows the Lake Hornavan fault zone and the northern rim of the Nasafjäll window and probably coincides with Saltfjorden (Fig. 10). In the basement culminations, negative  $\epsilon_{Nd}(T)$  values occur to both sides of this line. However, the  $\epsilon_{Nd}(T)$  values to the north have a larger variation and are generally more negative than the ones to the south. Furthermore, all granites to the south of Saltfjorden have Nd contents less than 50 ppm (Table 3, and Fig. 10), while most granites to the north have higher Nd contents. The southern palaeo-margin of the Archaean craton beneath the Scandinavian Caledonides can, however, not be defined by Nd-isotopic data.

In the Sm-Nd and the  $\epsilon_{Nd}(T)$ -Nd diagram (Fig. 10), the TGPB granites fall in two groups that differ by their Nd contents. Granites with Nd contents less than 60 ppm Nd have a very wide range of  $\epsilon_{Nd}(T)$  from +1.2 to -12.6, while granites with more than 60 ppm Nd have  $\epsilon_{Nd}(T)$  from +2.5 to -6.6 (Table 3, Fig. 10). Granites with more than 60 ppm Nd originate dominantly from the northern part of the investigated area, e.g., Kvaløya, Rombak-Sjangeli, and Efjord, while granites with less than 60 ppm Nd originate from the south, e.g., Glomfjord and Sjona (Fig. 10).  $\epsilon_{Nd}(T)$  of the older granites vary from 2.5 to -6.6 and they do not display a regular geographic zonation.  $\epsilon_{Nd}(T)$  of the younger granites vary also irregularly. However, for older and younger granites occurring in the same general area, the younger granites tend to have more negative  $\epsilon_{Nd}(T)$  values. This is especially obvious for

granites with less than 60 ppm Nd. The  $\epsilon_{Nd}(T)$  values suggest that the younger granites included Archaean crustal components to a larger extent than the older rocks and probably indicate a change in source rock character with time.

The contrasting  $\epsilon_{Nd}(T)$  of the younger and the older granites in the Svecofennian area suggests that the protolith character changed with time. Thus, the geographic distribution of  $\epsilon_{Nd}(T)$  values of granites from different tectonic settings (i.e., different age) can not be used combined to define the extent of Archaean influence. Instead, each age group has to be treated separately. The combination of both age groups to construct  $\epsilon_{Nd}(T)$  isolines will yield an irregular pattern, the strongly negative  $\epsilon_{Nd}(T)$  occurring at positions where sedimentary aprons emerged from the Archaean craton into the Svecofennian domain.

Pb-Pb data: As most  $^{207}\text{Pb}$  formed during the first two billion years of the Earth's history and the U/Pb ratio of silicic crust is higher than the one of the mantle, old crustal sources are characterized by higher  $^{207}\text{Pb}/^{204}\text{Pb}$  ratios than young crust when compared at the same  $^{206}\text{Pb}/^{204}\text{Pb}$  ratio. Therefore, lead isotopes can indicate the involvement of Archaean crust in the formation of Early Proterozoic and younger crust. Furthermore, Th and U fractionate strongly from each other during high-grade metamorphic and hydrothermal processes. U is lost from high-grade metamorphic terranes that will have high Th/U. In contrast, U is strongly enriched in hydrothermal and surface aqueous systems. Graphitic schists and hydrothermal systems often have very low Th/U. Over time the lead isotopic compositions of rocks that were exposed to such processes will become very distinctive. High-grade metamorphic terranes will evolve high  $^{208}\text{Pb}/^{204}\text{Pb}$  at comparatively low  $^{206}\text{Pb}/^{204}\text{Pb}$ , while graphitic schists and hydrothermal rocks will have very high  $^{206}\text{Pb}/^{204}\text{Pb}$  at low or moderate  $^{208}\text{Pb}/^{204}\text{Pb}$ . High-grade metamorphism occurs in collision zones involving older crust. A high Th/U signature in the Proterozoic granites could, therefore, indicate the presence of an older crustal component in their protoliths. Thus, high  $^{208}\text{Pb}/^{204}\text{Pb}$  and elevated  $^{207}\text{Pb}/^{204}\text{Pb}$  both indicate the availability of Archaean crust in the source area of the younger rocks. Lead that is mobilized from these sources and incorporated in younger rocks will keep its distinctive old lead signature.

Lead in the Early Proterozoic rocks of the basement culminations was redistributed during the Caledonian orogeny. Trace sulfide and galena lead isotopic compositions from these areas define mixing lines whose slopes in the  $^{206}\text{Pb}/^{204}\text{Pb}$  -  $^{207}\text{Pb}/^{204}\text{Pb}$  diagram yield source ages of ca 1.8 Ga for a Caledonian mixing age of ca 0.4 Ga (Johansson, 1983; Romer, 1989, 1990). These lead lines are in the  $^{206}\text{Pb}/^{204}\text{Pb}$  -  $^{207}\text{Pb}/^{204}\text{Pb}$  diagram parallel offset from each other (Fig. 17). The offset reflects contrasting  $^{207}\text{Pb}/^{204}\text{Pb}$  ratios in the 1.8 Ga old source. Increasingly higher  $^{207}\text{Pb}/^{204}\text{Pb}$  reflect higher average  $\mu_1$  ( $^{238}\text{U}/^{204}\text{Pb}$  before 1.8 Ga) which implies a higher contribution of Archaean crustal lead to the 1.8 Ga lead. In the Sjangeli supracrustal belt, for instance, Cu-deposits in mafic tuffitic units have distinctly lower  $\mu_1$  than Fe-deposits in pelitic schists. This difference could reflect the derivation of the tuffitic units from a magmatic source that did not involve significantly older crustal components and the derivation of the pelitic schists from older crustal sources with more evolved lead. High  $\mu_1$  lead occurs in the stratigraphically higher sections of the Sjangeli supracrustal belt. The variability of

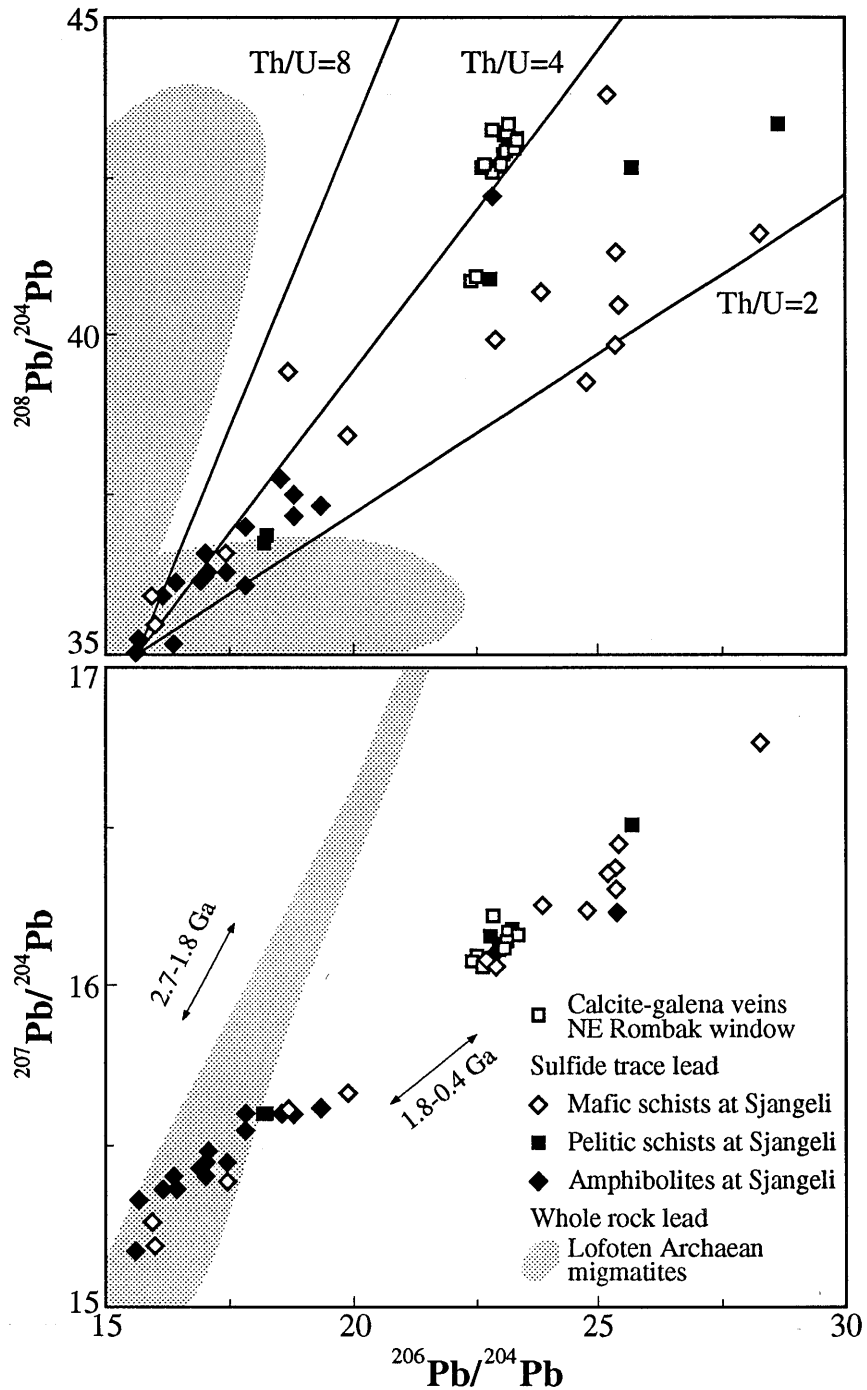


**Fig. 17:** The lead isotopic compositions from the Sjangeli supracrustal belt and granite-hosted galena-calcite veins of the northern part of the Sjangeli-Rombak basement culmination fall in the  $^{206}\text{Pb}/^{204}\text{Pb}$  -  $^{207}\text{Pb}/^{204}\text{Pb}$  diagram on a broad mixing trend. The slope of the mixing trend yields a mixing age of ca 0.4 Ga for a source age of ca 1.8 Ga. The width of the trend reflects the heterogeneous lead isotopic composition at 1.8 Ga and, thus, different pre-1.8 Ga  $^{238}\text{U}/^{204}\text{Pb}$  ratios. In the  $^{206}\text{Pb}/^{204}\text{Pb}$  -  $^{208}\text{Pb}/^{204}\text{Pb}$  diagram, the data mainly fall on a trend reflecting average Th/U ratios of 2 to 4. A few samples fall above (e.g., all galena-calcite vein samples) this trend. These data reflect higher Th/U ratios in their source rocks before the 0.4 Ga event (data from Romer, 1990, 1991, Romer and Wright, submit.).



the pre-1.8 Ga  $\mu_1$  suggests that Archaean crustal lead locally was available and that the supracrustal belts evolved close to the Archaean craton.

Lead isotopic compositions from the Rombak-Sjangeli basement culmination are highly variable in the  $^{206}\text{Pb}/^{204}\text{Pb}$  -  $^{208}\text{Pb}/^{204}\text{Pb}$  diagram (Fig. 17). The variation suggests that sources with both high Th/U and low Th/U were available for lead leaching at the time of the Caledonian orogeny. For instance, sulfide deposits hosted by mafic and pelitic schists generally have lead isotopic compositions indicating low Th/U ratios (Romer, 1989). In contrast, lead isotopic compositions from galena-calcite veins in granites indicate elevated Th/U ratios, i.e., the possible involvement of an older high-grade metamorphosed terrane. High Th/U ratios occur in the granites of the northeastern Rombak-Sjangeli basement culmination and the Kvaløya area. The Th/U of the granites ranges from 4 to 20. In contrast, granites from the Tysfjord area have Th/U ranging from 2 to 4. Furthermore, the Tysfjord granites, which geochemically mainly belong to the younger granite generation, have very high U and Th contents.

## 8. The Transscandinavian Granite Porphyry Belt

The TGPB is a more than 1000 km long continuous belt from southern Sweden to northern Sweden and Norway (Gaál and Gorbatshev, 1987), in part following the Protogine zone (P in Fig. 1), in part occurring beneath the Scandinavian Caledonides. The northward extension of the TGPB granites also comprises the coastal tectonic windows at Senja, and Kvaløya (Eriksson and Henkel, 1983). The TGPB rocks of southern Sweden (Fig. 1) have the same bimodal age distribution and geochemical signature as the granites in the basement culminations at Tysfjord, Rombak-Sjangeli, and Kvaløya, which suggests that along the TGPB similar tectonomagmatic processes occurred contemporaneously. Our chemical and chronological data corroborate favorably with the correlation from geophysical and gravimetric investigations (Eriksson and Henkel, 1983; Henkel and Eriksson, 1987).

The older granitoids of the TGPB granites vary in age from 1.84 to 1.76 Ga (Johansson, 1988) and overlap in time with the post-orogenic within-plate granites in the Svecofennian area of south-central Sweden (1.80 to 1.75 Ga, Zuber and Öhlander, 1990) to the east of the TGPB. The geochemical signature of the coeval granites in these two provinces, however, is distinctly different. The older TGPB granites have volcanic arc signatures, while late-Svecofennian granites have within-plate signatures (see Zuber and Öhlander, 1990). The younger granitoids within the TGPB range are 1.68 to 1.70 Ga old (Wilson et al., 1985; Patchett et al., 1987). These younger intrusions vary from gabbros to granites and show magma mixing (Wilson et al., 1985) and their granitic end members have the same geochemical characteristics as the within-plate granites of the Svecofennian domain of Bergslagen (Zuber and Öhlander, 1990). However, the within-plate granites of the TGPB are 50-100 Ma younger than the geochemically similar granites of the Bergslagen province.

The TGPB rocks represent the root of a magmatic arc that formed at the margin of the Svecofennian Baltic craton above an eastward dipping subduction zone (Johansson, 1988). The older granites probably mainly originate from the melting of

hydrated mafic material with variable, but generally minor contributions from older crustal sources. Their main and trace element contents are characteristic for rocks of magmatic arc affinity (Figs. 11e, 11g and 13c). In contrast, the younger granites generally contain much larger contributions of reworked Archaean crust, although there is a considerable overlap of the  $\epsilon_{Nd}(T)$  values. The younger granite generation probably involved much less of the hydrated mafic source. Their main and trace element contents are characteristic for within-plate granites (Figs. 11e, 11g and 13c).

Rock suites that formed by fractional crystallization processes in magmatic arcs define in the Rb/La - Ba/Zr diagram trends that follow the two axes, but that do not fall in the field where both Rb/La and Ba/Zr are large. In contrast, hybrid rocks have enhanced Rb/La and Ba/Zr ratios. The older granite generation has variably high Ba/Zr ratios at low Rb/La ratios (Fig. 16), which suggests that the geochemical variability of the older generation granites is largely due to fractional crystallization and only to a lesser extent to hybrid formation. In contrast, the younger generation of TGPB granites has dominantly low Ba/Zr ratios and very variable Rb/La ratios. The two groups appear to follow completely different fractionation trends in the Rb/La - Ba/Zr diagram (Fig. 16). The variation is mainly due to the kind of fractionating phases and their melt-solid distribution coefficients of the involved elements. The contrasting trends, thus, indicate contrasting fractionation histories that are due to differences in the initial chemical composition (determines which phases fractionate) and the probably contrasting oxygen fugacities (reflected by the presence and absence of magnetite, respectively). The contrasting fractionation trends probably reflect different kinds of source rocks in the two generations of granite.

## 9. Model

Any tectonic model for the Early Proterozoic evolution of the Rombak-Sjängeli area must take in consideration that the geometric relationships between the various units may have changed during later tectonic processes. For instance, NW striking strike-slip fault zones offset the TGPB (e.g., Eriksson and Henkel, 1983). These faults were mobile in part during the Caledonian orogeny (Romer and Bax, 1992), in part already earlier (Henkel and Eriksson, 1987). Furthermore, vertical displacements along such reactivated faults may have juxtaposed rocks from different crustal levels against each other. We chose to construct a tectonic model that explains the following large scale features:

- 1) The TGPB forms a magmatic belt along the western border of the Svecofennian area of the Baltic Shield. The TGPB granites range in age from ca 1.79 to 1.70 Ga and they are subduction related (Johansson, 1988). They have a bimodal age distribution and the two age groups have distinctly different chemical compositions. The older granites have magmatic arc affinity, while the younger granites have within-plate affinity. The TGPB probably formed in a similar tectonic setting as the high-K granites in the Andes and the North American Cordillera (Pitcher, 1982; Todd et al., 1988). The TGPB rocks include magnetite-series and ilmenite-series granites. The association of magnetite-series and ilmenite-series granites occurs above subduction

zones in East Asia, Japan, and northern America (e.g., Pitcher, 1982). For instance at Baja California, the ilmenite-series granites are flanked on both sides by magnetite-series granites (Gastil et al., 1990). The relation of the TGPB to the Baltic Shield suggests, that the TGPB formed above an eastward dipping subduction zone, the western plate being subducted, as otherwise traces of a suture zone should be found to the east of the TGPB on the Svecofennian part of the Baltic Shield.

2) The Archaean-Proterozoic boundary changes character along its strike. In Finland, the boundary is rather narrow and its definition by lithologic, chronologic, isotope geochemical, and geophysical means coincides within a narrow zone, which is few tens of kilometers wide (Vaasjoki and Sakko, 1988). Towards the west, the boundary between the Archaean and Svecofennian domain, as defined by the above methods, diverges and is at the front of the Caledonian orogen at least 250 km wide (from Lake Torneträsk in the north to Lake Hornavan in the south, Fig. 1). The westward widening of this boundary zone is not due to later strike-slip movements, the exposure of different crustal levels, and the locally variable protoliths of the granites. The various geological, geochemical, and geophysical definitions of the Archaean-Proterozoic boundary differ because they monitor contrasting characteristics. For instance, U-Pb dating in combination with lithologic mapping outlines the distribution of Archaean rocks, while isotope geochemistry (e.g.,  $\epsilon_{Nd}(T)$ , Pb-Pb) illustrates the geographic extent of incorporation and recycling of Archaean crustal material. The narrow Archaean-Proterozoic boundary in eastern Finland suggests that the sedimentary material transported from the Archaean craton towards the south either did not reach very far into the Svecofennian domain or was transported away by strike-slip movements along the boundary between the Archaean and the Svecofennian domain. In contrast, the wide zone of distinct Archaean influence in the Svecofennian domain of northern Sweden suggests that Archaean material reached far into the Svecofennian domain and was not transported away by tectonic processes.

3) The Early Proterozoic lead isotope zonation of the Baltic Shield is preserved in massive sulfide deposits. The zonation pattern within the Svecofennian domain is at a high angle to both the Archaean domain and the TGPB (Romer, 1991). The lead zonation pattern of the Svecofennian rocks appears to be inherited by deposits within the younger TGPB rocks. Areas in the Svecofennian domain that have comparatively high  $^{207}\text{Pb}/^{204}\text{Pb}$  ratios match with high  $^{207}\text{Pb}/^{204}\text{Pb}$  lead in the TGPB domain. The geographic extent of low  $^{207}\text{Pb}/^{204}\text{Pb}$  lead in the two domains matches also. TGPB lead has higher  $^{206}\text{Pb}/^{204}\text{Pb}$  ratios than the sulfide deposits of the Svecofennian domain, reflecting the lower age of the TGPB rocks. The correspondence of high and low  $^{207}\text{Pb}/^{204}\text{Pb}$  in the Svecofennian domain and the TGPB suggests that the TGPB lead was in part derived from reactivated Svecofennian crust (Romer and Wright, *subm.*).

4) There are two main areas of mafic to felsic volcanism within the Svecofennian domain: the Skellefte district to the north and the Bergslagen-Tampere area to the south. They are separated by the Bothnian greywacke basin (Fig. 18).

5) Tonalites related to island arc volcanism have an age of ca 1.94 Ga (Gautelis, Norvijaure, Outokumpu, and Jormua, Fig. 18). They are the oldest U-Pb zircon dated crustal rocks within the Svecofennian domain. They are coeval with volcanic rocks of

mafic to felsic composition (Kontinen, 1987). Ca 1.94 Ga old tonalitic rocks are so far only known from the northern Svecofennian volcanic province (Kontinen, 1987; Skiöld, pers. com., 1991).

6) Granitic magmatism related to subduction processes in the northern and southern Svecofennian province is roughly coeval (Patchett and Kuovo, 1986; Huhma, 1986; Skiöld, 1987, 1988; Patchett et al., 1987; Haapala et al., 1987). The granitic magmatism clusters in two age pulses at 1.90-1.85 Ga and 1.83-1.78 Ga (Patchett et al., 1987; Skiöld, 1988, Skiöld et al., 1988). The older granites have usually chemical compositions of magmatic arc affinity, while the younger granites display a within-plate affinity. The Svecofennian granites formed in a similar tectonic setting as the TGPB granites, yet they are 100 to 150 Ma older (Johansson, 1988; Öhlander et al., 1987; Zuber and Öhlander, 1990).

7) Metamorphism and crustal shortening in the Lapland Granulite Belt, the Svecofennian province and the TGPB domain follow each other in time. The Lapland Granulite Belt is oldest and the TGPB is youngest. Each domain becomes increasingly active as the tectonic activity in the previously active domain starts to vanish due to the "mechanical locking" of the involved crustal segments. The locking process corresponds either to the collision of crustal segments that are no longer subductible or the blocking of strike-slip movements. The locking results in the migration of the main-focus of crustal shortening and plate destruction into adjacent areas with deformable or subductible crust.

Our model attempts to explain these features as the result of early Proterozoic subduction and strike-slip processes in a three-plate scenario. The first plate (plate 1 to NE in Fig. 19) is the Archaean craton, now exposed as tonalitic to trondhjemitic gneisses in Lofoten/Vesterålen, northern Sweden, and northern/eastern Finland and granite-greenstone terranes in eastern Finland. This plate was segmented at ca 2.2 Ga by several continental and continent-marginal rifts (Skiöld and Cliff, 1984; Skiöld, 1987) and continent-marginal greywacke basins formed at Pohjanmaa and Peräpohja (Huhma et al., 1990; Park, 1991; Fig. 18). The second plate (plate 2 to the S in Fig. 19) comprises the Svecofennian domain and originally consisted of oceanic crust. In the Svecofennian domain, no exposures of Archaean continental crust was so far documented.  $\epsilon_{Nd}$  (T=1.8 Ga) values from the Bergslagen district suggest that most magmatic material did not involve significantly older crust (Patchett et al., 1987). However,  $\epsilon_{Nd}$  (T=1.8 Ga) from sedimentary rocks (Welin, 1987) and U-Pb ion-probe dating of detrital zircons (Huhma et al., 1991) indicates that Archaean crustal material was present in the source area of the sedimentary rocks. Furthermore, Archaean crust different from the one of plate 1 is also inferred from the lead isotope zonation (Romer, 1991). The Early Proterozoic internal structure of the Svecofennian plate is not well known. The plate most likely was highly heterogeneous. The Svecofennian domain contained several small volcanic arcs of different orientation. These arcs probably formed in island arc settings with changing subduction vergences and contrasting proximity to old crustal source areas. The third plate (plate 3 to the W in Fig. 19) is even less well known. It most likely was also composed of oceanic crust, as it later was destroyed beneath plates 1 and 2.

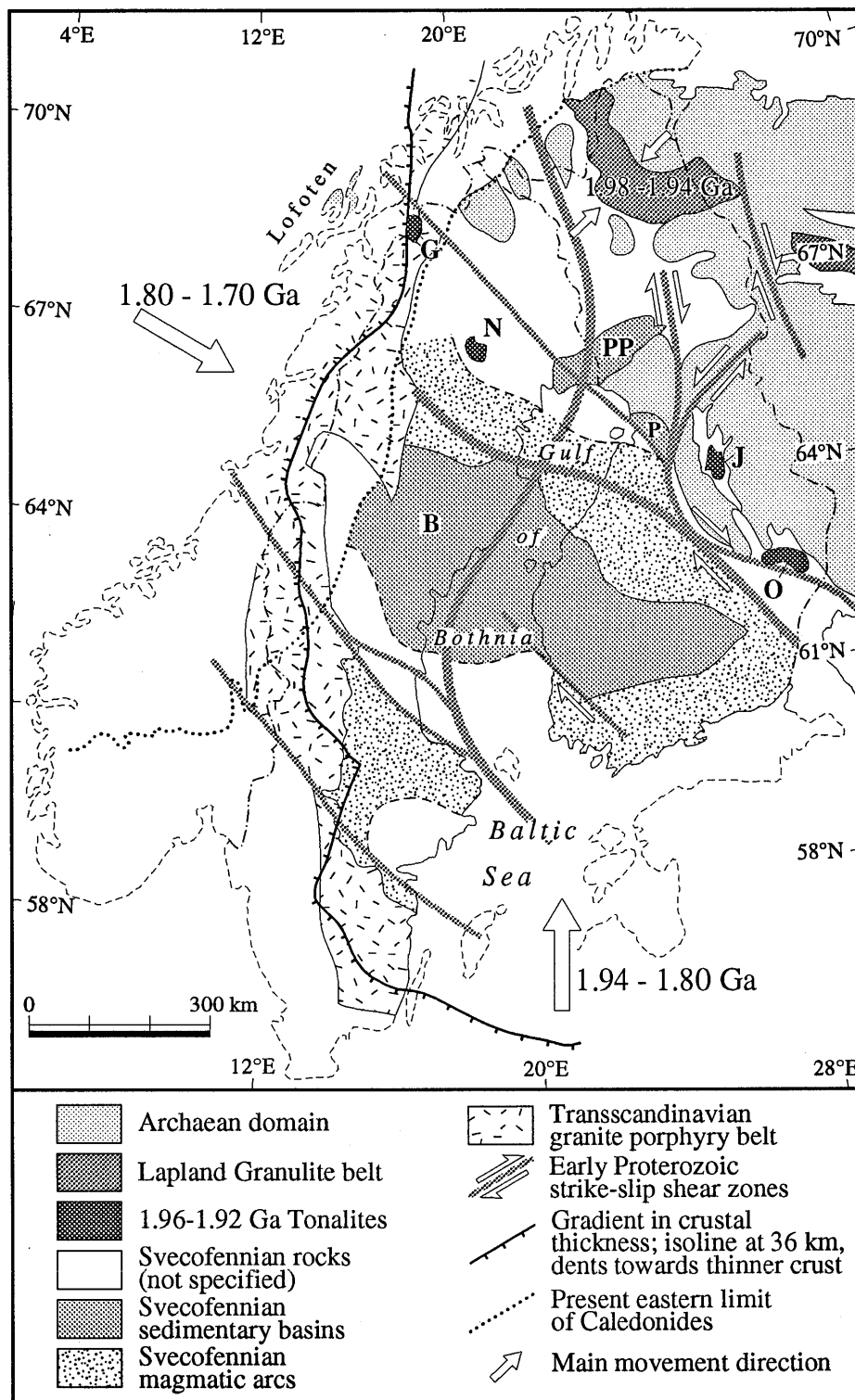


**Fig. 18:** Tectonic map of the Baltic Shield, showing the distribution of Archaean, Svecofennian, Sveconorwegian, and Caledonian rocks. Major fault and shear zones and of TGPB rocks are shaded. Note the westward broadening of the Archaean-Proterozoic boundary as defined by geophysical, geological, and geochemical methods. Oldest tonalitic complexes in the Svecofennian domain: G = Gautelis, N = Norvijaure, J = Jormua, O = Outokumpu. Greywacke basins in the Svecofennian domain: B = Bothnian basin, P = Pohjanmaa basin, PP = Peräpohja basin.

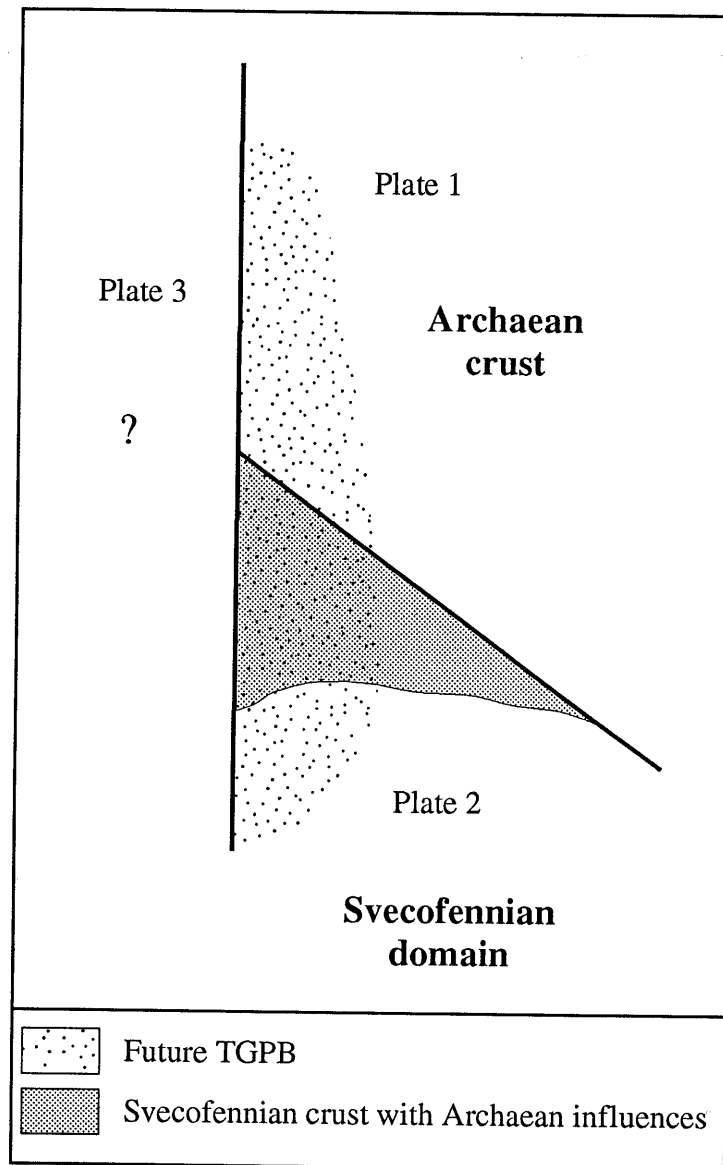


**Fig. 19:** Schematic three-plate scenario for the Baltic Shield at the early Proterozoic.

Before ca 1.94 Ga most of the NE-SW directed crustal shortening in the area of the Baltic Shield was accommodated by the closure of the oceanic segment of the future Lapland Granulite Belt (e.g., Gaál and Gorbatshev, 1987; Huhma and Meriläinen, 1991). The Lapland Granulite Belt formed, as the Archaean continental blocks collided at ca 1.94 Ga (Fig. 20). The Lapland Granulite Belt and the Kola suture zone became consolidated by the intrusion of post-collision granites. These intrusions ceased at ca 1.90 Ga (Huhma and Meriläinen, 1991). After the collision of the continental blocks,

the Archaean plate collage of northeastern Finland largely lost its ability to accommodate crustal shortening. At ca 1.90 Ga, plates 1 and 2 converged obliquely. The Archaean plate (plate 1) became deformed along old fault zones, where granites intruded along extensional segments. The focus of crustal shortening eventually moved southwards into the Svecofennian domain, where the oldest tonalitic intrusions have the same age as the collision of the Archaean continental blocks along the Lapland Granulite Belt suture.

Most of the crustal shortening occurred within the Svecofennian domain (plate 2, Fig. 20). The Svecofennian plate was subducted beneath the Archaean craton (Gaál and Gorbatshev, 1987; Park, 1991). Crustal shortening within the Svecofennian domain occurred along small plate-internal subduction zones. Such zones could have been situated to the south of the Skellefte district and to the south of the Bergslagen province, i.e., beneath these two volcanic arcs. The Svecofennian oceanic plate, furthermore, accommodated N-S crustal shortening along dextral NW striking strike-slip shear zones. Dextral strike-slip movements, for instance along the Raahe-Ladoga zone (i.e., the boundary between the Archaean and Svecofennian domain in Finland), transported not subducted volcanic arcs to the northwest. The westward widening transition zone between the Archaean block and the Svecofennian block (south of the Skellefte district) indicates that these westward escaping buoyant fragments accumulated in the west. The accumulating non-subductible fragments are all fault-bound. They consist of Proterozoic volcanic arcs, sediments derived from the Archaean craton, and probably minor slices of scraped off Archaean crust.

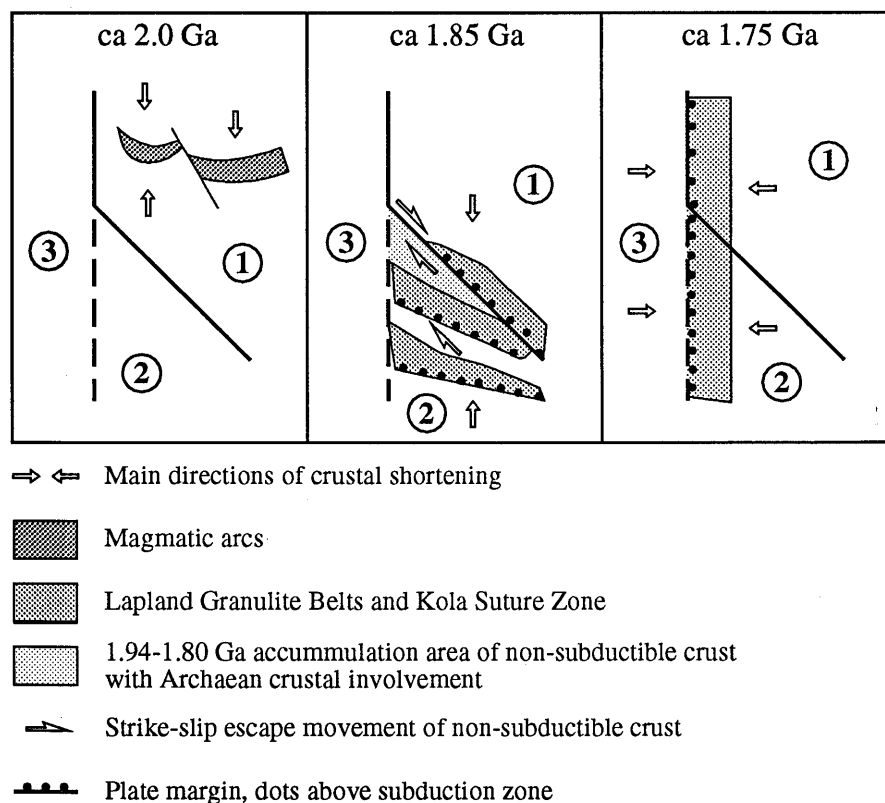


**Fig. 20:** Schematic distribution of crustal shortening on the Baltic Shield at ca 2.0 Ga, 1.85 Ga, and 1.75 Ga. For discussion see text.

There are two possible processes to explain the accumulation of these crustal fragments in the area of northern Sweden. One possibility is that the margin of the Archaean craton was bending to the southwest. The fragments, that were strike-slip transported to the northwest, were thrust onto the Archaean block at the site of the bend. Subsequently arriving non-subductible blocks were then thrust over the earlier arrived fragments. The Archaean block acted as buttress against which the buoyant fragments were thrust. The fragments consist of volcanic arcs and deltaic sedimentary piles, which now are juxtaposed against each other. Wright (1988) presented a model for the Kiruna area which involved Proterozoic thrusting to the northwest, similar to the processes required by the above scenario. In such a model, the early Proterozoic margin of the Baltic Shield would tectonically resemble the present west coast of North America, where the Pacific plate to the south moves along strike-slip zones against the North American plate and to the north is subducted beneath the North American plate. Far travelled terranes accumulate in the "bend" of the margin of the North American plate in the area of the Gulf of Alaska (Monger et al., 1982; Park et al., 1984).

The second process requires a buttress to the west against which the buoyant fragments are thrust. The third plate to the west could be such a buttress. The plate boundary between plates 2 and 3 must not be conservative.

Eventually, both processes result in a heterogeneous collage of thrust terranes in northwestern Sweden. These fault-bound terranes have contrasting lithologies and different metamorphic and structural histories. Lithologic units across terrane boundaries are not correlative. Later granite intrusions along terrane boundaries yield granites with very different  $\epsilon_{Nd}(T)$  values because of the lithologically heterogeneous nature of the protoliths and their variable source ages. Volcanic source rocks probably formed in island arc settings and had rather little involvement of older silicic crust, while sedimentary protoliths probably predominantly originated from the Archaean craton to the north, and consisted of pelitic and greywacke rocks.

Possible traces of Svecofennian strike-slip fault zones and destructive margins are shown in Fig. 18. These zones are magnetically very distinct as they offset magnetic patterns and juxtapose crustal segments of contrasting magnetic character and pattern (e.g., Henkel, 1991). These zones also represent boundaries between areas of contrasting lithologic and metamorphic record and distinctly different Svecofennian lead isotopic composition (Romer, 1991).

The westward transfer of non-subductible segments of plate 2 resulted in the subduction of plate 3 beneath plate 2 along an east-dipping approximately N-S striking subduction zone. The TGPB rocks that formed at the margin of plate 2 above that subduction zone. As the northward continuation of the TGPB rocks crosses the westward projection of the Raahe-Ladoga zone, it is likely that plate 3 also was subducted beneath plate 1.

The contrasting character of the Archaean-Proterozoic boundary in Finland and Sweden reflects the different tectonic behavior of plate 2 during its transport relative to plate 1. In Finland, plate 2 was transported relative to plate 1 mainly by dextral strike-slip movements. The Archaean-Proterozoic boundary as defined by different geological, geochemical, and geophysical methods falls therefore within a narrow band (Vaasjoki and Sakko, 1988). Southwestward extending sedimentary aprons, emerging



from the Archaean craton into the Svecofennian domain, were transported to the northwest. Therefore in Finland, there is no Archaean influence apparent to the SW of this major strike-slip fault zone (Vaasjoki and Sakko, 1988). In northern Sweden, the sedimentary aprons and not subducted volcanic terranes, which originated from the southeast, were assembled into an irregular collage. The different terranes within plate 2 were thrust to the NW (Wright, 1988), i.e., roughly parallel to the direction of strike-slip movements of plate 2 relative to plate 1.

Later intrusions (1.83-1.78 Ga) in northern Sweden recycled volcanic and sedimentary material to a variable extent. Granites being mainly derived from sedimentary source rocks show a distinct Archaean influence, i.e., negative  $\epsilon_{Nd}(T)$  values, while granites derived from volcanic source rocks show less negative  $\epsilon_{Nd}(T)$  values. The tectonic juxtaposition of areas with contrasting source histories and derivation from different tectonic environments made the source area of the granites lithologically very heterogeneous. Therefore, the apparent boundary of Archaean involvement in Svecofennian rocks, as defined by  $\epsilon_{Nd}(T)$  isolines is very irregular.

Internal subduction within plate 2 resulted in the consumption of subductible oceanic crust. Within-plate granitic magmatism (ca 1.83-1.78 Ga) related with the collision of non-subductible crustal fragments "stitched" these together and caused the thickening and strengthening of plate 2 (Park, 1991). Therefore, there was little possibility for additional internal shortening of plate 2 after 1.80 Ga. K-Ar mica and U-Pb zircon dating of rocks from the Raahe-Ladoga zone that yield ages for the last major movements of 1830-1810 Ma (Haudenschild, 1988; Vaasjoki and Sakko, 1988; Korsman, 1988) which suggests that with the stabilization and cratonization of plate 2, strike-slip movements between plate 1 and 2 became less important and eventually ceased.

The subduction of plate 3 beneath the combined plates 1 and 2 became the dominant tectonic process on the Baltic Shield at ca 1.79 Ga. The late-orogenic TGPB granites intruded between 1.80 and 1.76 Ga along this N-S striking subduction zone into plates 1 and 2. At the same time, granites of post-orogenic and anorogenic character intruded the Svecofennian domain (e.g., Revsund-type granites). The 1.80-1.76 Ga old granites in the two areas are related to completely different processes. The granites of the TGPB domain are related to the destruction of plate 3 beneath plates 1 and 2. These granites have a magmatic arc affinity. In contrast, the coeval granites within the Svecofennian domain have within-plate affinity (Zuber and Öhlander, 1990) and they represent the aftermath of the subduction processes and crustal shortening processes within plate 2. The subduction of plate 3 beneath plates 1 and 2 along the TGPB eventually ceased or moved its focus farther to the west. The area of the TGPB subduction zone became intruded by granites of post-orogenic and anorogenic affinity between ca 1.73 and 1.68 Ga (Patchett et al., 1987; Jarl and Johansson, 1988; Fig. 7).

## 10. Summary

The intersection of the boundary zone between the Archaean (ca 2.7 Ga) and the Svecofennian domain (ca 2.0-1.8 Ga) with the ca 1.8-1.7 Ga Transscandinavian Granite Porphyry Belt (TGPB) is exposed in basement culminations of the 0.5-0.4 Ga old Caledonian orogen. The Transscandinavian Granite Porphyry Belt (TGPB), which extends along the western margin of the Baltic Shield from southern Sweden to northern Norway, forms a belt of granitoids that formed above an eastward dipping subduction zone at ca 1.8-1.7 Ga. The granites have a bimodal age distribution. One group has U-Pb zircon ages of  $1791 \pm 10$  Ma. The other group yields U-Pb zircon ages of  $1711 \pm 26$  Ma. With increasing time, the trace element pattern of the TGPB rocks changes from magmatic arc to within-plate geochemical affinity. Superimposed on these geochemical variations are chemical variations due to contrasting character of the protoliths for the granites of these two areas. Granites to the north, in the Archaean domain, have high Th/U ratios, while granites to the south, in the Svecofennian domain, have low Th/U ratios. This suggests that the northern granites mainly incorporated rocks with lower crustal rocks, while the southern granites mainly incorporated upper crustal rocks. To the north, the  $\epsilon_{Nd}(T)$  for the old and the young TGPB granite generations overlap and fall in the range of +2.5 to -6.2. In contrast, the  $\epsilon_{Nd}(T)$  of the two TGPB granite generations in the southern windows varies systematically. The older granites have  $\epsilon_{Nd}(T)$  varying from 0.2 to -6.6, while the younger granites have  $\epsilon_{Nd}(T)$  ranging from 0.0 to -12.6. This suggests, that in the southern area the protolith became increasingly dominated by older crustal material, while in the northern area the source of crustal material did not change its character.

## 11. Acknowledgments

This paper is part of ILP Geotranssect EU 13 (Lofoten-Torneträsk-Gällivare Caledonide Deep Section). RLR gratefully acknowledges James E. Wright, Rice University, Houston TX, for giving him access to his laboratory to do the U-Pb dating. BK and BS did the Rb-Sr and Sm-Nd analyses at Mineralogisk-Geologisk Museum, Oslo. RLR acknowledges support from Luleå University during his visit to Rice. We thank Milan Vnuk, Luleå University, for a great job with the artwork.

## 12. References

- Adamek, P.M., 1975. Geology and mineralogy of the Kopparåsen uraninite-sulphide mineralization, Norrbotten County, Sweden. *Sver. geol. Unders.*, C712: 67pp.
- Andresen, A., 1980. The age of the Precambrian basement in western Troms, Norway. *Geol. Fören. Stockholm Förh.*, 101: 291-298.
- Andresen, A. and Tull, J.F., 1986. Age and tectonic setting of the Tysfjord gneiss granite, Etfjord, North Norway. *Norsk geol. Tidsskr.*, 66: 69-80.
- Arth, J.G., 1979. Some trace elements in trondjemites — their implications to magma genesis and paleotectonic setting. In: F. Barker (Ed.) *Trondjemites, dacites, and related rocks. Devel. in Petrology 6*: 123-132, Elsevier, Amsterdam.
- Barker, F., 1979. Trondjemite: Definition, environment and hypotheses of origin. In: F. Barker (Ed.) *Trondjemites, dacites, and related rocks. Devel. in Petrology 6*: 1-12, Elsevier, Amsterdam.
- Bartley, J.M., 1981. Field relations, metamorphism, and age of the Middagstind quartz syenite, Hinnøy, north Norway. *Norsk geol. Tidsskr.*, 61: 237-248.
- Batchelor, R.A. and Bowden, P., 1985. Petrogenetic interpretation of granitoid rock series using multicationic parameters. *Chem. Geol.*, 48: 43-55.
- Bax, G., 1989. Caledonian structural evolution and tectonostratigraphy in the Rombak-Sjangeli Window and its covering sequences, northern Scandinavian Caledonides. *Norges Geol. Unders. Bull.*, 415: 87-104.
- Bax, G., Kathol, B. and Romer, R.L., 1991. Geology and tectonic stratigraphy at the Caledonian thrust front in the Torneträsk area, Sweden. In: Andresen, A. and Steltenpohl, M.G. (Eds.). *A geotraverse excursion through the Scandinavian Caledonides: Torneträsk-Ofoten-Tromsø, 4-11 august 1991*, p.1-18. IGCP Project 233: Terranes in the Circum-Atlantic Paleozoic Orogens, Tromsø.
- Berthelsen, A., 1987. A tectonic model for the crustal evolution of the Baltic Shield. In: J.-P. Schaer and J. Rodgers (Eds.) *Comparative anatomy of mountain chains*. Princeton Univ. Press, p. 31-57.
- Berthelsen, A. and Marker, M., 1986. 1.9-1.8 Ga old strike-slip megashears in the Baltic Shield, and their plate tectonic implications. *Tectonophysics*, 128: 163-181.
- Brattli, B. and Prestvik, T., 1987. Tysfjord granite and overlying rocks in the area of Linnajavrre, central-north Norway. *Norges geol. Unders. Bull.*, 410: 65-72.
- Coleman, R.G. and Donato, M.M., 1979. Oceanic plagiogranite revisited. In: F. Barker (Ed.) *Trondjemites, dacites, and related rocks. Devel. in Petrology 6*: 149-168, Elsevier, Amsterdam.
- Debon, F. and LeFort, P., 1983. A chemical-mineralogical classification of common plutonic rocks and associations. *Trans. R. Soc. Edinburgh: Earth Sci.*, 73: 135-149.
- Eriksson, L. and Henkel, H., 1983. Deep structures in the Precambrian interpreted from magnetic and gravity maps of Scandinavia. *Int. Basement Tectonics Ass. Publ.*, 4: 351-358.
- Faure, G., 1986. *Principles of isotope geology (2nd Ed.)*. John Wiley & Sons, New

- York, 589pp.
- Frietsch, R., 1988. Precambrian metallogeny of Finland, Norway and Sweden. Proc. Seventh Quadrennial IAGOD Symp, 11-22, E. Schweizerbart'sche Verlagsbuchhandlung, Stuttgart
- Gaál, G. and Gorbatshev, R., 1987. An outline of the Precambrian evolution of the Baltic Shield. *Precamb. Res.*, 35: 15-52.
- Gastil, G., Diamond, J., Knaack, C., Walawender, M., Marshall, M., Boyles, C., Chadwick, B. and Erskine, B., 1990. The problem of the magnetite/ilmenite boundary in southern and Baja California, California. In: J.L. Anderson (Ed.) *The nature and origin of Cordilleran magmatism*. *Geol. Soc. Am. Mem.* 174: 19-32.
- Gee, D.G. and Zachrisson, E., 1979. The Caledonides in Sweden. *Sveriges geol. Unders.*, C769: 1-48.
- Gunner, J.D., 1981. A reconnaissance Rb-Sr study of Precambrian rocks from the Sjangeli-Rombak window and the pattern of initial  $^{87}\text{Sr}/^{86}\text{Sr}$  ratios from Northern Scandinavia. *Norsk geol. Tidsskr.*, 61: 281-290.
- Griffin, W.L., Taylor, P.N., Hakkinen, J.W., Heier, K.S., Iden, I.K., Krogh, E.J., Malm, O., Olsen, K.I., Ormaasen, D.E., and Tveten, E., 1978. Archaean and Proterozoic crustal evolution in Lofoten-Vesterålen, N Norway. *J. geol. Soc. London*, 135: 629-647.
- Haapala, I., Front, K., Rantala, E. and Vaarma M., 1987. Petrology of Nattanen-type granite complexes, northern Finland. *Precamb. Res.*, 35: 225-240.
- Haudenschild, U., 1988. K-Ar age determination on biotite and muscovite in the Pihtipudas-Iisalmi and Jroinen-Sulkava areas, Eastern Finland. *Geol. Surv. Finl., Bull.*, 343: 33-50.
- Heier, K.S. and Compston, W., 1969. Interpretation of Rb-Sr age patterns in high-grade metamorphic rocks, Northe Norway. *Norsk geol. Tidsskr.*, 49: 257-283.
- Henkel, H., 1991. Magnetic crustal structures in northern Fennoscandia. *Tectonophysics*, 192: 57-79.
- Henkel, H. and Eriksson, L., 1987. Regional aeromagnetic and gravity studies in Scandinavia. *Precamb. Res.*, 35: 169-180.
- Huhma, H., 1986. Sm-Nd, U-Pb and Pb-Pb isotopic evidence for the origin of the Early Proterozoic Svecokarelian crust in Finland. *Bull. Geol. Surv. Finland*, 337: 1-48.
- Huhma, H. and Meriläinen, K., 1991. Provenance of paragneisses from the Lapland Granulite Belt. In: P. Tuisku and K. Laajoki (eds.) *IGCP 275 and IGCP 304: Metamorphism, deformation and structure of the crust (MDSC)*. *Res Terrae*, Oulu University, Finland, Ser. A, 5: 26.
- Huhma, H., Cliff, R.A., Perttunen, V. and Sakko, M., 1990. Sm-Nd and Pb isotopic study of mafic rocks associated with early Proterozoic continental rifting: the Peräpohja schist belt in northern Finland. *Contrib. Mineral. Petrol.*, 104: 369-379.
- Huhma, H., Claesson, S., Kinny, P.D. and Williams, I.S., 1991. The growth of Early Proterozoic crust: new evidence from Svecofennian detrital zircons. *Terra Nova*, 3: 175-178.
- Jacobsen S.B. and Wasserburg, G.J., 1978. Interpretation of Nd, Sr and Pb isotope data

- from Archean migmatites in Lofoten-Vesterålen, Norway. *Earth Planet. Sci. Lett.*, 41: 245-253.
- Jahn, B.-M., Vidal, P. and Kröner, A., 1984. Multi-chronometric age and origin of Archean tonalitic gneisses in Finnish Lapland: a case for long crustal residence time. *Contrib. Mineral. Petrol.*, 86: 398-408.
- Jarl, L.-G. and Johansson, Å., 1988. U-Pb ages of granitoids from the Småland-Värmland granite-porphyry belt, southern and central Sweden. *Geol. Fören. Stockholm Förh.*, 110: 21-28.
- Johansson, Å., 1983. Lead isotope composition of Caledonian sulfide-bearing veins in Sweden. *Econ. Geol.*, 78: 1674-1688.
- Johansson, Å., 1988. The age and geotectonic setting of the Småland-Värmland granite-porphyry belt. *Geol. Fören. Stockholm Förh.*, 110: 105-110.
- Kontinen, A., 1987. An Early Proterozoic ophiolite — the Jormua mafic-ultramafic complex, northeastern Finland. *Precamb. Res.*, 35: 313-341.
- Korneliussen, A. and Sawyer, E.W., 1989. The geochemistry of Lower Proterozoic mafic to felsic igneous rocks, Rombak Window, North Norway. *Norges geol. Unders. Bull.*, 415: 7-21.
- Korsman, K., 1988. Tectono-metamorphic evolution of the Raahe-Ladoga zone, eastern Finland. *Geol. Surv. Finl., Bull.*, 343: 3.
- Krill, A.G. and Fareth, E., 1984. Rb-Sr whole-rock dates from Senja, North Norway. *Norsk Geol. Tidsskr.*, 64: 171-172.
- Krogh, T.E., 1973. A low contamination method for hydrothermal decomposition of zircon and extraction of U and Pb for isotopic age determinations. *Geochim. Cosmochim. Acta*, 37: 485-494.
- Kulling, O., 1964. Översikt över norra Norrbottensfjällens kaledonberggrund [Overview on the Caledonides of northern Norrbotten county, Sweden; Swedish with English summary]. *Sveriges geol. Unders.*, Ba19: 1-166.
- Ludwig, K.R., 1986. ISOPLOT200: A plotting and regression program for isotope geochemists, for use with HP Series 200 computers. U.S. Geol. Surv., Open-File Report 85-513, 105pp.
- Mearns, E.W., 1986. Sm-Nd ages in Norwegian garnet peridotites. *Lithos*, 19: 269-278.
- Monger, J.W.H., Price, R.A., and Tempelman-Kluit, D.J., 1982. Tectonic accretion and the origin of the two major metamorphic and plutonic belts in the Canadian Cordillera. *Geology*, 10: 70-75.
- Nordkalott Project, 1988. Metamorphic, structural and isotopic age map, northern Fennoscandia. 1:1 mill. Geological Surveys of Finland, Norway and Sweden, Helsinki.
- Öhlander, B., Skiöld, T., Hamilton, P.J., and Claesson, L.-Å., 1987. The western border of the Archean province of the Baltic Shield: evidence from northern Sweden. *Contrib. Mineral. Petrol.*, 95: 437-450.
- Öhlander, B., Skiöld, T., and Nisca, D.H., 1990. Delineation and origin of the Archean-Proterozoic boundary in northern Sweden. Second Symposium on the Baltic Shield, Lund, Sweden, June 5-7, 1990, Abstract volume, p. 69.
- Papanastassiou, D.A. and Wasserburg, G.J., 1969. Initial strontium isotopic abundances and the resolution of small time differences in the formation of

- planetary objects. *Earth Planet. Sci. Lett.*, 5: 361-376.
- Park, A.F., 1991. Continental growth by accretion: A tectonostratigraphic terrane analysis of the evolution of the western and central Baltic Shield, 2.50 to 1.75 Ga. *Geol. Soc. Am. Bull.*, 103: 522-537.
- Park, A.F., Bowes, D.R., Halden, N.M., and Koistinen, T.J., 1984. Tectonic evolution at an Early Proterozoic continental margin: The Svecokareliides of eastern Finland. *J. Geodynamics*, 1: 359-386.
- Patchett, P.J. and Kuovo, O., 1986. Origin of continental crust of 1.9-1.7 Ga age: Nd isotopes and U-Pb zircon ages in the Svecokarelian terrain of southern Finland. *Contrib. Mineral. Petrol.*, 92: 1-12.
- Patchett, P.J., Todt, W. and Gorbatshev, R., 1987. Origin of continental crust of 1.9-1.7 Ga age: Nd isotopes in the Svecofennian orogenic terrains of Sweden. *Precamb. Res.*, 35: 145-167.
- Pearce, J.A., Harris, N.G.W. and Tindle, A.G., 1984. Trace element discrimination diagrams for the tectonic interpretation of granitic rocks. *J. Petrol.*, 25: 956-983.
- Pharao, T.C. and Pearce, J.A., 1984. Geochemical evidence for the geotectonic setting of early Proterozoic metavolcanic sequences in Lapland. *Precamb. Res.*, 25: 283-208.
- Pitcher, W.S., 1982. Granite types and tectonic environment. K.S. Hsü (Ed.) *Mountain building processes*, Academic Press, London, 19-40.
- Pupin, J.P., 1985. Magmatic zoning of hercynian granitoids in France based on zircon typology. *Schweiz. mineral. petrol. Mitt.*, 65: 29-56.
- Rapp, R.P., Watson, E.B. and Miller, C.F., 1991. Partial melting of amphibolite/eclogite and the origin of Archean trondhjemites and tonalites. *Precamb. Res.*, 51: 1-25.
- Roddick J.C. and Compston, W., 1977. Strontium isotopic equilibration: a solution to a paradox. *Earth Planet. Sci. Lett.*, 34: 238-246.
- Romer, R.L., 1987. The geology, geochemistry and metamorphism of the Sjangeli area, a tectonic basement window in the Caledonides of Northern Sweden. *Res. Rep. University of Luleå, TULEA 1987:16*, 124 pp.
- Romer, R.L., 1989. Interpretation of the lead isotopic composition from sulfide mineralizations in the Proterozoic Sjangeli area, northern Sweden. *Norges geol. Unders. Bull.*, 415: 57-69.
- Romer, R.L., 1990. Lead mobilization during foreland metamorphism in orogenic belts: Examples from northjern Sweden. *Geol. Rundsch.*, 79: 693-707.
- Romer, R.L., 1991. The Late Archaean to Early Proterozoic lead isotopic evolution of the Northern Baltic Shield of Norway, Sweden and Finland. *Precamb. Res.*, 49: 73-95.
- Romer, R.L. and Bax, G., 1990. The rhombohedral framework of the Scandinavian Caledonides. *Geol. Soc. Am. Annual Meeting, Abstracts with Program 22*: 367.
- Romer, R.L. and Bax, G., 1992. The rhombohedral framework of the Scandinavian Caledonides and their foreland. *Geol. Rundschau*, 81:
- Romer, R.L. and Wright, J.E., 1992. U-Pb dating of columbites: A geochronologic tool to date magmatism and ore deposits. *Geochim. Cosmochim. Acta*, xx

- Romer, R.L. and Wright, J.E., submit. Lead mobilization during tectonic reactivation of the western Baltic Shield.
- Sawyer, E.W. and Korneliussen, A., 1989. The geochemistry of Lower Proterozoic siliciclastic turbidites from the Rombak Window: implications for paleogeography and tectonic settings. *Norges geol. Unders. Bull.*, 415: 23-38.
- Skiöld, T., 1987. Aspects of the Proterozoic geochronology of northern Sweden. *Precamb. Res.*, 35: 161-167.
- Skiöld, T., 1988. Implications of new U-Pb zircon chronology to Early Proterozoic crustal accretion in northern Sweden. *Precamb. Res.*, 38: 147-164.
- Skiöld, T. and Cliff, R.A., 1984. Sm-Nd and U-Pb dating of Early Proterozoic mafic-felsic volcanism in northernmost Sweden. *Precambrian Res.*, 38: 147-164.
- Skiöld, T., Öhlander, B., Vocke, R.D. jr. and Hamilton, P.J., 1988. Chemistry of Proterozoic orogenic processes at a continental margin in northern Sweden. *Contrib. Mineral. Petrol.*, 96: 193-207.
- Skyseth, T. and Reitan, P., 1990. The geochemistry and geology of the carbonate-hosted, disseminated gold deposit at Gautelisfjell, Rombak Proterozoic Basement Window, Northern Norway. *Internat. Symp. Geochem. Prosp.*, Prague; *Meth. Geochem. Prosp.*, Extended Abstr., p.210
- Stendal, H., 1981. Feltundersøgelser af kontaktrelationer mellem den sydlige del af Tysfjord vinduet og de overliggende metasedimenter med henblik på Mo-U mineraliseringer. Sørfold, Nordland. *Norges geol. Unders. Rapp. Nr 1850/30C*: 18pp. (in Danish).
- Stendal, H., 1990. Mineraliseringspotentialet af granitiske bjergarter i den sydlige del af Tysfjordvinduet, Nordland, Norge. *Geolognytt*, 1/90, 106-107. (in Danish).
- Stendal, H. and Petersen, M.D., 1989. Feltrapport, Kvaløya, Troms 1988. Open file Rapport 89-10-HSt. Geologisk Cewntralinstitut. Københavns Universitet, 29pp. (in Danish).
- Todd, V.R., Erskine, B.G. and Morton, D.M., 1988. Metamorphic and tectonic evolution of the northern Peninsular Ranges Batholith, southern California. In: W.G. Ernst (Ed.). *Metamorphism and crustal evolution of the Western United States*. Rubey volume VII: 894- 937.
- Vaasjoki, M. and Sakko, M., 1988. Evolution of the Raahe-Ladoga zone in Finland: Isotopic constraints. *Geol. Surv. Finl., Bull.*, 343: 7-32.
- Welin, E., 1987. The depositional evolution of the Svecofennian supracrustal sequence in Finland and Sweden. *Precamb. Res.*, 35: 95-113.
- Wilson, M.R., Hamilton, P.J., Fallick, A.E., Aftalion, M. and Michard, A., 1985. Granites and early Proterozoic crustal evolution in Sweden: evidence from Sm-Nd, U-Pb and O isotope systematics. *Earth Planet. Sci. Lett.*, 72: 376-388.
- Wright, S.F., 1988. Early Proterozoic deformational history of the Kiruna district, northern Sweden. Unpubl. PhD Thesis Univ. Minnesota, 170pp.
- Zuber, J.A. and Öhlander, B., 1990. Geophysical and geochemical evidence of Proterozoic collision in the western marginal zone of the Baltic Shield. *Geol. Rundsch.*, 79: 1-11.

Sample	SiO <sub>2</sub>	Al <sub>2</sub> O <sub>3</sub>	Fe <sub>2</sub> O <sub>3</sub>	MnO	TiO <sub>2</sub>	MgO	CaO	K <sub>2</sub> O	Na <sub>2</sub> O	P <sub>2</sub> O <sub>5</sub>	Sum	LOI	Ba	Cr	Cu	Ni
<b>Sjangeli: Archaean tonalites</b>																
STE3	70.8	15.4	2.00	0.04	0.26	0.88	2.21	1.17	6.78	0.13	99.6	0.3	387	63	8.3	13
STE4	63.8	16.5	4.86	0.06	0.43	2.09	3.91	1.38	5.68	0.12	98.8	1.0	428	57	21	23
STES	67.6	17.0	2.82	0.03	0.20	1.25	3.85	1.25	5.70	0.09	99.8	0.6	388	57	29	41
<b>Gautelis: 1.94 Ga tonalites</b>																
TS84/43	72.88	14.97	1.58	0.03	0.22	0.41	1.82	2.76	5.01	0.07	100.43	0.68	565	22	8	7
TS85/44	72.48	14.62	1.42	0.03	0.19	0.62	1.32	2.20	5.76	0.07	99.25	0.54	1100	12	3	3
TS86A/45	73.48	14.94	1.42	0.02	0.18	0.35	1.84	2.67	5.13	0.06	100.65	0.54	764	11	3	3
TS86B/46	72.64	15.20	1.11	0.02	0.17	0.26	2.31	1.16	5.86	0.05	99.46	0.68	356	14	3	3
TS87/47	70.75	15.48	1.28	0.02	0.18	0.35	1.80	3.55	4.71	0.06	99.89	0.68	992	15	3	3
TS89/50	70.77	15.84	1.71	0.03	0.21	0.36	1.64	3.28	5.41	0.08	99.87	0.53	736	10	3	3
TS90/51	74.54	15.01	1.27	0.03	0.20	0.36	2.34	0.92	6.02	0.07	191.27	0.51	346	15	3	3
TS91/52	71.37	14.60	1.60	0.03	0.20	0.42	1.46	3.55	4.66	0.06	98.51	0.56	876	13	3	3
TS92/53	76.54	13.13	0.93	0.02	0.09	0.12	0.67	5.49	3.47	0.01	100.75	0.28	253	10	3	3
TS93/54	69.99	15.05	1.99	0.02	0.22	0.46	1.90	3.06	4.89	0.07	98.19	0.53	810	16	3	3
TS95/55	60.50	17.35	5.68	0.08	0.64	2.25	4.55	2.75	4.80	0.32	99.67	0.76	1100	23	19	17
TS105/64	60.96	16.92	5.31	0.07	0.62	2.21	4.10	2.90	4.73	0.29	98.88	0.77	1300	24	14	15
K140.5	67.29	14.91	4.47	0.05	0.54	1.54	3.60	2.12	4.50	0.13	99.98	0.83	967	9	11	7
K143.5	71.94	15.27	1.31	0.04	0.17	0.42	1.74	1.52	6.59	0.05	99.83	0.78	719	n.d.	4	n.d.
K144.5	69.25	14.95	3.13	0.06	0.44	1.01	3.21	1.94	4.92	0.12	99.85	0.83	722	7	2	8
<b>Sjangeli: older granites</b>																
STB2**	67.8	14.2	4.58	0.07	0.57	0.89	1.85	5.34	3.26	0.19	98.7	0.9	1768	34	28	19
STE2**	72.3	14.0	2.38	0.02	0.26	0.81	1.40	4.52	3.92	0.12	99.7	0.6	1639	52	20	8.2
<b>Cuncojavrrre: older granite</b>																
K124.5	63.21	17.57	3.39	0.16	0.67	0.62	1.31	5.90	6.07	0.16	99.87	0.82	802	n.d.	5	5
<b>Gautelisvatn: older granites</b>																
K142.5	60.55	18.49	4.49	0.05	0.67	2.19	2.03	1.53	8.54	0.19	99.44	0.70	361	22	3	15
K145.5	72.55	14.53	1.35	0.03	0.18	0.32	0.76	5.64	4.13	0.05	99.90	0.35	1101	n.d.	2	2
K152.5	67.00	14.73	4.19	0.08	0.62	0.76	1.93	5.75	4.00	0.18	99.72	0.48	1008	8	28	6

**Table 4:** Chemical whole-rock XRF analyses for granites and tonalites of the Kvaløya, Rombak-Sjangeli, and Tysfjord basement culminations. For description of analytical method and precision see Korneliussen and Sawyer (1989). Ce, Sm, Hf, Ta, Th, and U concentrations were obtained through neutron activation analyses. XRF analyses were performed at the Geological Survey of Norway (NGU), neutron activation analyses were performed at (Becquerel Laboratories Inc., Mississauga, Ont., Canada) through contract work with NGU.



Table 4: Cont'd.

Sample	SiO <sub>2</sub>	Al <sub>2</sub> O <sub>3</sub>	Fe <sub>2</sub> O <sub>3</sub>	MnO	TiO <sub>2</sub>	MgO	CaO	K <sub>2</sub> O	Na <sub>2</sub> O	P <sub>2</sub> O <sub>5</sub>	Sum	LOI	Ba	Cr	Qu	NI
<b>Kvaløya: older granites</b>																
KR9.88	68.	15.05	3.06	0.04	0.44	0.74	2.02	4.67	4.10	0.17	98.69	0.40	1300	11	9	8
KR10A.88	68.63	15.40	2.68	0.03	0.39	0.55	1.83	5.13	4.13	0.13	99.37	0.46	1100	9	9	3
KR11.88	70.95	14.59	2.05	0.02	0.24	0.39	1.48	4.79	4.04	0.08	99.40	0.76	898	8	3	3
KR12.88	69.61	14.91	2.75	0.04	0.44	0.58	1.79	4.79	4.04	0.12	99.58	0.51	1200	9	7	3
KR13.88**													1700	11	11	6
KR14.88	72.60	14.08	1.62	0.02	0.19	0.31	1.31	5.18	3.67	0.05	99.29	0.26	618	7	8	3
KR15.88	70.10	15.06	2.36	0.03	0.29	0.51	1.61	4.91	4.15	0.09	99.68	0.56	896	11	8	3
KR16.88	71.02	14.46	2.31	0.03	0.35	0.48	1.61	4.97	3.80	0.10	99.47	0.32	973	9	6	5
<b>Nordal: older granites</b>																
K275.3	69.37	13.44	4.74	0.06	0.59	0.54	1.70	5.33	2.90	0.15	99.28	0.46	760	6	6	
ES-22	72.97	13.85	2.48	0.04	0.26	0.23	1.21	5.76	3.10	0.03	100.39	0.46	599	8	n.d.	7
ES-33	75.32	13.70	1.48	0.03	0.20	0.19	0.97	5.56	3.20	0.02	101.08	0.41	500	n.d.	n.d.	n.d.
ES-81	66.40	15.83	3.82	0.06	0.51	0.59	2.04	5.45	4.10	0.13	99.40	0.47	1300	n.d.	n.d.	n.d.
ES-83	66.04	15.26	4.87	0.06	0.64	0.96	2.25	5.53	3.40	0.18	99.77	0.58	1200	13	8	6
K63.5	66.13	13.99	5.40	0.09	0.78	1.81	2.76	4.36	3.51	0.28	99.66	0.51	895	37	12	14
K72.5	70.69	14.98	1.93	0.04	0.29	0.64	1.48	4.80	4.53	0.07	100.03	0.59	983	6	5	8
<b>Serdal: older granites</b>																
KS3.3	75.89	13.47	1.58	0.03	0.14	0.13	0.76	5.18	3.80	0.02	101.39	0.39	173	n.d.	n.d.	n.d.
KS5.3**	76.76	12.49	1.36	0.02	0.10	0.08	0.72	5.06	3.30	0.01	100.33	0.44	77	n.d.	6	n.d.
<b>Svandal (Rombakstøt): older granites</b>																
KR30.88	70.89	14.42	2.78	0.04	0.31	0.31	1.20	5.77	3.59	0.07	99.84	0.46	722	12	3	14
KR31.88	69.24	15.37	3.19	0.04	0.36	0.38	1.24	6.17	3.68	0.08	100.19	0.45	983	13	6	13
KR32.88	69.93	14.83	3.13	0.04	0.36	0.33	1.24	6.22	3.54	0.07	100.20	0.50	1100	13	3	13
KR33.88**	68.50	15.57	3.55	0.05	0.42	0.39	1.30	6.38	3.69	0.09	100.39	0.46	1200	12	7	16
KR34.88	68.16	15.98	3.20	0.04	0.46	0.38	1.36	6.26	4.04	0.08	100.46	0.49	1300	12	3	11
KR37.88	63.54	18.09	4.50	0.07	0.52	0.52	2.86	4.40	4.68	0.14	99.90	0.59	1800	16	7	16
KR38.88	62.71	17.60	4.75	0.06	0.60	0.71	2.30	5.83	4.03	0.22	99.45	0.64	2000	18	12	9
KR39.99	62.01	18.27	3.75	0.06	0.46	0.52	2.38	6.10	4.50	0.13	99.04	0.87	3000	12	7	7
KR40.88	63.36	17.34	4.43	0.07	0.50	0.44	2.40	6.05	4.42	0.12	99.60	0.47	2000	11	9	11
KR41.88	64.12	17.78	3.83	0.06	0.42	0.40	2.39	5.90	4.57	0.11	100.16	0.62	2200	13	14	8

Table 4: Cont'd.

Sample	SiO <sub>2</sub>	Al <sub>2</sub> O <sub>3</sub>	Fe <sub>2</sub> O <sub>3</sub>	MnO	TiO <sub>2</sub>	MgO	CaO	K <sub>2</sub> O	Na <sub>2</sub> O	P <sub>2</sub> O <sub>5</sub>	Sum	LOI	Ba	Cr	Qi	Ni
<b>Tysfjord (Hellemobotn): older granites</b>																
MH1-42	68.41	16.3	2.48	0.04	0.34	0.32	1.61	5.51	4.72	0.11	100.2	0.35	788	6	3	8
MH2-43	68.82	16.55	2.26	0.04	0.28	0.31	1.49	5.89	4.59	0.09	100.68	0.37	854	8	3	6
MH3-44	67.61	16.69	2.15	0.04	0.3	0.26	1.46	5.83	4.82	0.09	99.73	0.5	884	6	3	5
MH4-45	66.67	15.82	3.26	0.05	0.42	0.49	1.65	5.23	4.37	0.12	98.96	0.87	751	7	5	9
MH5-46	16.43	2.25		0.04	0.28	0.29	1.56	5.54	4.75	0.08	100.7	0.51	751	7	5	9
<b>Tysfjord (Særfolda): older granite</b>																
HS5750**	70.37	14.77	3.19	0.07	0.48	0.67	1.36	5.57	4.80	0.11		0.43				
HS32775-2**	65.86	14.38	4.01	0.02	0.31	0.12	2.59	4.72	4.90	0.04		1.25				
<b>Eifjord: older granites</b>																
IL890195**	69.29	14.24	3.76	0.06	0.40	0.21	1.57	5.82	3.49	0.07		0.12	869	3	3	3
IL890142**	71.05	15.22	1.76	0.04	0.20	0.34	0.95	5.07	4.50	0.05		0.30	789	20	3	3
IL88007**	72.11	13.94	2.60	0.04	0.25	0.26	0.96	5.57	3.67	0.04		0.34				
<b>Hogtuva: older granites</b>																
IL870390**	71.35	14.88	1.54	0.04	0.26	0.04	0.57	6.18	4.31	0.04	xx					
IL870577**	69.52	14.15	1.48	0.04	0.22	0.05	0.98	5.85	3.72	0.05						
IL870320**	66.67	15.13	2.82	0.08	0.39	0.14	1.61	5.73	4.09	0.14						
IL870525**	59.82	18.78	2.99	0.05	0.65	0.18	2.79	5.95	4.74	0.18						
IL870468**	56.94	17.17	4.96	0.08	0.58	0.26	3.92	3.98	4.46	0.26						
<b>Glomfjord: older granite</b>																
KG3.88**	70.06	15.51	1.89	0.07	0.30	0.37	1.22	5.57	4.69	0.08		0.19	504	14	3	9
<b>Sjangel: younger granite</b>																
STB5**	75.9	12.2	2.76	0.04	0.19	0.29	0.71	4.71	3.29	0.06	100.2	0.5	265	20	14	6.6
<b>Cunojavrr: younger granites</b>																
K125.5	76.04	13.06	0.65	0.01	0.03	0.05	0.70	4.61	4.39	0.01	99.78	0.24	10	6	n.d.	3
K126.5	75.33	13.45	0.59	0.01	0.04	0.08	0.40	4.76	4.69	0.01	99.82	0.45	24	3	2	3

Table 4: Cont'd.

Sample	SiO <sub>2</sub>	Al <sub>2</sub> O <sub>3</sub>	Fe <sub>2</sub> O <sub>3</sub>	MnO	TiO <sub>2</sub>	MgO	CaO	K <sub>2</sub> O	Na <sub>2</sub> O	P <sub>2</sub> O <sub>5</sub>	Sum	LOI	Ba	Cr	Qu	NI
<b>Lappvikind: younger granites</b>																
U1675	77.26	12.86	1.27	0.02	0.09	0.15	0.73	4.38	3.50	0.01	100.56	0.30	100	n.d.	n.d.	n.d.
U1677	77.52	12.81	1.49	0.01	0.09	0.07	0.59	5.07	3.40	0.01	101.23	0.18	26	n.d.	n.d.	n.d.
U1687	78.82	12.24	1.43	0.01	0.01	0.09	0.59	5.23	3.00	0.01	101.50	0.19	85	n.d.	n.d.	n.d.
U1692	77.28	12.59	1.16	0.01	0.07	0.13	0.64	4.71	3.30	0.01	100.21	0.32	57	n.d.	n.d.	n.d.
U1702	75.09	13.04	2.44	0.02	0.18	0.38	0.67	5.00	3.60	0.02	100.84	0.40	262	n.d.	7	n.d.
U1734	73.47	14.65	1.78	0.02	0.23	0.33	0.43	5.32	4.30	0.04	100.88	0.31	440	n.d.	n.d.	n.d.
U1739	71.13	14.60	4.29	0.03	0.16	0.69	1.09	2.54	5.20	0.02	100.56	0.81	377	n.d.	n.d.	n.d.
U1745	71.76	14.86	2.04	0.03	0.38	0.45	0.48	5.54	4.40	0.08	100.36	0.34	807	n.d.	n.d.	n.d.
U1757	72.35	14.70	1.96	0.03	0.24	0.21	0.97	5.37	3.90	0.04	99.88	0.11	688	n.d.	n.d.	n.d.
U1769	71.58	15.23	1.89	0.02	0.27	0.25	0.49	6.24	3.70	0.05	100.25	0.53	643	n.d.	n.d.	n.d.
<b>Nordal: younger granites</b>																
K272.3	76.65	12.48	1.35	0.01	0.09	0.07	0.74	5.29	3.30	0.01	100.47	0.50	80	n.d.	9	n.d.
ES-24	76.91	12.44	1.70	0.02	0.14	0.15	0.78	5.43	3.10	0.01	101.08	0.41	214	n.d.	n.d.	n.d.
<b>Særdal: younger granites</b>																
KS30.3	64.04	15.05	5.75	0.09	0.67	2.03	2.94	3.82	3.90	0.15	99.06	0.62	702	n.d.	n.d.	n.d.
KS31.3	70.93	13.90	3.33	0.03	0.48	0.22	1.12	5.06	3.40	0.11	99.33	0.75	757	n.d.	5	n.d.
KS35.3**	67.12	13.37	2.70	0.04	0.30	0.24	1.20	5.16	3.00	0.06	99.33	6.14	856	n.d.	n.d.	5
KS36.3	71.24	13.93	3.54	0.04	0.47	0.40	1.06	6.45	2.50	0.12	100.15	0.40	800	n.d.	11	5
<b>Stasjonsholmen: younger granites</b>																
KR1.88	73.97	12.51	1.82	0.02	0.18	0.17	0.78	5.63	3.12	0.03	98.48	0.25	298	7	9	15
KR2A.88**	73.03	13.06	1.73	0.02	0.20	0.22	0.71	5.25	3.41	0.04	98.02	0.36	262	8	6	15
KR2B.88													310	8	3	12
KR2C.88	73.96	13.33	1.62	0.02	0.18	0.24	0.52	5.56	3.20	0.05	99.18	0.51	280	8	7	14
KR3.88	69.60	14.54	3.45	0.05	0.46	0.42	1.66	5.54	3.66	0.11	99.85	0.36	717	12	3	14
KR4.88	72.13	13.95	2.33	0.03	0.25	0.17	1.09	6.15	3.32	0.04	99.76	0.30	574	8	3	12
KR5A.88**													194	21	3	22
KR5B.88	76.20	12.53	1.80	0.03	0.15	0.10	0.68	5.53	3.02	0.02	100.51	0.46	208	9	3	18
KR5E.88																

Table 4: Cont'd.

Sample	SiO <sub>2</sub>	Al <sub>2</sub> O <sub>3</sub>	Fe <sub>2</sub> O <sub>3</sub>	MnO	TiO <sub>2</sub>	MgO	CaO	K <sub>2</sub> O	Na <sub>2</sub> O	P <sub>2</sub> O <sub>5</sub>	Sum	LOI	Ba	Cr	Cu	Ni
<b>Tysfjord (Hellemobotn): younger granites</b>																
KH50A-1	73.25	14.09	2.6	0.04	0.26	0.21	0.81	4.8	4.25	0.04	100.56	0.2	294	7	10	17
KH51-3**	72.02	15.06	3.01	0.05	0.32	0.25	1.06	5.98	3.87	0.06	101.89	0.22	443	3	3	150
KH52-4	73.66	14.12	2.02	0.03	0.19	0.08	0.86	5.62	3.8	0.03	100.58	0.18	288	7	3	120
KH55-7	72.86	14.22	2.11	0.03	0.28	0.46	0.87	5.64	3.78	0.06	100.62	0.31	706	10	3	97
KH56B-9																6
KH56C-10	71.67	13.6	2.48	0.03	0.31	0.31	0.96	5.38	3.52	0.07	98.53	0.2	348	8	3	21
KH57A-11	75.37	13.11	1.73	0.03	0.15	0.09	0.44	5.66	3.62	0.02	100.41	0.19	107	7	3	21
KH57B-12																
KH58-13	79.55	11.76	1.12	0.02	0.07	0.005	0.64	4.41	3.58	0.005	101.36	0.24	5	6	3	19
KH59-14	76.95	12.61	1.65	0.03	0.16	0.08	0.64	5.16	3.34	0.02	100.81	0.17	85	7	3	7
KH60-15**	74.74	12.6	1.81	0.03	0.18	0.15	0.7	4.86	3.64	0.03	98.9	0.17	79	8	3	12
KH61-16	75.97	11.88	1.88	0.03	0.18	0.12	0.64	4.72	3.26	0.02	98.94	0.23	71	8	3	12
KH62-17	70.14	14.36	3.1	0.05	0.36	0.73	1.24	5.47	3.98	0.06	99.76	0.26	244	6	3	20
KH63-18	66.61	13.09	8.17	0.14	0.99	0.77	2.07	4.08	3.41	0.15	99.87	0.38	191	11	3	52
GH1-33	74.63	13.63	2.03	0.03	0.23	0.24	0.86	4.96	3.67	0.04	100.52	0.21	295	6	3	16
GH2A-34	72.29	13.85	2.5	0.04	0.27	0.1	0.95	5.28	3.89	0.05	99.58	0.35	140	6	3	36
GH2B-35	78.3	12.73	0.28	0.005	0.03	0.005	0.66	5.34	3.55	0.005	101.03	0.19	94	3	3	19
GH3-36	77.9	12.82	1.09	0.02	0.08	0.005	0.54	5.09	3.71	0.02	101.37	0.18	13	6	3	14
GH4-37	67.49	17.44	2.03	0.03	0.5	0.95	1.01	4.66	6.36	0.11	101.04	0.47	237	7	3	24
GH5-39	64.39	13.25	8.84	0.13	1.14	1.08	2.56	3.81	3.43	0.19	99.18	0.38	235	7	3	42
GH6-40	70.09	12.84	5.22	0.1	0.63	0.51	1.49	4.88	3.16	0.12	99.33	0.3	208	9	3	25
GH6B-41	65.15	13.31	8.82	0.15	1.11	0.76	2.12	4.02	3.57	0.17	99.65	0.46	193	7	3	49
<b>Tysfjord (Gjerdal): younger granites</b>																
KG65A-19																
KG65B-20	74.54	12.55	2.02	0.04	0.17	0.005	0.85	5.21	3.6	0.01	99.21	0.22	187	8	3	28
KG65C-21																
KG66A-22																
KG66B-23	72.57	13.75	2.77	0.06	0.23	0.005	1.04	5.74	3.77	0.02	100.04	0.16	220	7	3	28
KG67-24	70.61	15.17	1.22	0.02	0.09	0.005	0.92	7.25	3.85	0.005	99.42	0.34	232	6	3	15
KG68-25	73.29	13.39	2.29	0.04	0.28	0.17	0.9	5.12	4.37	0.07	100.33	0.41	370	6	3	13
KG69-26**	68.53	15.43	3.1	0.07	0.32	0.005	1.25	6.42	4.1	0.02	99.38	0.13	455	7	3	15
KG70-27																

Table 4: Cont'd.

Sample	SiO <sub>2</sub>	Al <sub>2</sub> O <sub>3</sub>	Fe <sub>2</sub> O <sub>3</sub>	MnO	TiO <sub>2</sub>	MgO	CaO	K <sub>2</sub> O	Na <sub>2</sub> O	P <sub>2</sub> O <sub>5</sub>	Sum	LOI	Ba	Cr	Cl	NI
<b>Tysfjord (Veikvatn): younger granites</b>																
KV71A-28	76.35	12.1	1.99	0.03	0.13	0.005	0.49	5.23	3.72	0.005	100.21	0.23	26	7	3	24
KV72A-29	75.16	12.33	2.06	0.03	0.15	0.005	0.63	5.3	3.69	0.01	99.63	0.28	50	3	3	27
KV73-30**	76.73	12.43	1.44	0.02	0.1	0.03	0.43	5.12	3.77	0.005	100.32	0.23	43	3	3	33
KV74-31	75.61	11.85	2.26	0.04	0.15	0.005	0.5	5.34	3.63	0.005	99.6	0.26	42	7	3	46
KV75-32	74.63	13.63	2.03	0.03	0.23	0.24	0.86	4.96	3.67	0.04	100.52	0.21				
<b>Eifjord: younger granites</b>																
IL890016**	69.80	15.58	1.85	0.05	0.18	0.14	0.85	6.17	4.72	0.04		0.13	616	3	3	3
IL890007**	77.44	11.63	1.49	0.03	0.12	0.17	0.32	5.08	3.44	0.01		0.29	124	3	5	3
<b>Glomfjord: younger granite</b>																
KG1.88**	78.11	11.93	0.70	0.04	0.11	0.04	0.40	4.45	4.07	0.01		0.16	37	6	3	3
<b>Tysfjord (Særfolda): younger granites</b>																
HS5767**	77.27	12.18	1.95	0.03	0.19	0.15	0.55	4.65	4.00	0.03		0.41				
HS5701**	73.92	12.85	1.86	0.03	0.22	0.33	0.58	5.47	4.10	0.03		0.28				
HS5807**	75.91	13.02	1.63	0.04	0.20	0.15	0.45	5.53	3.80	0.02		0.39				
HS32793-2**	73.69	12.73	2.70	0.02	0.25	0.27	0.28	5.35	3.20	0.02		0.68				
HS5789**	73.38	13.17	1.81	0.05	0.28	0.24	0.54	5.31	4.20	0.03		0.39				
HS5738**	76.10	12.44	1.94	0.03	0.13	0.20	0.18	4.75	4.40	0.01		0.32				
HS32753-2**	72.92	12.58	3.65	0.04	0.16	0.69	0.40	5.66	2.70	0.02		0.57				
HS5727**	74.73	12.03	1.86	0.02	0.13	0.17	0.29	4.69	4.10	0.01		0.37				

Sample	La	Pb	Sr	V	Y	Zn	Zr	Nb	Rb	Ce	Sm	Hf	Ta	Th	U
<b>Sjangeli: Archaean tonalites</b>															
STE3	18		184	38	8	27	95	n.d.	35						
STE4	33		539	83	13	72	108	n.d.	90						
STE5	n.d.		569	41	11	30	18	n.d.	52						
<b>Gautelis: 1.94 Ga tonalites</b>															
TS84/43	37	5	319	19	9	36	117	15	61	53	4	3	1	9	2
TS85/44	29	10	432	16	13	14	122	12	46	49	3	4	1	9	4
TS86A/45	32	11	494	15	8	21	109	9	63	54	3	3	1	8	2
TS86B/46	39	14	636	12	9	14	122	10	37	67	4	3	1	11	2
TS87/47	53	11	443	15	13	19	111	11	77	88	5	3	1	15	2
TS89/50	43	12	365	17	8	22	132	11	81	72	4	3	1	11	2
TS90/51	35	10	523	18	10	14	123	14	27	61	4	3	1	8	6
TS91/52	37	12	366	15	12	23	120	12	89	65	4	3	1	11	3
TS92/53	40	14	117	3	34	13	105	21	192	81	5	4	4	42	10
TS93/54	16	12	450	23	3	23	116	9	58	25	2	4	1	5	1
TS95/55	33	12	1100	92	13	78	119	9	107	66	8	4	1	5	1
TS105/64	41	13	974	85	14	61	112	9	85	76	7	3	2	8	1
K140.5	24	12	377	56	16	36	180	12	55						
K143.5	26	11	490	15	11	17	112	9	34						
K144.5	45	12	692	34	18	31	219	19	54						
<b>Sjangeli: older granites</b>															
STB2**	61	21	164	37	35	128	326	11	227						
STE2**	19	24.9	312	26	4.0	41	94	n.d.	75						
<b>Cunofavre: older granite</b>															
K124.5	12	12	47	16	16	57	26	7	163						
<b>Gautelisvatn: older granites</b>															
K142.5	43	16	353	63	22	43	206	18	47						
K145.5	18	14	229	19	10	34	107	8	106						
K152.5	65	28	178	31	47	58	270	20	197						

Table 4: Cont'd.

Sample	La	Pb	Sr	V	Y	Zn	Zr	Nb	Pb	Ce	Sm	Hf	Ta	Th	U
<b>Kvaløya: older granites</b>															
KR9.88	130	19	411	42	21	48	229	15	145	200	7	8	2	17	2
KR10A.88	120	19	331	35	17	40	200	17	172	190	6	8	2	18	1
KR11.88	95	20	295	27	10	28	196	11	154	160	5	6	n.d.	19	1
KR12.88	230	20	380	39	23	41	274	19	141	360	10	13	2	37	2
KR13.88**	140	14	430	46	25	41	254	17	156	260	10	11	1	17	1
KR14.88	63	23	210	23	5	29	142	8	184	100	3	5	1	21	1
KR15.88	83	21	271	28	11	41	199	11	187	170	5	9	2	20	1
KR16.88	99	21	301	31	18	39	190	14	152	170	7	9	2	15	1
<b>Nordal: older granites</b>															
K275.3	91	25	120	30	63	90	198	24	239						
ES-22	97	27	103	10	57	70	109	19	246						
ES-33	63	22	118	10	26	14	199	16	230						
ES-81	105	25	229	23	43	43	352	18	133						
ES-89	96	20	234	43	46	81	367	19	197						
K63.5	58	26	212	58	33	75	248	18	193						
K72.5	33	14	372	32	15	21	174	15	138						
<b>Sørdal: older granites</b>															
KS3.3	60	33	3	9	51	35	142	13	349						
KS5.3**	52	38	3	n.d.	88	33	156	14	366						
<b>Svartdal (Rombaksbotn): older granites</b>															
KR30.88	110	28	100	23	60	55	283	22	211	230	11	13	2	26	5
KR31.88	53	23	110	26	45	60	329	20	205	110	9	12	1	8	2
KR32.88	60	27	112	24	44	61	380	17	191	130	10	15	1	10	4
KR33.88**	120	19	126	27	55	62	400	21	205	270	15	14	2	18	3
KR34.88	130	23	129	25	50	64	405	18	167	250	15	15	3	20	5
KR37.88	41	22	244	36	28	86	329	21	246	78	5	15	2	5	3
KR38.88	37	20	227	42	17	67	422	10	150	66	4	14	1	3	2
KR39.88	42	17	314	34	22	64	313	14	127	82	5	11	n.d.	4	1
KR40.88	73	27	244	34	39	108	513	12	136	130	8	22	1	9	4
KR41.88	60	21	245	31	32	91	424	12	130	97	7	15	n.d.	8	3

Table 4: Cont'd.

Sample	La	Pb	Sr	V	Y	Zn	Zr	Nb	Rb	O <sub>2</sub>	Sm	Hf	Ta	Th	U
<b>Tysfjord (Hellemobotn): older granites</b>															
MH1-42	98	32	197	25	34	34	209	18	194	180	10	7	1	31	7
MH2-43	73	30	203	24	24	35	185	13	201	130	5	7	1	24	3
MH3-44	90	30	200	22	25	30	213	11	190	160	6	7	1	28	3
MH4-45	80	32	192	24	31	35	157	18	206	160	7	8	1	26	4
MH5-46	56	32	192	24	31	35	157	13	206	98	6	6	1	23	5
<b>Tysfjord (Sørfolda): older granites</b>															
HS5750**		30	185		40		435	20	205						
HS32775-2**		37	615		46		625	47	297						
<b>Efford: older granites</b>															
IL890195**		47	127	3	99	124	523	40	281						
IL890142**		22	170	12	27	24	201	16	115						
IL88007**															
<b>Hegtuva: older granites</b>															
IL870390**		30	101		28			18	230						
IL870577**		26	178		30			15	220						
IL870320**		129	233		35			16	237						
IL870525**		23	680		13			8	72						
IL870468**		25	934		21			11	111						
<b>Glomfjord: older granites</b>															
KG3.88**		26	156	22	33	39	242	18	172						
<b>Sjangeli: younger granite</b>															
STB5**	44	20	48	10	48	67	171	11	312						
<b>Cunejvrrre: younger granites</b>															
K125.5	5	40	12	9	34	13	59	11	183						
K126.5	n.d.	39	15	5	42	12	26	61	360						

Table 4: Cont'd.



Sample	La	Pb	Sr	V	Y	Zn	Zr	Nb	Rb	Ce	Sm	Hf	Ta	Th	U
<b>Lappvikstind: younger granites</b>															
U1675	60	34	41	n.d.	84	23	133	17	272						
U1677	81	33	24	n.d.	93	22	166	16	350						
U1687	77	28	29	n.d.	43	28	158	13	276						
U1692	82	38	23	n.d.	94	26	121	13	339						
U1702	94	22	69	n.d.	48	38	188	15	300						
U1734	42	41	59	n.d.	34	32	93	14	337						
U1739	51	17	52	5	31	27	167	17	283						
U1745	134	131	161	14	66	65	349	30	290						
U1757	99	20	152	11	36	40	217	21	261						
U1769	87	19	113	10	31	31	278	30	265						
<b>Nordal: younger granites</b>															
K272.3	98	63	24	n.d.	142	38	168	17	391						
ES-24	8	30	46	n.d.	76	45	214	15	319						
<b>Sardal: younger granites</b>															
KS30.3	85	20	18	25	53	35	345	24	275						
KS31.3	87	31	18	22	53	47	314	21	229						
KS35.3**	79	25	162	13	63	45	342	22	357						
KS36.3	89	24	118	15	48	59	338	17	242						
<b>Stasjonsholmen: younger granites</b>															
KR1.88	100	38	57	16	55	49	195	16	239	210	11	10	2	39	9
KR2A.88**	81	28	64	20	30	19	182	18	363	150	6	6	2	57	8
KR2B.88	71	23	82	18	36	17	152	21	329	140	7	6	5	49	27
KR2C.88	48	24	70	17	22	24	143	21	365	100	4	5	4	42	15
KR3.88	85	20	126	27	54	57	355	21	214	160	12	15	2	23	5
KR4.88	110	25	88	17	48	49	247	18	227	210	11	13	1	27	5
KR5A.88**	180	28	51	15	102	44	195	17	263	260	18	11	1	43	10
KR5B.88	140	36	52	15	69	51	182	17	270	240	14	8	2	38	8
KR5E.88	72									130	8	5	2	45	18

Table 4: Cont'd.

Sample	La	Pb	Sr	V	Y	Zn	Zr	Nb	Rb	Ca	Sm	Hf	Ta	Th	U
<b>Tysfjord (Hellebobotn): younger granites</b>															
KH50A-1	35	32	87	19	46	27	332	23	317	86	5.6	16	4	82	17
KH51-3**	150	23	64	15	59	50	329	30	214	290	17	14	3	58	9
KH52-4	120	34	61	12	44	39	202	18	244	210	12	7	1	60	12
KH55-7	97	5	172	24	15	23	252	12	173	230	8	8	1	29	3
KH56B-9	6									17	nd.	5	nd.	40	3
KH56C-10	130	30	76	18	60	37	260	27	265	210	12	10	3	53	10
KH57A-11	53	39	27	13	40	31	177	22	370	85	6	9	2	52	10
KH57B-12	28									59	4	8	6	35	23
KH58-13	28	41	6	12	64	18	123	16	266	72	4	7	1	56	22
KH59-14	53	32	38	14	27	24	165	18	281	110	5	6	1	46	11
KH60-15**	130	32	38	14	60	29	180	18	262	230	13	8	2	70	20
KH61-16	52	32	34	12	29	30	190	22	262	99	5	9	2	67	10
KH62-17	210	35	67	16	66	62	391	28	258	370	18	16	2	69	11
KH63-18	585	37	60	25	191	156	939	69	323	940	47	34	6	206	42
GH1-33	39	21	75	18	40	25	211	27	299	110	4	11	5	59	15
GH2A-34	140	43	49	13	128	48	296	26	340	270	16	13	5	68	24
GH2B-35	20	32	44	12	64	3	172	55	269	59	5	14	5	27	29
GH3-36	17	58	18	12	34	24	114	22	280	50	1	7	3	58	13
GH4-37	210	11	40	19	105	39	514	54	184	410	21	19	6	67	10
GH5-39	677	29	91	38	211	119	1200	78	213	1000	60	45	6	218	45
GH6-40	410	35	60	20	130	100	655	48	257	650	33	26	4	110	26
GH6B-41	722	34	57	24	232	184	1100	79	332	1150	57	43	8	249	53
<b>Tysfjord (Gjerdal): younger granites</b>															
KG65A-19	180									350	26	11	3	93	13
KG65B-20	88	48	41	12	93	86	279	32	310	170	17	14	3	26	11
KG65C-21	15500									19100	739	30	29	1300	135
KG66A-22	1710									2710	131	21	5	163	24
KG66B-23	130	48	48	11	90	115	396	44	302	240	20	17	3	141	35
KG67-24	44	70	55	11	39	46	53	18	325	82	3	3	2	45	11
KG68-25	110	39	83	16	50	75	271	27	237	200	11	9	2	24	4
KG69-26**	190	44	86	13	76	85	513	37	189	350	24	21	2	12	2
KG70-27	99									180	13	9	1	12	2

Table 4: Cont'd.

Sample	La	Pb	Sr	V	Y	Zn	Zr	Nb	Rb	O <sub>2</sub>	Sm	Hf	Ta	Th	U
<b>Tysfjord (Veikvatn): younger granite</b>															
KV71A-28	130	42	13	11	157	144	357	23	410	230	21	19	2	25	8
KV72A-29	150	52	23	11	173	71	308	42	400	260	21	16	4	48	17
KV73-30**	120	50	23	11	107	35	221	43	390	210	14	14	4	50	15
KV74-31	150	49	13	11	158	140	412	34	425	270	20	22	3	53	14
KV75-32	210									350	26	19	4	51	13
<b>Eifjord: younger granites</b>															
IL890016**		23	95	3	24	45	238	14	145						
IL890007**		23	14	3	34	64	177	34	212						
<b>Glomfjord: younger granite</b>															
KG1.88**		21	21	14	17	15	114	22	204						
<b>Tysfjord (Sørfolda): younger granites</b>															
HS5767**		25	31		24		329	14	245						
HS5701**		26	47		58		284	24	249						
HS5807**		32	60		58		253	21	263						
HS32793-2**		13	46		13		346	34	266						
HS5789**		71	54		48		323	29	276						
HS5738**		27	9		73		395	64	351						
HS32753-2**		18	41		88		291	38	354						
HS5727**		22	6		116		355	79	491						

Table 4: Cont'd.